

NASA CONTRACTOR  
REPORT

NASA CR-1209



NASA CR-1209

0060325

TECH LIBRARY KAFB, NM

LOAN COPY: RETURN TO  
AFWL (WLIL-2)  
KIRTLAND AFB, N MEX

ROLL AND YAW COMPENSATION  
FEASIBILITY STUDY

*by P. D. Fremming*

*Prepared by*

LING-TEMCO-VOUGHT CORPORATION

Dallas, Texas

*for Langley Research Center*

NATIONAL AERONAUTICS AND SPACE ADMINISTRATION • WASHINGTON, D. C. • JANUARY 1969



0060325

NASA CR-1209

## ROLL AND YAW COMPENSATION FEASIBILITY STUDY

By P. D. Fremming

Distribution of this report is provided in the interest of information exchange. Responsibility for the contents resides in the author or organization that prepared it.

Issued by Originator as Report No. 3-32000/7R-36

Prepared under Contract No. NAS 1-5592 by  
LING-TEMCO-VOUGHT CORPORATION  
Dallas, Texas

for Langley Research Center

NATIONAL AERONAUTICS AND SPACE ADMINISTRATION

---

For sale by the Clearinghouse for Federal Scientific and Technical Information  
Springfield, Virginia 22151 - CFSTI price \$3.00



## TABLE OF CONTENTS

	<u>Page No.</u>
LIST OF FIGURES . . . . .	v
LIST OF TABLES . . . . .	vi
LIST OF SYMBOLS . . . . .	vii
1.0 SUMMARY . . . . .	1
2.0 INTRODUCTION . . . . .	4
3.0 REQUIREMENTS . . . . .	6
4.0 DISCUSSION OF METHOD . . . . .	8
4.1 Servo Multiplier . . . . .	8
4.2 Logarithmic Multiplier . . . . .	9
4.3 Field Effect Transistor . . . . .	9
4.4 Quarter Square Multiplier . . . . .	12
4.5 Pre-Programmed Gain Changing Multiplier . . . . .	13
4.6 Magnetic Amplifier Multiplier . . . . .	14
5.0 SELECTION OF METHOD . . . . .	16
5.1 Stability and Control Analysis . . . . .	16
5.2 Simulation Results . . . . .	29
5.3 Circuit Analysis . . . . .	48
5.4 Reliability . . . . .	59
5.5 Trade Study . . . . .	60
5.6 Conclusion . . . . .	69
6.0 BREADBOARD RESULTS . . . . .	71
6.1 Circuit Changes . . . . .	71
6.2 Final Circuit . . . . .	74
6.3 Test Results . . . . .	76
6.4 Reliability . . . . .	88

TABLE OF CONTENTS (Continued)

		<u>Page No.</u>
7.0	CHECKOUT METHOD . . . . .	89
8.0	FINAL DESIGN . . . . .	95
	8.1 GSE Requirements . . . . .	95
	8.2 Package Design . . . . .	99
	8.3 Vehicle Changes . . . . .	99
9.0	CONCLUSIONS AND RECOMMENDATIONS . . . . .	103
10.0	REFERENCES . . . . .	104

## LIST OF FIGURES

<u>Figure Number</u>	<u>Title</u>	<u>Page No.</u>
1	Scout Control System Block Diagram With Roll And Yaw Compensation	5
2	Euler Angle Coordinate Transfer	18
3	Effect of Lower Stage Disturbance on Upper Stage Heading Errors	23
4	Analog Simulation Equations	30
5	Definitions	31
6	Analog Simulation Equations Third Stage Coast	32
7	Scout First Stage at $t = 30$ sec. Response to Sidewind	34
8	Scout First Stage at $t = 30$ sec. Response to Roll Moment	35
9	Scout Third Stage Coast Control Operation	37
10	Roll and Yaw Compensation Schematic	49
11	Simplified System Schematic	50
12	IGFET Demodulator	55
13	Typical Demodulator Characteristics	58
14	Reliability Block Diagram Unit No. I	67
15	Reliability Block Diagram Unit No. II	68
16	Control Electronics Schematic Final Circuit	75
17	Final Breadboard Gain Variation with Temperature	87
18	Acceptance Test Box, Schematic	96
19	Acceptance Test Set	97
20	Test Point Unit, Wiring Changes	98
21	Roll and Yaw Compensation Unit	100
22	Unit Installation	101
23	Wiring Mod	102

## LIST OF TABLES



<u>Number</u>	<u>Title</u>	<u>Page No.</u>
I	Values Used in Analog Study	33
II	Inclination Deviation Due to First Three Stages	46
III	Pre-Amplifier Electrical Characteristics	53
IV	Reliability Summary	60
V	Part Failure Rate Tabulation Unit I	61
VI	Part Failure Rate Tabulation Unit II	64
VII	Failure Rate Tabulation by Functional Component	66
VIII	Failure Rate Tabulation by Functional Component	66
IX	Comparison of Original and Revised Requirements	70
X	LTV Pre-Amplifier Characteristics	72
XI	Control Electronics Components	73
XII	Switching Transistor Characteristics	85

# LIST OF SYMBOLS


<u>Symbol</u>	<u>Parameter</u>	<u>Unit/s</u>
$\Theta$	pitch attitude	radians
$\Phi$	roll attitude	
$\Psi$	yaw attitude	
$\Theta_e$	pitch error	
$\Phi_e$	roll error	
$\Psi_e$	yaw error	radians
P	roll rate	radians/second
Q	pitch rate	
R	yaw rate	
$Q_C$	pitch rate command = $-g/v \cos \gamma$	
$Q_{CP}$	roll compensation gain	
$Q_{CR}$	yaw compensation gain	radians/second
$\alpha$	angle of attack	radians
$\beta$	sideslip	
$\gamma$	climb angle	
$\zeta$	heading	
$\delta$	control deflection	radians
d	reference length	feet
S	reference area	feet <sup>2</sup>
q	dynamic pressure	pounds/feet <sup>2</sup>
$I_X$	roll moment of inertia	slug-feet <sup>2</sup>
$I_Y$	yaw moment of inertia	slug-feet <sup>2</sup>
$I_{SP}$	boost specific impulse	seconds
m	vehicle mass	slugs
g	gravity	feet/second <sup>2</sup>
T	booster thrust	pounds



# LIST OF SYMBOLS (Continued)

<u>Symbol</u>	<u>Parameter</u>	<u>Unit/S</u>
$V$	axial velocity	feet/second
$l_v$	distance, C.G. to jet vane	feet
$l_E$	distance, C.G. to jet exit	feet
$r_v$	radius to jet vane	feet
$N_{\delta v}$	jet vane normal force effectiveness	
$K_{D\theta}$	pitch displacement gain	constant
$K_{D\phi}$	roll displacement gain	constant
$K_{D\psi}$	yaw displacement gain	constant
$K_{R\theta}$	pitch rate gain	seconds
$K_{R\phi}$	roll rate gain	
$K_{R\psi}$	yaw rate gain	
$T_\theta$	pitch servo time constant	
$T_\phi$	roll servo time constant	
$T_\psi$	yaw servo time constant	seconds
$\theta_{DB}$	pitch deadband	radians
$\phi_{DB}$	roll deadband	radians
$\psi_{DB}$	yaw deadband	radians
$C_{l\delta}$	fin tip roll control effectiveness	radians <sup>-1</sup>
$C_{lP}$	roll damping coefficient	
$C_{M\delta}$	fin tip pitch control effectiveness	
$C_{M\dot{Q}}$	pitch damping coefficient	
$C_{M\alpha}$	pitch static stability coefficient	
$C_{N\alpha}$	normal force slope	radians <sup>-1</sup>
$\theta$	pitch axis	notation only
$\phi$	roll axis	notation only
$\psi$	yaw axis	notation only

LIST OF SYMBOLS (Continued)

<u>Symbol</u>	<u>Parameter</u>	<u>Unit/S.</u>
UL	upper left jet	notation only
UR	upper right jet	
LL	lower left jet	
LR	lower right jet	
UP	upper pitch jet	
LP	lower pitch jet	
W	wind	
YPR	yaw-pitch-roll rotation order	
PYR	pitch-yaw-roll rotation order	
C	command	notation only

## 1.0

### SUMMARY

Analysis, computer simulation, circuit design, breadboard testing, preliminary packaging design, and preliminary vehicle and GSE design have been performed to show the feasibility of using roll and yaw compensation to reduce the inclination error of the Scout launch vehicle. The recommended circuit configuration, a discussion of the recommended checkout method and equipment, and a description of the installation requirements are included in this report.

From the analyses, it has been concluded that a pre-programmed type of multiplier is the only system currently known to have sufficient accuracy to meet the requirements of roll and yaw compensation. Analysis has shown that a gyro drift rate caused by the compensation unit of greater than 0.5 degrees per hour would degrade the inclination accuracy improvements realized by the addition of the roll and yaw compensation. Since a steady voltage across the gyro torquer produces a drift rate, it is concluded that the null uncertainty of the compensation unit must be less than 0.0002 volts to meet the drift requirements. Only the pre-programmed multiplier can meet this null requirement. This device achieves the required multiplication by changing the gain of the compensator as a function of the pitch program rate on command from the Intervalometer. The design has shown the feasibility of setting the compensation gains by the adjustment of potentiometers only and does not require the pre-wiring of jumpers and fixed resistors. This gain setting can be accomplished at the normal system calibration during performance of Standard Procedure 4-3-7.

Analysis has shown that a reduction in system complexity, size, weight, and cost can be achieved if the compensation is required to operate only for pitch down program rates. Since pitch up program rates have not previously occurred for orbital missions, the assumption of only pitch down rates is made. Also, in the event pitch up rates are required for orbital missions, the system can be de-energized such that no compensation occurs for the time of the pitch-up step. Further simplification is achieved by limiting the compensation to program rates of 0.06 to 4.0 degrees per second. The limited pitch rate range allows for the use of the potentiometers for gain adjustment and also is consistent with the maximum and minimum pitch rates expected during flight.

Digital computer simulation has shown that the inclination error is not reduced by roll compensation in the upper stages but is reduced by roll compensation in the first stage. This is caused by an induced roll error in the upper stages which tends to pull the velocity vector back towards nominal and compensates for the error without roll compensation. With roll compensation, no induced roll error exists in the upper stages and therefore the inclination error is not inherently compensated. The following three sigma inclination errors have resulted from the simulation:

	<u>Without Roll/Yaw Compensation</u>	<u>With Roll/Yaw Compensation</u>	<u>With Roll Comp. 1st stage only, Yaw Comp. 1st, 2nd, and 3rd</u>	<u>With Roll/Yaw Compensation first stage only</u>
3 $\sigma$ *	$\pm .799$	$\pm .318$	$\pm .276$	$\pm .322$

\* Does not include Fourth Stage tip-off.

The circuit configuration can be packaged utilizing printed circuit boards in a 3.5 x 5.25 x 2 inch assembly weighing 1.96 pounds. An additional 0.5 pound is required for installation hardware and wiring. The

package would be installed in the vehicle lower "D" section. The analysis indicates that the roll and yaw compensation can be tested at the vehicle and bench system level using existing Scout ground support equipment. It is further determined that the only new GSE required is a test box and a test cable to be used with existing standard laboratory equipment for acceptance testing of the roll and yaw compensation unit. Modification must be made to the existing Guidance Test Point Unit accumulation for bench system testing.

It is concluded that this study and the breadboard evaluation has shown the feasibility of producing hardware which will improve the orbital inclination accuracy of the Scout launch vehicle, and it is recommended that flight hardware be developed and incorporated in the Scout vehicle.

Studies of methods of improving the orbital inclination accuracy of the Scout launch vehicle have indicated that crosswind and thrust misalignment are the predominant sources of error in the lower stages of the vehicle. These sources produce a yaw displacement error which, in the presence of a pitch rate, causes a roll displacement error that is not sensed by the guidance system. This error can be reduced by the addition of Roll Compensation, i.e., by torquing the Roll Miniature Integrating Gyro (MIG) as a function of the product of the yaw displacement error and the commanded pitch rate. In a similar manner a roll displacement error in the presence of a pitch rate causes a yaw displacement error. This error can be reduced by the addition of Yaw Compensation, i.e., by torquing the Yaw Miniature Integrating Gyro as a function of the product of the roll displacement error and the commanded pitch rate. Computer simulation has shown that significant improvements in the orbital inclination error caused by the lower stages can be achieved by implementation of roll and yaw compensation. A block diagram showing the addition of roll and yaw compensation to the existing Scout guidance system is shown in figure 1.

The following sections are presented to show the feasibility of producing hardware for the addition of roll and yaw compensation to the Scout launch vehicle.

SCOUT CONTROL SYSTEM BLOCK  
DIAGRAM WITH ROLL AND YAW  
COMPENSATION

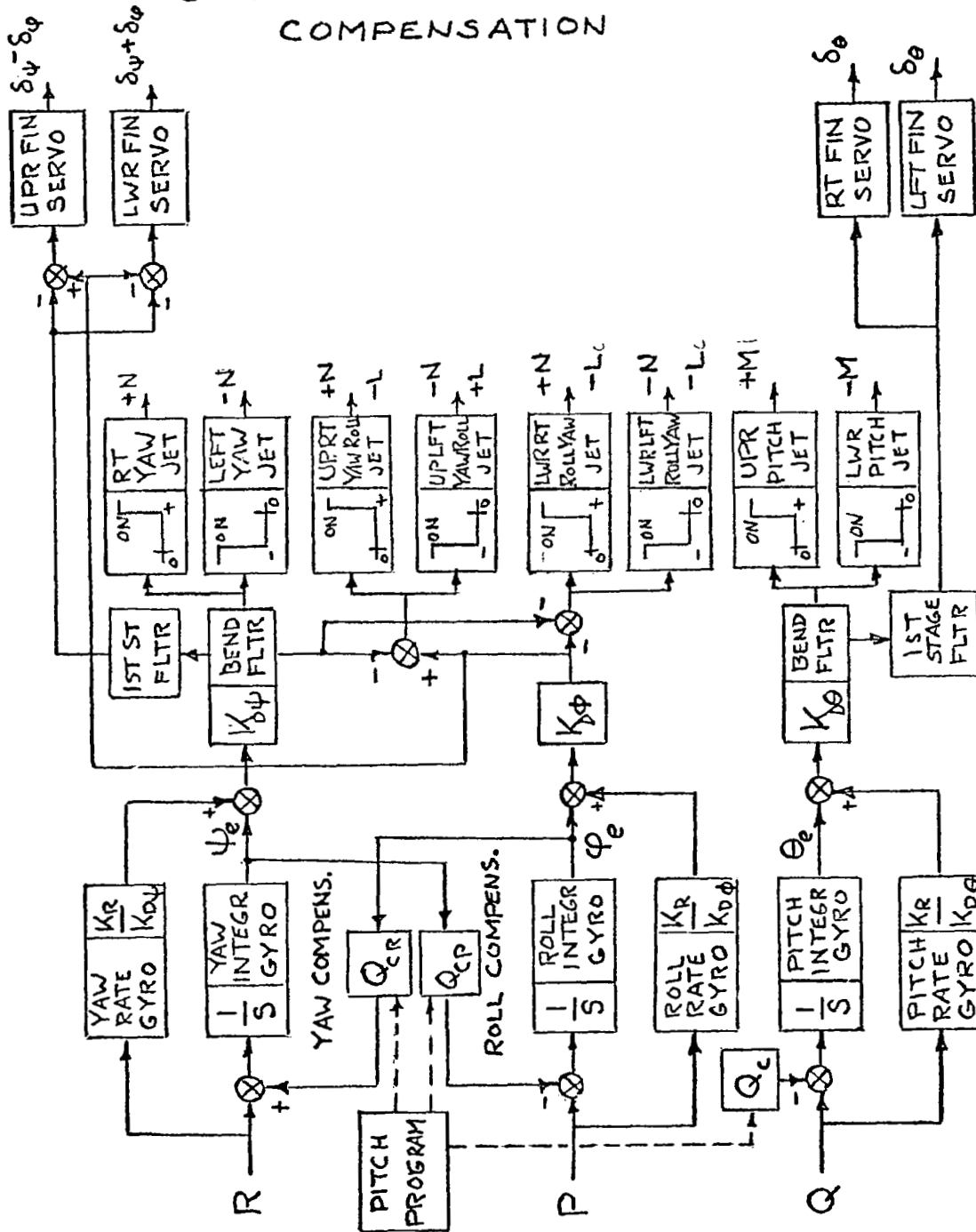
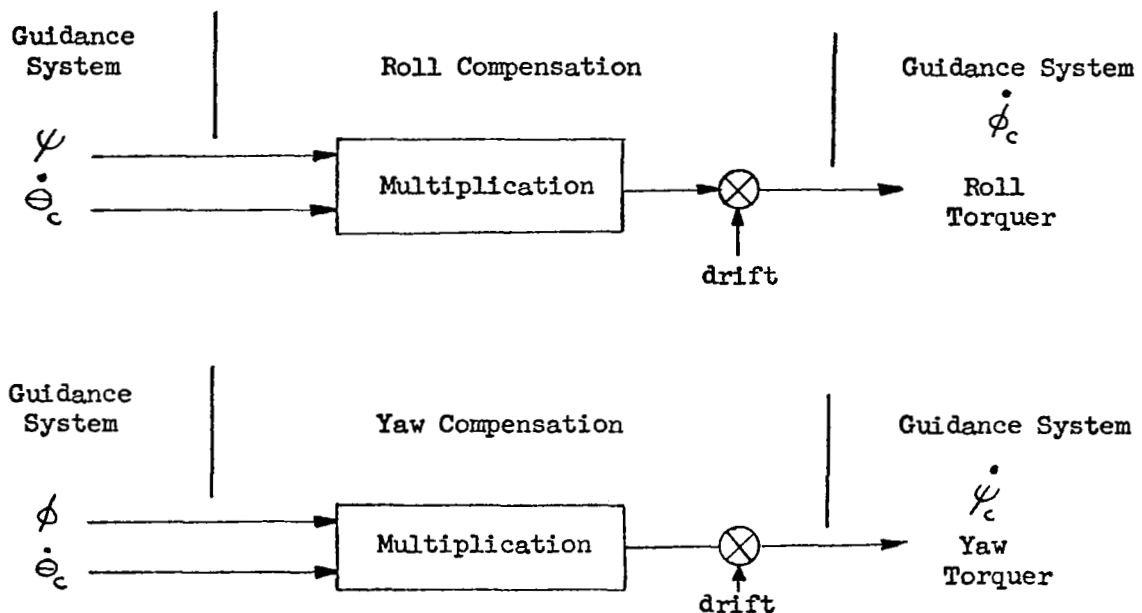


FIGURE 1

## 3.0

REQUIREMENTS

The initial requirements and design constraints for Yaw/Roll Compensation are as follows:



where:  $\psi = 0$  to  $10^\circ$  (0 to .1745 RAD) maximum Yaw displacement  
 $\phi = 0$  to  $10^\circ$  (0 to .1745 RAD) maximum Roll displacement  
 $\dot{\theta}_c = 0.03$  to  $10^\circ/\text{sec}$  pitch program rate (Programmer Capability)  
 $\dot{\phi}_c = \dot{\psi}_c = 0$  to  $1.745^\circ/\text{sec}$  maximum roll and yaw torquing rates  
 $\text{drift} = 0$  to  $.5^\circ/\text{hour}$  maximum  
 $\psi \times \dot{\theta}_c$  and  $\phi \times \dot{\theta}_c$  tolerance at  $\pm 5\%$

Additional requirements include: the capability of compensating for both pitch down and pitch up program commands; a packaged volume no greater than 30 cu. in.; a weight no greater than 2 pounds; and a 28 volt battery power drain no greater than .1 ampere hour. The selection of the method of Yaw/Roll Compensation is to be based on the following:



1. Complexity
2. Accuracy
3. Reliability
4. Pre-Flight Preparation
5. Power Requirements
6. Size and Weight
7. Cost

#### 4.0

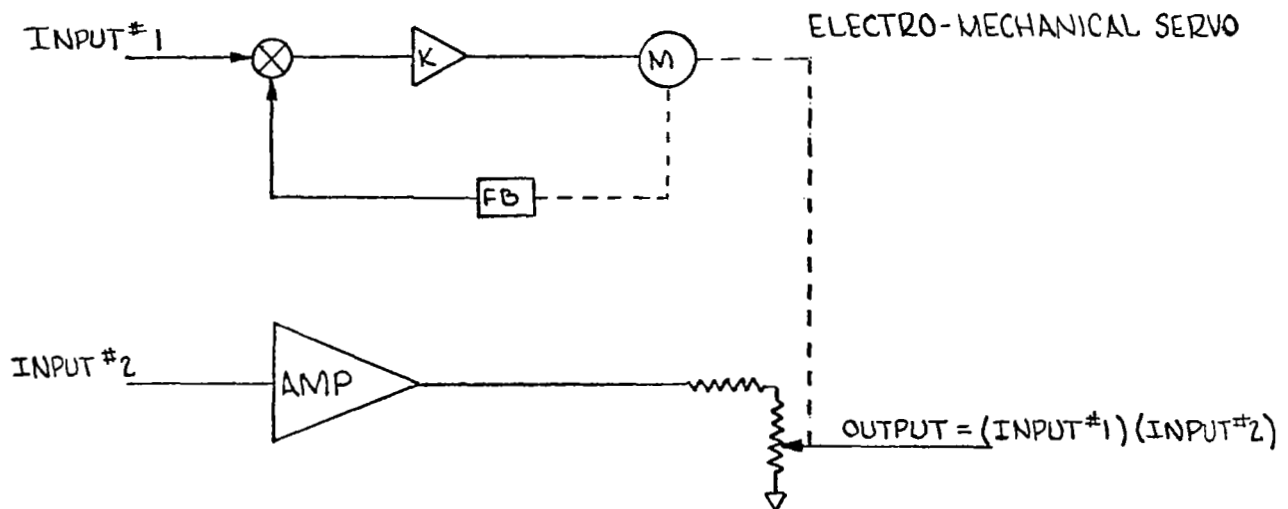
#### DISCUSSION OF METHODS

Numerous methods are available for the multiplication of two signals. However, most of them can be logically eliminated based on the requirements given for Yaw/Roll Compensation. The methods considered and a discussion of each are as follows:

#### 4.1

#### Servo Multiplier

The output of any basic amplifier stage is the product of the input and the gain of that amplifier. Therefore, if the gain of an amplifier is varied as the function of a signal level, the output of the amplifier will be the product of that signal and the amplifier input signal. One method of achieving this gain variation is by driving a potentiometer with an electro-mechanical servo:



Input #1 positions the potentiometer which varies the gain between the output and input #2. Two obvious disadvantages to this method are size and weight since the motors, tachometers, gear trains, etc. are large and heavy compared with electronic components. Also, calculations show a

required change in gain of approximately 300 to 1. Using the potentiometer in series with the output torquer (Roll or Yaw), a 300 to 1 change in resistance would result in inaccuracies especially at low resistances due to the resolution of the potentiometer. A possible solution would be to switch in smaller potentiometers as a function of the input level such that several potentiometers in series would result in the required resistance range. The increased complexity of this switching logic would further add to the disadvantages previously discussed.

#### 4.2 Logarithmic Multiplier

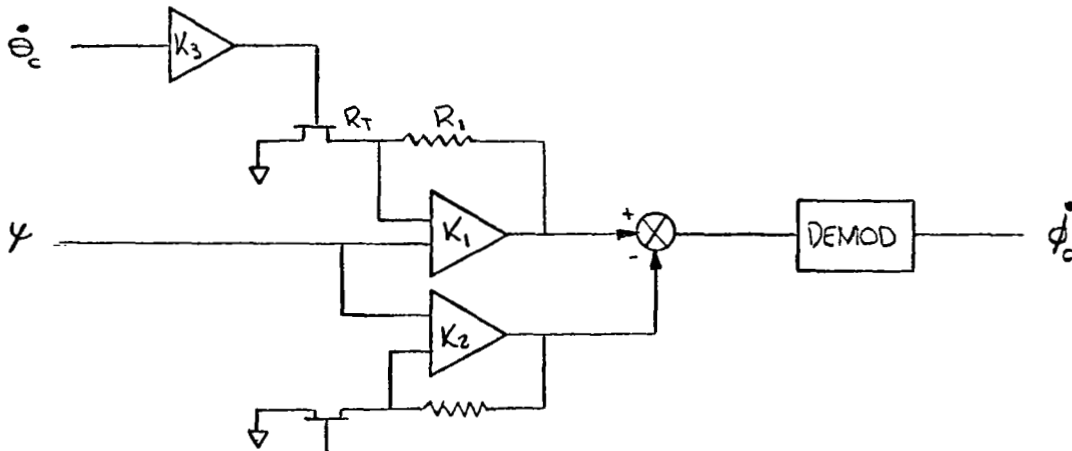
Since the antilog of the sum of the logarithms of two numbers is equal to the product of those numbers, the logarithmic circuit can be used for multiplier applications. The logarithmic circuit, usually a diode resistor network, has inherently high drift due to temperature change. A typical value is 10 mv/°C. Therefore, a 46°C temperature change (25°C to 71°C, Scout maximum temperature requirement) would result in a 460 mv drift or an equivalent torquing rate of approximately 0.6°/sec. Obviously this is unacceptable because an error in excess of 100% would result for certain torquing rates.

#### 4.3 Field Effect Transistor Multiplier

The FET device displays a variable resistance as a function of the gate voltage level. This characteristic can be used in a manner similar to the electro-mechanical servo to provide the multiplication of two signals. Examination of typical characteristic curves for FET's shows two linear resistances regions:



A block diagram for implementing the FET multiplier is shown below:



The gain,  $K_1$ , is equal to  $1 + R_T/R_1$  and can never be less than 1. This configuration allows for a linear gain change with variation of the FET resistance  $R_T$ . Also, the feedback amplifier configuration supplies a nearly constant current through the FET. This is important since the characteristic curve of the FET will vary with current. Since the FET resistance does not decrease to zero and due to the feedback amplifier configuration, the gain  $K_1$  will not be zero for a zero program command. A compensating circuit  $K_2$

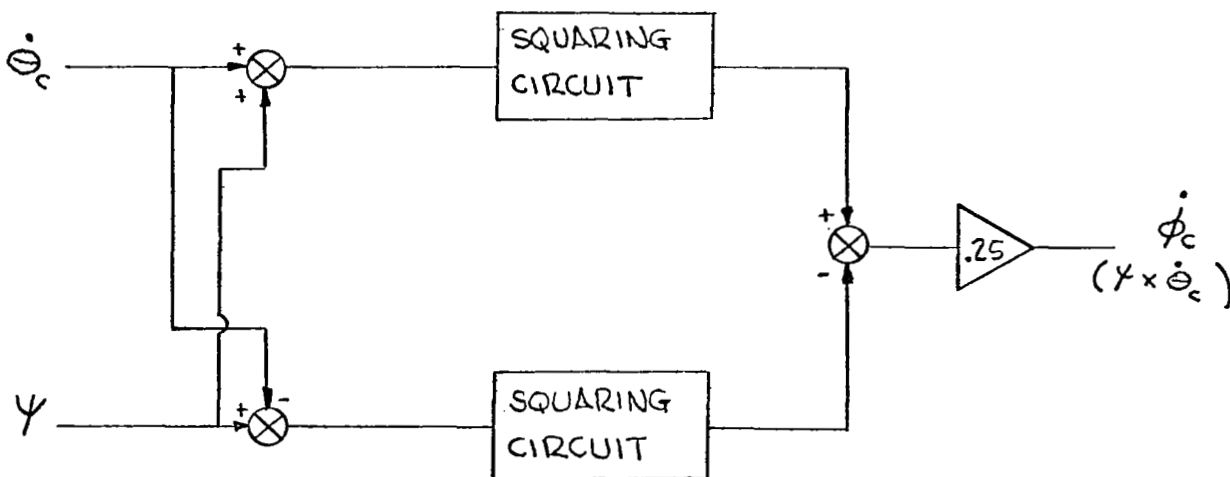
equal to the minimum value of  $K_1$ , is added to provide a zero gain at zero program command. The FET in the compensating circuit also corrects for variations in the characteristic curve due to temperature change. The FET multiplier appears to be more accurate and less complex than any multiplier currently available. However, examination of the typical FET characteristic curve indicates one linear region of a small resistance change with a large variation in gate voltage. A second linear region has a large resistance change with a very small variation in gate voltage. Typical values for resistance variation are 25 to 50 ohms from 0 to 2 volts and 1000 to 100,000 ohms from 3.6 to 3.8 volts. One region would result in a very small gain change for a large input variation while the other region would result in a large gain change for a very small variation in input voltage. Obviously any attempt to increase the gain range or the input signal range would result in additional circuitry such as amplifiers, bias level circuitry, and temperature compensation circuitry. It is felt that the additional circuitry required makes the FET multiplier undesirable from the standpoint of complexity as well as accuracy. For example, if the 3.6 to 3.8 volt signal level is biased to 0 to 0.2 volts (negative 3.6 bias level), as little as  $\pm 1\%$  variation in the -3.6 volt bias would result in a  $\pm 18\%$  shift in the 0 to 0.2 volt signal level. Therefore it is concluded that attempts to correct for the small linear region of resistance change in the FET would result in an unsatisfactory system in terms of complexity, accuracy and reliability. However, should future developments result in increasing the linear resistance range of the FET's, it is felt that the FET multiplier would ultimately be superior to any of those currently studied.

#### 4.4 Quarter Square Multiplier

Analog computers often use the following expression to implement the multiplication of two variables:

$$\frac{1}{4} [(X+Y)^2 - (X-Y)^2]$$

Simplifying the above expression yields the multiplication of the variables  $X$  and  $Y$  ( $X \cdot Y$ ). The quarter square expression can be implemented electronically by the following block diagram.

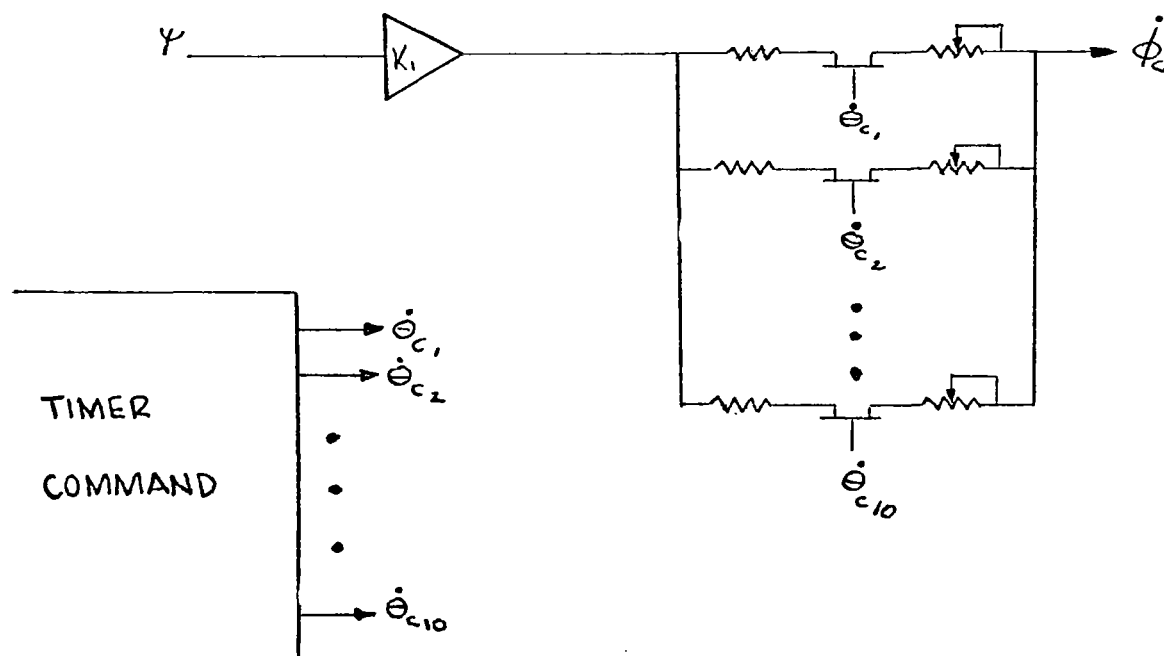


The squaring circuit is the critical element in terms of accuracy and drift. Usually a resistor diode network or a transistor circuit, the squaring element is subject to parameter change due to temperature, operating current, and manufacturing processes. A typical value for accuracy is  $\pm 1\%$  of full scale output. For a full scale output of 1.745 degrees per second, the accuracy of the multiplier is  $\pm 0.01745$  degrees per second for any output

level. For system operation near the full scale output, this accuracy is adequate. However, it is probable that the system will be operating most of the time below 0.01745 degrees per second compensation rate. In this case the error of the quarter square multiplier will be greater than  $\pm 100\%$ . Although the quarter square multiplier results in a relatively simple circuit, it is concluded that it cannot provide adequate accuracy for Yaw/Roll Compensation.

#### 4.5 Pre-Programmed Gain Changing Multiplier

Changing the gain of an amplifier to provide a multiplication can be accomplished by switching fixed resistors at a predetermined time. Switching commands available at the Scout Intervalometer connect the Programmer power supply voltage (approximately 13.5 volts) to each Programmer channel. This command can be used to switch fixed resistors in the Yaw and Roll Compensation circuits to provide an accurate multiplication at each program rate.

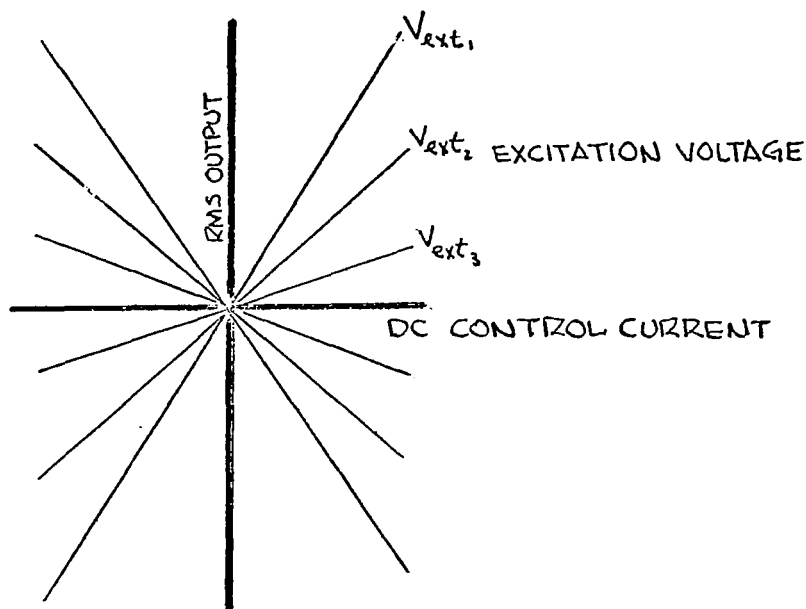


This method of multiplication can be extremely accurate since the major source of error is the resistor tolerances. The FET in this application is used as a switch providing a few hundred ohms when closed and several megohms when open. The potentiometer is provided for fine adjustment of the gain and to correct for any variations in the FET saturation resistance. For a low demodulator drift, the accuracy of the total system will be dependent on the resistor and potentiometer tolerances. This accuracy could be less than  $\pm 5\%$  if required. The major disadvantage to this method is the requirement of pre-flight adjustment of the compensation circuit. However, in terms of accuracy, complexity and size, it is concluded that this method is adequate for Yaw and Roll Compensation and therefore a detailed design of this method is included in section 5. An alternate to this method would be the use of existing relay contacts within the intervalometer. However, since this would require an additional connector and internal wiring modifications to the intervalometer, the use of the FET's for switching is considered superior.

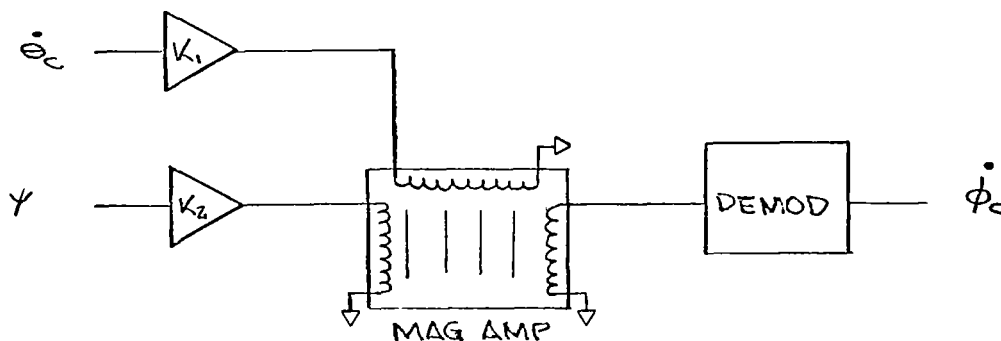
#### 4.6 Magnetic Amplifier Multiplier

Magnetic amplifiers are available that have a linear input-output relationship which varies linearly with excitation voltage. Therefore, using the excitation as a signal input, the magnetic amplifier can be used as a multiplier. A typical characteristic of the multiplying magnetic amplifier is shown.





Since the magnetic amplifier provides multiplication in four quadrants, the total system is relatively simple.



The amplifiers  $K_1$  and  $K_2$  are primarily required for impedance matching. Complexity and a minimum of pre-flight preparation are the major advantages to this system since the multiplication is proportional and operates in all four quadrants. However, hysteresis inherent in magnetic core material causes uncertainties in the output null. Since any output null is reflected on the gyro torquer as a drift, the output null must be held to a minimum. Calculations show that as little as 0.001 volts across the torquer produces a gyro drift rate of 1.35 degrees per hour. Analysis of available magnetic multipliers shows the best units to have an accuracy of 1% of the full scale output for a full scale of 2 volts or a null uncertainty of 0.02 volts. Since a null uncertainty of this magnitude would cause an excessive drift rate and since the null uncertainty is inherent with the magnetic core material, it is concluded that the magnetic multiplier is unacceptable for Yaw and Roll Compensation.

## 5.0

### SELECTION OF METHOD

In surveying the methods of electronic multiplication, it is concluded that only the pre-programmed gain changing multiplier meets the requirements of Yaw and Roll Compensation. Therefore a detailed trade study to determine the selection of the method is not required. However, during the performance of design and analysis of the multiplier, it has become evident that improvements in system complexity, reliability, size, and weight can be realized if certain of the system requirements are revised. For example, system complexity can be reduced if the Yaw and Roll Compensation is required to perform only for pitch down program commands. Also, if the range of pitch program steps is reduced from the required 0.03 to 10 degrees per second the complexity of Yaw and Roll Compensation can be improved. Obviously, any improvement in complexity will be reflected in improvements in reliability, size, and weight. Therefore a trade study is conducted in the following paragraphs to determine the improvements in system complexity by reducing the requirements of Yaw and Roll Compensation.

### 5.1 Stability and Control Analysis

#### 5.1.1 Analytical Derivations

To provide a better understanding of the vehicle attitude response and resulting flight path errors, the equations of motion were manipulated algebraically to provide various useful closed form expressions. Using the definitions of the body inertial orientation Euler angles in the pitch-yaw-roll sequence and the attitude errors sensed by the control system displacement gyros, an integral expression for the roll ( $\phi$ ) and yaw ( $\psi$ ), attitudes in terms of the history of roll ( $\phi_e$ ) and Yaw ( $\psi_e$ ) errors vs. pitch attitude ( $\theta$ ) was derived, as shown in equations (1) through (9)

of paragraph 5.1.1.1. The part of the Euler angle response not attributable to the instantaneous gyro error is directly proportional to the difference between the actual pitch rate (  $Q$  ) and the roll or yaw compensation gain pitch rate (  $Q_{CP}$  or  $Q_{CQ}$  ). The effect of compensation gain is therefore linear and complete compensation corresponds to the case where roll and yaw Euler angles are equal to roll and yaw gyro errors. When the gyro errors are set at zero, the roll and yaw Euler angles at one pitch attitude propagate to the values at another pitch attitude according to equations (14), which were derived from equations (9).

In equations (9) the uncompensated error in Euler angles for a small pitch attitude change becomes:

$$\Delta \phi = \int \psi_e d\theta \quad ; \quad \Delta \psi = \int \phi_e d\theta$$

The sinusoidal variation of  $\Delta \phi$  and  $\Delta \psi$  with  $\theta$  in equations (14) is also equivalent to representing  $\phi = \frac{d\psi}{d\theta}$  and  $\psi = \frac{d\phi}{d\theta}$ . The attitude response of the vehicle may be described in a plot of  $\psi$  vs.  $\theta$ , or the trace made on the surface of a sphere by the nose of the vehicle in response to roll and yaw disturbances during a commanded pitch rate. The geometry involved is illustrated in Figure 2. An initial roll angle becomes a yaw angle and an initial yaw angle becomes a roll angle after 90 degrees of pitch as seen in this diagram.

EULER ANGLE COORDINATE TRANSFER:  
 CONVENTIONAL YAW PITCH ROLL YPR SYSTEM  
 USED IN DIGITAL SIMULATION  
 TO PITCH YAW ROLL PYR SYSTEM USED IN  
 ANALYSIS AND ANALOG SIMULATION

$$\sin \theta_{PYR} \cos \psi_{PYR} = \sin \theta_{YPR}$$

$$\sin \psi_{PYR} = \sin \psi_{YPR} \cos \theta_{YPR}$$

$$\sin \phi_{PYR} \cos \psi_{PYR} = \sin \phi_{YPR} \cos \psi_{YPR} - \cos \phi_{YPR} \sin \psi_{YPR} \sin \theta_{YPR}$$

APPROXIMATELY:

$$\theta_{PYR} = \theta_{YPR}$$

$$\psi_{PYR} = \psi_{YPR} \cos \theta$$

$$\phi_{PYR} = \phi_{YPR} - \psi_{YPR} \sin \theta$$

OR:

$$\psi_{YPR} = \psi_{PYR} / \cos \theta$$

$$\phi_{YPR} = \phi_{PYR} + \psi_{PYR} \tan \theta$$

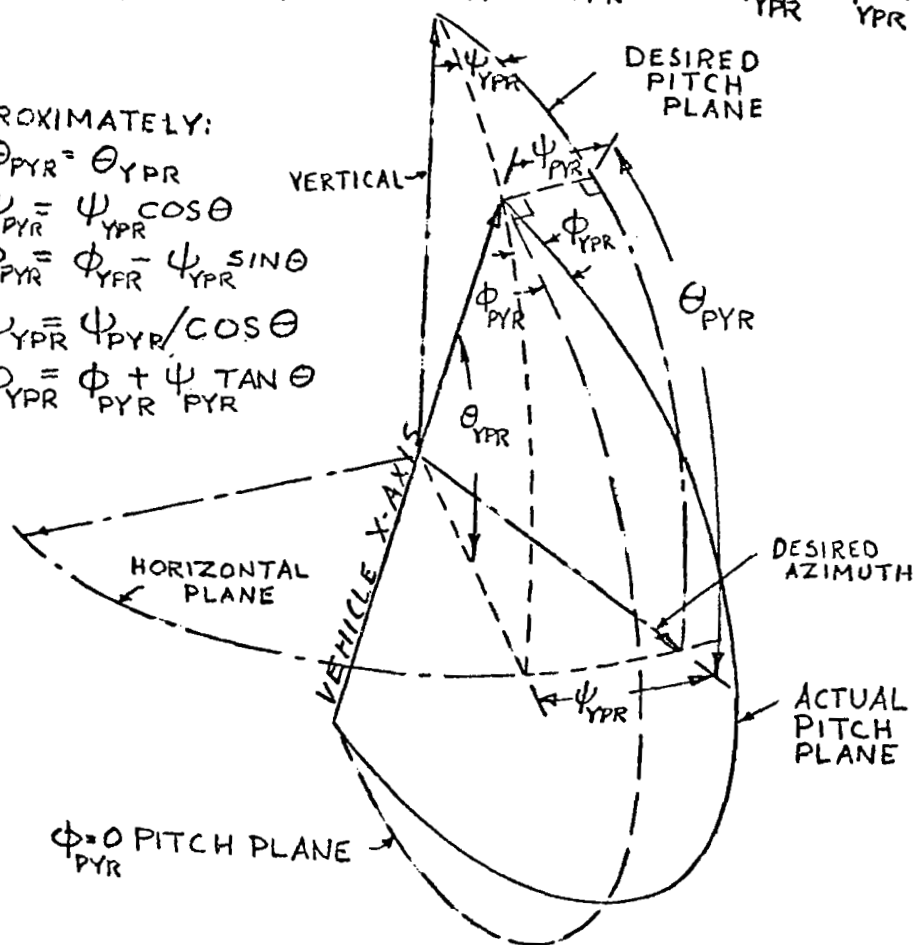


FIGURE 2

### 5.1.1.1. EULER ANGLE $\Phi, \Psi$ RESPONSE TO CONTROL ERROR $\Phi_e, \Psi_e$

EULER ANGLE RATES IN P, Y, R SYSTEM :

$$\begin{aligned}\dot{\Phi} &= P - Q \Psi \\ \dot{\Psi} &= R + Q \Phi\end{aligned}\quad \left. \vphantom{\begin{aligned}\dot{\Phi} &= P - Q \Psi \\ \dot{\Psi} &= R + Q \Phi\end{aligned}} \right\} (1)$$

DISPLACEMENT GYRO ERROR RATES :

$$\begin{aligned}\dot{\Phi}_e &= P - Q_{cp} \Psi_e \\ \dot{\Psi}_e &= R + Q_{cr} \Phi_e\end{aligned}\quad \left. \vphantom{\begin{aligned}\dot{\Phi}_e &= P - Q_{cp} \Psi_e \\ \dot{\Psi}_e &= R + Q_{cr} \Phi_e\end{aligned}} \right\} (2)$$

$$\begin{aligned}\dot{\Phi} &= \dot{\Phi}_e + Q_{cp} \Psi_e - Q \Psi \\ \dot{\Psi} &= \dot{\Psi}_e - Q_{cr} \Phi_e + Q \Phi\end{aligned}\quad \left. \vphantom{\begin{aligned}\dot{\Phi} &= \dot{\Phi}_e + Q_{cp} \Psi_e - Q \Psi \\ \dot{\Psi} &= \dot{\Psi}_e - Q_{cr} \Phi_e + Q \Phi\end{aligned}} \right\} (3)$$

$$\text{IF } \frac{du}{dt} = \frac{du}{d\theta} \frac{d\theta}{dt} = Q \frac{du}{d\theta}$$

$$\begin{aligned}\frac{d\Phi}{d\theta} &= \frac{d\Phi_e}{d\theta} + \frac{Q_{cp}}{Q} \Psi_e - \Psi \\ \frac{d\Psi}{d\theta} &= \frac{d\Psi_e}{d\theta} - \frac{Q_{cr}}{Q} \Phi_e + \Phi\end{aligned}\quad \left. \vphantom{\begin{aligned}\frac{d\Phi}{d\theta} &= \frac{d\Phi_e}{d\theta} + \frac{Q_{cp}}{Q} \Psi_e - \Psi \\ \frac{d\Psi}{d\theta} &= \frac{d\Psi_e}{d\theta} - \frac{Q_{cr}}{Q} \Phi_e + \Phi\end{aligned}} \right\} (4)$$

IF  $S = \frac{d}{d\theta}$  , THE LAPLACE OPERATOR,

$$\begin{aligned}(S^2 + 1)\Phi &= \left(S^2 + \frac{Q_{cr}}{Q}\right) \Phi_e - \left(1 - \frac{Q_{cp}}{Q}\right) S \Psi_e \\ (S^2 + 1)\Psi &= \left(S^2 + \frac{Q_{cp}}{Q}\right) \Psi_e + \left(1 - \frac{Q_{cr}}{Q}\right) S \Phi_e\end{aligned}\quad \left. \vphantom{\begin{aligned}(S^2 + 1)\Phi &= \left(S^2 + \frac{Q_{cr}}{Q}\right) \Phi_e - \left(1 - \frac{Q_{cp}}{Q}\right) S \Psi_e \\ (S^2 + 1)\Psi &= \left(S^2 + \frac{Q_{cp}}{Q}\right) \Psi_e + \left(1 - \frac{Q_{cr}}{Q}\right) S \Phi_e\end{aligned}} \right\} (5)$$

$$\left. \begin{aligned} \Phi_{i,o}(s) &= \frac{s^2}{s^2+1} \Phi_e(s) + \frac{1}{s^2+1} \frac{Q_{cr}}{Q} \Phi_e(s) - \left(1 - \frac{Q_{cp}}{Q}\right) \frac{s}{s^2+1} \Psi_e(s) \\ \Psi_{i,o}(s) &= \frac{s^2}{s^2+1} \Psi_e(s) + \frac{1}{s^2+1} \frac{Q_{cp}}{Q} \Psi_e(s) + \left(1 - \frac{Q_{cr}}{Q}\right) \frac{s}{s^2+1} \Phi_e(s) \end{aligned} \right\} (6)$$

TAKING THE INVERSE LAPLACE TRANSFORMS

$$\left. \begin{aligned} \mathcal{L}^{-1} \frac{1}{s^2+1} \frac{1}{s} &= 1 - \cos \Theta & (= U - U \cos \Theta) \\ \mathcal{L}^{-1} \frac{1}{s^2+1} &= \sin \Theta & (= U_0 - U_0 \cos \Theta + U \sin \Theta) \\ \mathcal{L}^{-1} \frac{s}{s^2+1} &= \cos \Theta & (= U_0 \sin \Theta + U \cos \Theta) \\ \mathcal{L}^{-1} \frac{s^2}{s^2+1} &= U_0 - \sin \Theta & (= U_0 \cos \Theta - U \sin \Theta) \end{aligned} \right\} (7)$$

(U = UNIT STEP AT t=0, U<sub>0</sub> = UNIT IMPULSE AT t=0)

RESPONSE AT TIME t, DUE TO AN IMPULSE

$\Phi_{e_0} dt$  OR  $\Psi_{e_0} dt$  AT TIME t<sub>0</sub> IS

$$\left. \begin{aligned} d\Phi_{i,o}(\Theta) &= \left[ U_0 \Phi_{e_0} - \left(1 - \frac{Q_{cr}}{Q}\right) \Phi_{e_0} \sin \Theta_{i,o} - \left(1 - \frac{Q_{cp}}{Q}\right) \Psi_{e_0} \cos \Theta_{i,o} \right] d\Theta \\ d\Psi_{i,o}(\Theta) &= \left[ U_0 \Psi_{e_0} - \left(1 - \frac{Q_{cp}}{Q}\right) \Psi_{e_0} \sin \Theta_{i,o} + \left(1 - \frac{Q_{cr}}{Q}\right) \Phi_{e_0} \cos \Theta_{i,o} \right] d\Theta \end{aligned} \right\} (8)$$

BUILDING UP THE  $\Phi_e$  AND  $\Psi_e$  TIME HISTORIES AS A SEQUENCE OF IMPULSES BETWEEN t<sub>0</sub> AND t, THE  $\Phi$  AND  $\Psi$  RESPONSE WILL BE :

$$\left. \begin{aligned} \Phi_{i,o}(\Theta) &= \Phi_{e_i} - \int_0^1 \left[ \left(1 - \frac{Q_{cr}}{Q}\right) \Phi_{e_i} \sin \Theta_{i,i} + \left(1 - \frac{Q_{cp}}{Q}\right) \Psi_{e_i} \cos \Theta_{i,i} \right] d\Theta_i \\ \Psi_{i,o}(\Theta) &= \Psi_{e_i} - \int_0^1 \left[ \left(1 - \frac{Q_{cp}}{Q}\right) \Psi_{e_i} \sin \Theta_{i,i} - \left(1 - \frac{Q_{cr}}{Q}\right) \Phi_{e_i} \cos \Theta_{i,i} \right] d\Theta_i \end{aligned} \right\} (9)$$

PROPAGATION OF ERROR ACCUMULATED AT  $t_1$  TO  $t_2$

WHERE  $\Phi_e = \Psi_e = 0$  FROM  $t_1$  TO  $t_2$

$$\begin{aligned} \sin \theta_{2,i} &= \sin(\theta_{1,i} + \theta_{2,1}) = \sin \theta_{1,i} \cos \theta_{2,1} + \cos \theta_{1,i} \sin \theta_{2,1} \\ \cos \theta_{2,i} &= \cos(\theta_{1,i} + \theta_{2,1}) = \cos \theta_{1,i} \cos \theta_{2,1} - \sin \theta_{1,i} \sin \theta_{2,1} \end{aligned} \quad \left. \vphantom{\begin{aligned} \sin \theta_{2,i} &= \sin(\theta_{1,i} + \theta_{2,1}) \\ \cos \theta_{2,i} &= \cos(\theta_{1,i} + \theta_{2,1}) \end{aligned}} \right\} (10)$$

$$\begin{aligned} \Phi_{2,0} &= \int_0^2 (a \sin \theta_{2,i} + b \cos \theta_{2,i}) d\theta_i \\ \Psi_{2,0} &= \int_0^2 (b \sin \theta_{2,i} - a \cos \theta_{2,i}) d\theta_i \end{aligned} \quad \left. \vphantom{\begin{aligned} \Phi_{2,0} &= \int_0^2 (a \sin \theta_{2,i} + b \cos \theta_{2,i}) d\theta_i \\ \Psi_{2,0} &= \int_0^2 (b \sin \theta_{2,i} - a \cos \theta_{2,i}) d\theta_i \end{aligned}} \right\} (11)$$

$$\begin{aligned} \Phi_{2,0} &= \int_0^2 (a \sin \theta_{1,i} + b \cos \theta_{1,i}) \cos \theta_{2,1} d\theta_i \\ &\quad + \int_0^2 (a \cos \theta_{1,i} - b \sin \theta_{1,i}) \sin \theta_{2,1} d\theta_i \\ \Psi_{2,0} &= \int_0^2 (b \sin \theta_{1,i} - a \cos \theta_{1,i}) \cos \theta_{2,1} d\theta_i \\ &\quad + \int_0^2 (b \cos \theta_{1,i} + a \sin \theta_{1,i}) \sin \theta_{2,1} d\theta_i \end{aligned} \quad \left. \vphantom{\begin{aligned} \Phi_{2,0} &= \int_0^2 (a \sin \theta_{1,i} + b \cos \theta_{1,i}) \cos \theta_{2,1} d\theta_i \\ &\quad + \int_0^2 (a \cos \theta_{1,i} - b \sin \theta_{1,i}) \sin \theta_{2,1} d\theta_i \\ \Psi_{2,0} &= \int_0^2 (b \sin \theta_{1,i} - a \cos \theta_{1,i}) \cos \theta_{2,1} d\theta_i \\ &\quad + \int_0^2 (b \cos \theta_{1,i} + a \sin \theta_{1,i}) \sin \theta_{2,1} d\theta_i \end{aligned}} \right\} (12)$$

BUT

$$\begin{aligned} \Phi_1 &= \int_0^1 (a \sin \theta_{1,i} + b \cos \theta_{1,i}) d\theta_i \\ \Psi_1 &= \int_0^1 (b \sin \theta_{1,i} - a \cos \theta_{1,i}) d\theta_i \end{aligned} \quad \left. \vphantom{\begin{aligned} \Phi_1 &= \int_0^1 (a \sin \theta_{1,i} + b \cos \theta_{1,i}) d\theta_i \\ \Psi_1 &= \int_0^1 (b \sin \theta_{1,i} - a \cos \theta_{1,i}) d\theta_i \end{aligned}} \right\} (13)$$

THEREFORE SINCE  $a = b = 0$  WHEN  $t_i > t_1$

$$\begin{aligned} \Phi_2 &= \Phi_1 \cos \theta_{2,1} - \Psi_1 \sin \theta_{2,1} \\ \Psi_2 &= \Psi_1 \cos \theta_{2,1} + \Phi_1 \sin \theta_{2,1} \end{aligned} \quad \left. \vphantom{\begin{aligned} \Phi_2 &= \Phi_1 \cos \theta_{2,1} - \Psi_1 \sin \theta_{2,1} \\ \Psi_2 &= \Psi_1 \cos \theta_{2,1} + \Phi_1 \sin \theta_{2,1} \end{aligned}} \right\} (14)$$

### 5.1.2 Behavior Predicted From Analytical Expressions

The behavior observed in digital solution of the complete vehicle equations of motion may be predicted from the simplified concepts presented previously. When a yawing moment is applied, the vehicle seeks an equilibrium yaw gyro error, as shown in Figure 3b. If this error is held as the vehicle pitches through a given increment, a roll angle will build up (equation 9) along with a small decrease in yaw angle. When the yawing moment is removed the constant gyro error will be removed, leaving the vehicle with a roll Euler angle and a slight yaw angle in opposition to the initial yaw angle as shown in Figure 3b. Further pitch occurs in a skewed plane, causing the yaw angle to increase in the direction opposing the initial error.

In the presence of a roll error caused by a rolling moment, the yaw Euler angle error builds up due to pitch rate applied in a skewed plane. When the rolling moment and roll error are removed, the pitch plane is reoriented such that further pitch occurs at a yaw Euler angle which remains fairly constant at the value existing at roll moment removal.

The vehicle thrust vector is pointed by the attitude motions previously described. A component of velocity,  $\dot{V} \Delta t \Delta \psi_{p,y,r}$  is built up normal to the desired pitch plane whenever longitudinal acceleration occurs with a yaw Euler angle error  $\Delta \psi_{p,y,r}$  for a length of time  $\Delta t$ . During any time interval the vehicle velocity increment  $\Delta V$  and an increment in pitch angle  $\Delta \Theta_c$  will be commanded by the pitch programmer. The velocity vector diagrams corresponding to the yaw Euler angle variation with pitch angle will then appear as shown in Figure 3a.



# EFFECT OF LOWER STAGE DISTURBANCE ON UPPER STAGE HEADING ERRORS

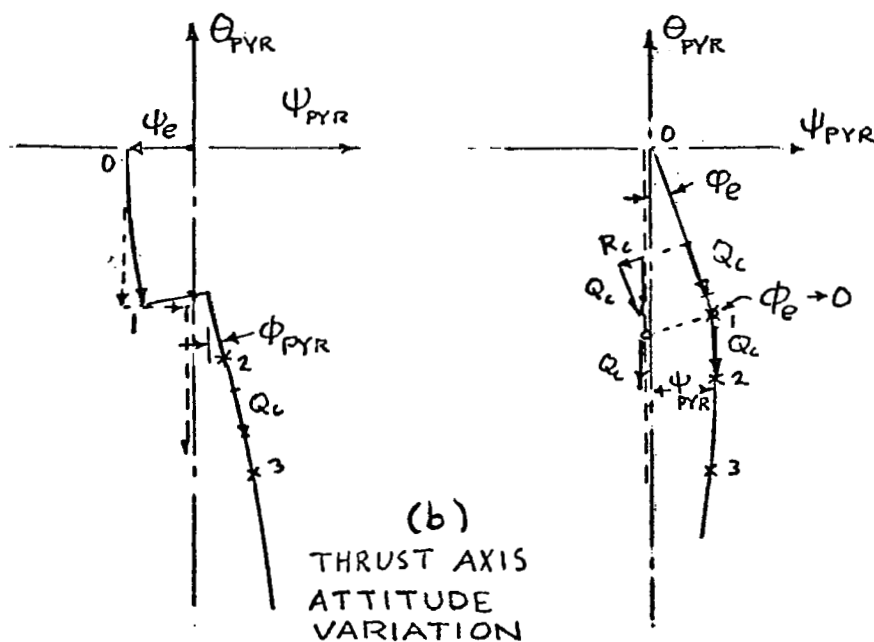
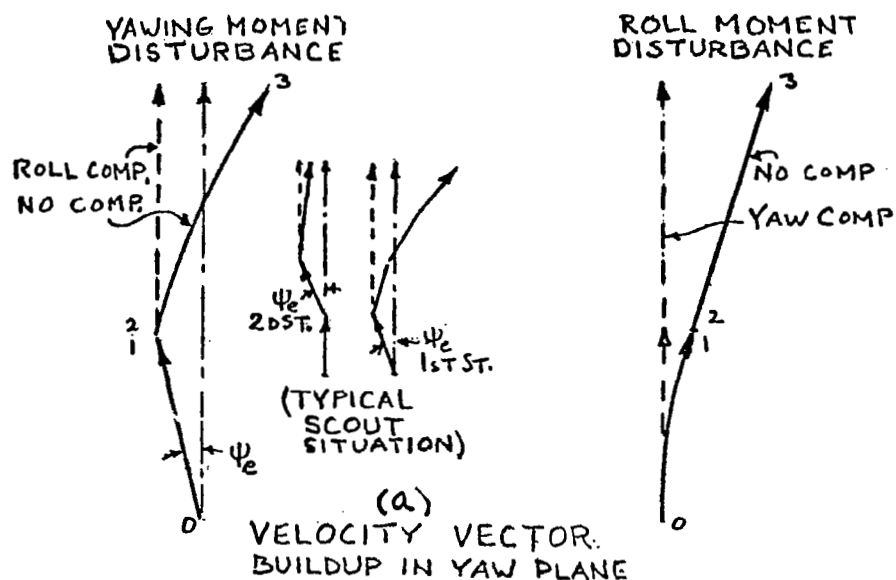


FIGURE 3

On Scout the first stage programmed pitch angle is four times greater than that of the second stage. The first stage roll Euler angle sensitivity to yaw disturbance is therefore four times greater than that of the second stage. The vehicle velocity added following stage burnout is also significant from the standpoint of propagating the effects of disturbances that occur during stage boost. Twice as much velocity is added after first stage burnout than after second stage burnout so first stage propagated errors are significantly greater than errors propagated from similar second stage disturbances.

In the case of a first stage yaw disturbance the propagated out-of-plane error is much larger than the initial error and of opposite sign (Figure 3a). (Initial errors are those generated during the period of a disturbance). Therefore roll compensation which removes the propagated error only will reduce the final error. The propagated out-of-plane error following an upper stage disturbance also opposes the initial error but is much smaller than the initial error. Removal of this propagated error by roll compensation increases the final flight path error.

In the case of roll disturbances, the initial error affects thrust vector pointing very little. The propagated out-of-plane error is the major part of the final error and is in the same direction as the initial error. Therefore yaw compensation reduces trajectory errors due to roll disturbances occurring during operation of all stages.

#### 5.1.3 Effect of Roll-Yaw Compensation on Dynamic Stability: Roots of Characteristic Equation

The linearized roll, yaw and side force equations were solved for the system characteristic equation using an ideal no-lag control system in paragraph 5.1.3.1. Dynamic Stability roots were found using the first stage

flight parameters at  $t = 30$  sec. used in the analog computer study. The roll and yaw rigid body roots were found to change by negligible amounts as the command pitch rate was increased from zero to  $0.1 \text{ rad/sec}$ .

$$\left. \begin{aligned} (S^2 + Q_{CR} Q_{CP}) \Psi_e - SR - Q_{CR} P &= 0 \\ (S^2 + Q_{CR} Q_{CP}) \Phi_e - SP + Q_{CP} R &= 0 \end{aligned} \right\} (1)$$

$$\left. \begin{aligned} P &= \frac{\left(\frac{P}{S_\phi}\right) K_{D\phi}}{1 - K_{R\phi}\left(\frac{P}{S_\phi}\right)} \Phi_e \\ R &= \frac{\left(\frac{R}{S_\psi}\right) K_{D\psi}}{1 - K_{R\psi}\left(\frac{R}{S_\psi}\right)} \Psi_e + \frac{\left(\frac{R}{S_\phi}\right) K_{D\phi}}{1 - K_{R\psi}\left(\frac{R}{S_\psi}\right)} \left(1 + \frac{K_{R\phi}\left(\frac{P}{S_\phi}\right)}{1 - K_{R\phi}\left(\frac{P}{S_\phi}\right)}\right) \Phi_e \end{aligned} \right\} (2)$$

$$\left. \begin{aligned} &= \frac{\left(\frac{R}{S_\psi}\right) K_{D\psi}}{1 - K_{R\psi}\left(\frac{R}{S_\psi}\right)} \Psi_e + \frac{\left(\frac{R}{S_\phi}\right) K_{D\phi}}{\left(1 - K_{R\psi} \frac{R}{S_\psi}\right) \left(1 - K_{R\phi} \frac{P}{S_\phi}\right)} \Phi_e \\ (S^2 + Q_{CR} Q_{CP}) \Psi_e - \frac{S \left(\frac{R}{S_\psi}\right) K_{D\psi} \Psi_e}{1 - K_{R\psi}\left(\frac{R}{S_\psi}\right)} - \frac{S \left(\frac{R}{S_\phi}\right) K_{D\phi} \Phi_e}{\left(1 - K_{R\psi} \frac{R}{S_\psi}\right) \left(1 - K_{R\phi} \frac{P}{S_\phi}\right)} \\ &- \frac{Q_{CR} \left(\frac{P}{S_\phi}\right) K_{D\phi} \Phi_e}{1 - K_{R\phi}\left(\frac{P}{S_\phi}\right)} = 0 \\ (S^2 + Q_{CR} Q_{CP}) \Phi_e - \frac{S \frac{P}{S_\phi} K_{D\phi} \Phi_e}{1 - K_{R\phi}\left(\frac{P}{S_\phi}\right)} + \frac{Q_{CP} K_{D\phi} \frac{R}{S_\phi} \Phi_e}{\left(1 - K_{R\psi} \frac{R}{S_\psi}\right) \left(1 - K_{R\phi} \frac{P}{S_\phi}\right)} \\ &+ \frac{Q_{CP} K_{D\psi} \left(\frac{R}{S_\psi}\right) \Psi_e}{1 - K_{R\psi}\left(\frac{R}{S_\psi}\right)} = 0 \end{aligned} \right\} (3)$$

WHICH IS OF THIS FORM :

$$A\psi_e + B\phi_e = 0$$

$$C\psi_e + D\phi_e = 0$$

(4)

WHICH PRODUCES THE CHARACTERISTIC EQUATION :

$$AD - BC = 0, \text{ WHERE :}$$

(5)

$$A = \left[ \left( 1 - K_{R\psi} \frac{R}{\delta_\psi} \right) (S^2 + Q_{CR} Q_{CP}) - K_{D\psi} \frac{R}{\delta_\psi} S \right] \left( 1 - K_{R\phi} \frac{P}{\delta_\phi} \right)$$

$$B = -Q_{CR} K_{D\phi} \left( \frac{P}{\delta_\phi} \right) \left( 1 - K_{R\psi} \frac{R}{\delta_\psi} \right) - K_{D\phi} \left( \frac{R}{\delta_\phi} \right) S$$

$$C = Q_{CP} K_{D\psi} \frac{R}{\delta_\psi} \left( 1 - K_{R\phi} \frac{P}{\delta_\phi} \right)$$

$$D = \left[ \left( 1 - K_{R\phi} \frac{P}{\delta_\phi} \right) (S^2 + Q_{CR} Q_{CP}) - K_{D\phi} \left( \frac{P}{\delta_\phi} \right) S \right] \left( 1 - K_{R\psi} \frac{R}{\delta_\psi} \right) + Q_{CP} K_{D\phi} \left( \frac{R}{\delta_\phi} \right)$$

(6)

$$AD = \left[ \left( 1 - K_{R\psi} \frac{R}{\delta_\psi} \right) (S^2 + Q_{CR} Q_{CP}) - K_{D\psi} \frac{R}{\delta_\psi} S \right] \left[ \left( 1 - K_{R\phi} \frac{P}{\delta_\phi} \right) (S^2 + Q_{CR} Q_{CP}) - K_{D\phi} \frac{P}{\delta_\phi} S \right] \left( 1 - K_{R\phi} \frac{P}{\delta_\phi} \right) \left( 1 - K_{R\psi} \frac{R}{\delta_\psi} \right) + Q_{CP} K_{D\phi} \frac{R}{\delta_\phi} \times \left[ \left( 1 - K_{R\psi} \frac{R}{\delta_\psi} \right) (S^2 + Q_{CR} Q_{CP}) - K_{D\psi} \frac{R}{\delta_\psi} S \right] \left( 1 - K_{R\phi} \frac{P}{\delta_\phi} \right)$$

(7)

$$BC = -Q_{CR} Q_{CP} K_{D\phi} \frac{P}{\delta_\phi} K_{D\psi} \frac{R}{\delta_\psi} \left(1 - K_{R\psi} \frac{R}{\delta_\psi}\right) \left(1 - K_{R\phi} \frac{P}{\delta_\phi}\right) - Q_{CP} K_{D\psi} \frac{R}{\delta_\psi} K_{D\phi} \frac{R}{\delta_\phi} S \left(1 - K_{R\phi} \frac{P}{\delta_\phi}\right) \quad \left. \begin{array}{l} (7) \\ \text{CONT.} \end{array} \right\}$$

DIVIDING BY  $\left(1 - K_{R\phi} \frac{P}{\delta_\phi}\right) \left(1 - K_{R\psi} \frac{R}{\delta_\psi}\right)$  AND SETTING  $AD - BC = 0$ :

$$\left[ \left(1 - K_{R\psi} \frac{R}{\delta_\psi}\right) (S^2 + Q_{CR} Q_{CP}) - K_{D\psi} \frac{R}{\delta_\psi} S \right] \left[ \left(1 - K_{R\phi} \frac{P}{\delta_\phi}\right) (S^2 + Q_{CR} Q_{CP}) - K_{D\phi} \frac{P}{\delta_\phi} S \right] + Q_{CR} Q_{CP} K_{D\phi} \left(\frac{P}{\delta_\phi}\right) K_{D\psi} \left(\frac{R}{\delta_\psi}\right) + Q_{CP} K_{D\phi} \left(\frac{R}{\delta_\phi}\right) \times (S^2 + Q_{CR} Q_{CP}) = 0 \quad (8)$$

SUBSTITUTING :

$$\frac{R}{\delta_\psi} = \frac{N_\delta (S - Y_\beta)}{\Delta_\psi}, \quad \frac{R}{\delta_\phi} = \frac{-(Q_o) N_\beta L_\delta}{\Delta_\psi \times \Delta_\phi} \quad \left. \begin{array}{l} \\ (9) \end{array} \right\}$$

$$\frac{P}{\delta_\phi} = \frac{L_\delta}{\Delta_\phi}, \quad \Delta_\phi = S - L_p, \quad \Delta_\psi = S^2 + (-Y_\beta - N_R) + N_\beta + N_R Y_\beta$$

MULTIPLY BY  $\Delta_\phi \Delta_\psi$  AND THE CHARACTERISTIC EQUATION IS:

$$\left[ (\Delta_\psi - K_{R\psi} N_\delta (S - Y_\beta)) (S^2 + Q_{CR} Q_{CP}) - K_{D\psi} N_\delta (S - Y_\beta) S \right] \times \left[ (S - L_p - K_{R\phi} L_\delta) (S^2 + Q_{CR} Q_{CP}) - K_{D\phi} L_\delta S \right] + Q_{CR} Q_{CP} K_{D\phi} L_\delta K_{D\psi} N_\delta (S - Y_\beta) - Q_{CP} Q_o K_{D\phi} L_\delta N_\beta \left( S + \frac{Q_{CR} Q_{CP}}{S} \right) = 0 \quad (10)$$

## 5.2 Simulation Results

Analog and digital simulations have been performed to show the results of the addition of Roll and Yaw Compensation to the Scout launch vehicle. The analog simulation considers the possible inaccuracies resulting from the addition of compensation, i.e., drift and gain error, and determines the design requirements for the compensation circuitry. Also certain interfaces such as the effect of the addition of compensation on the hydrogen peroxide propellant consumption as well as the effect on vehicle stability are included in the simulation. The digital simulation is primarily trajectory runs with and without compensation, to show the improvements in the vehicle inclination accuracy.

### 5.2.1 Analog Study

The analog simulation was set up using a five degree of freedom, linear, fixed coefficient, rigid vehicle. Figures 4 through 6 and Table I present the equations and values used. Flight conditions assumed were for the first stage at 30 seconds after launch and for the third stage during coast. Pitch-Yaw-Roll Euler angles were compared with gyro attitude errors with and without roll or yaw compensation. Pitch program rates were varied from  $0.55^\circ/\text{sec}$  to  $5.5^\circ/\text{sec}$  with flight path curvature arbitrarily set to match these rates. A step sidewind and step rolling moment disturbance were used. Typical responses are shown in figures 7 and 8. The yaw Euler angle due to roll disturbance and the roll Euler angle due to yaw disturbance were found to agree with approximate analytical expressions without compensation and were reduced to zero by compensation. As predicted by

# ANALOG SIMULATION EQUATIONS FIRST STAGE

$$\dot{P} = L_{\delta\varphi} \delta\varphi + L_P P + L_0$$

$$\dot{Q} = M_{\delta\theta} \delta\theta + M_Q Q + M_\alpha(\alpha + \alpha_w) + M_0$$

$$\dot{R} = N_{\delta\psi} \delta\psi + N_R R + N_\beta(\beta + \beta_w) + N_0$$

$$\dot{\alpha} = Q - Q_0 - P_\beta - L_\alpha \alpha - L_{\alpha_w} \alpha_w$$

$$\dot{\beta} = -R - Q_0 \varphi + P_\alpha + Y_\beta \beta + Y_{\beta_w} \beta_w$$

$$\dot{\varphi} = P - \dot{\theta} \psi$$

$$\dot{\theta} = Q - R \varphi$$

$$\dot{\psi} = R + Q \varphi$$

$$\gamma = \theta - \alpha - \beta \varphi$$

$$\gamma = \psi + \beta - \alpha \varphi$$

$$\dot{\psi}_e = R + Q_{cR} \varphi_e$$

$$\dot{\varphi}_e = P - Q_{cP} \psi_e$$

$$\dot{\theta}_e = Q - Q_c$$

$$\delta\psi = K_{\delta\psi} (\psi_e + K_R/K_D R) \frac{1}{(1 + \tau_\psi s)}$$

$$\delta\varphi = K_{\delta\varphi} (\varphi_e + K_R/K_D P) \frac{1}{(1 + \tau_\varphi s)}$$

$$\delta\theta = K_{\delta\theta} (\theta_e + K_R/K_D Q) \frac{1}{(1 + \tau_\theta s)}$$

FIGURE 4



# DEFINITIONS:

$$L_{\delta\psi} = C_{\ell\delta} dSg / I_x - N_{\delta v} r_v / I_x$$

$$M_{\delta\theta}, N_{\delta\psi} = C_{m\delta} dSg / I_y - N_{\delta v} l_v / I_y$$

$$L_p = C_{\ell p} (d/2v) dSg / I_y$$

$$M_Q, N_R = C_{mQ} d/2v dSg / I_y - T \ell_E^2 / g I_{SP} I_y$$

$$M_{\alpha}, -N_{\beta} = C_{m\alpha} dSg / I_y$$

$$L_{\alpha}, -Y_{\beta} = C_{N\alpha} Sg / mV + T / mV$$

$$L_{\alpha_w} - Y_{\beta_w} = C_{N\alpha} Sg / mV$$

$L_0, M_0, N_0$  ROLL, PITCH, YAW ANG. ACCEL. DUE  
TO APPLIED MOMENT RAD/SEC<sup>2</sup>

$L_{\delta i}, M_{\delta i}, N_{\delta i}$  REACTION CONTROL ROLL, PITCH, YAW  
ANG. ACCEL. ( $i = UL, UR, LL, LR, UL, PL$ ) RAD/SEC<sup>2</sup>

$L_{\delta\psi}, M_{\delta\theta}, N_{\delta\psi}$  FIRST STAGE ROLL, PITCH, YAW  
CONTROL EFFECTIVENESS, RAD/SEC<sup>2</sup>/RAD

FIGURE 5

# ANALOG SIMULATION EQUATIONS

## THIRD STAGE COAST

$$\dot{P} = -L_{\delta_{UR}} \delta_{UR} + L_{\delta_{LR}} \delta_{LR} + L_{\delta_{UL}} \delta_{UL} - L_{\delta_{LL}} \delta_{LL}$$

$$\dot{R} = +N_{\delta_{UR}} \delta_{UR} + N_{\delta_{LR}} \delta_{LR} - N_{\delta_{UL}} \delta_{UL} - N_{\delta_{LL}} \delta_{LL}$$

$$\dot{Q} = M_{\delta_{UP}} \delta_{UP} - M_{\delta_{LP}} \delta_{LP}$$

$$x_{\psi} = \frac{d_1}{\psi_{DB}} (\psi_e + K_R / K_{D\psi} R)$$

$$x_{\phi} = \frac{d_1}{\phi_{DB}} (\phi_e + K_R / K_{D\phi} P)$$

$$x_{\theta} = \frac{d_1}{\theta_{DB}} (\theta_e + K_R / K_{D\theta} Q)$$

$$x_{UR} = -x_{\psi} + x_{\phi} = -x_{UL}$$

$$x_{LR} = -x_{\psi} - x_{\phi} = -x_{LL}$$

$$x_{UP} = -x_{\theta} = -x_{LP}$$

JET  
ARRANGEMENT

UP

UL > V < UR

LL > ^ < LR  
LP

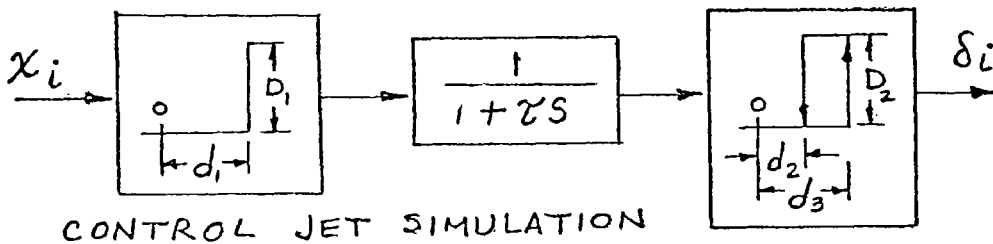
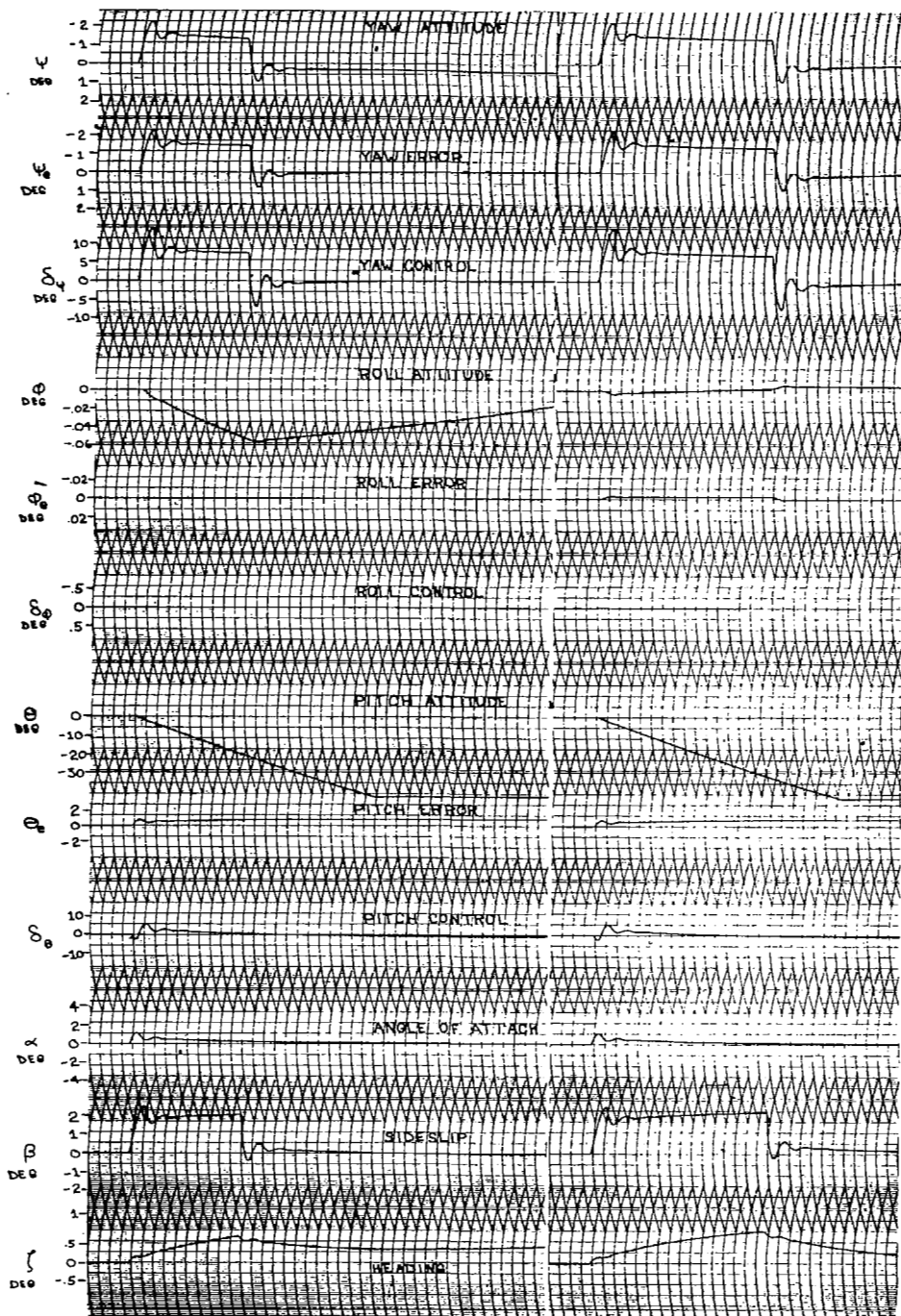


FIGURE 6

TABLE I  
VALUES USED IN ANALOG STUDY

1ST STAGE PARAMETERS		3D STAGE COAST PARAMETERS	
$L_{\delta\phi}$	-15.62 R/SEC <sup>2</sup> /RAD	$L_{\delta i}$	.1355 R/SEC <sup>2</sup>
$L_p$	-.023 1/SEC	$M_{\delta i}$	.0143 R/SEC <sup>2</sup>
$M_{\delta\theta}, N_{\delta\psi}$	-1.02 R/SEC <sup>2</sup> /RAD	$N_{\delta i}$	.0215 R/SEC <sup>2</sup>
$M_Q, N_R$	-.297 1/SEC		
$M_\alpha, -N_\beta$	-3.63 1/SEC <sup>2</sup>		
$L_\alpha, -Y_\beta$	.164 1/SEC		
$L_{\alpha_w}, -Y_{\beta_w}$	.090 1/SEC		
CONTROL SYSTEM:			
$K_{\theta\psi}$	5	$\theta_{DB}$	.004 RAD
$K_{\phi}$	2	$\psi_{DB}$	.004 RAD
$K_R/K_D \phi, \psi$	.4 SEC	$\phi_{DB}$	.00715 RAD
$\tau_{\theta, \psi}$	.133 SEC	$K_R/K_D \theta, \psi$	.50 SEC
$\tau_\phi$	.0445 SEC	$K_R/K_D \phi$	.45 SEC
$Q_C, Q_{CP}, Q_{CR}$	-.0096 R/SEC	$Q_C, Q_{CP}, Q_{CR}$	-.035 R/SEC
DISTURBANCES:		$D_2 = D_1 = d_1 = 1$	
$L_o$	.90 R/SEC <sup>2</sup>	$d_3$	ROLL YAW PITCH .85 .85
$M_o, N_o$	.043 R/SEC <sup>2</sup>	$d_2$	.15 .10
$\alpha_w, \beta_w$	.0715 RAD	$\tau$	.03 .025

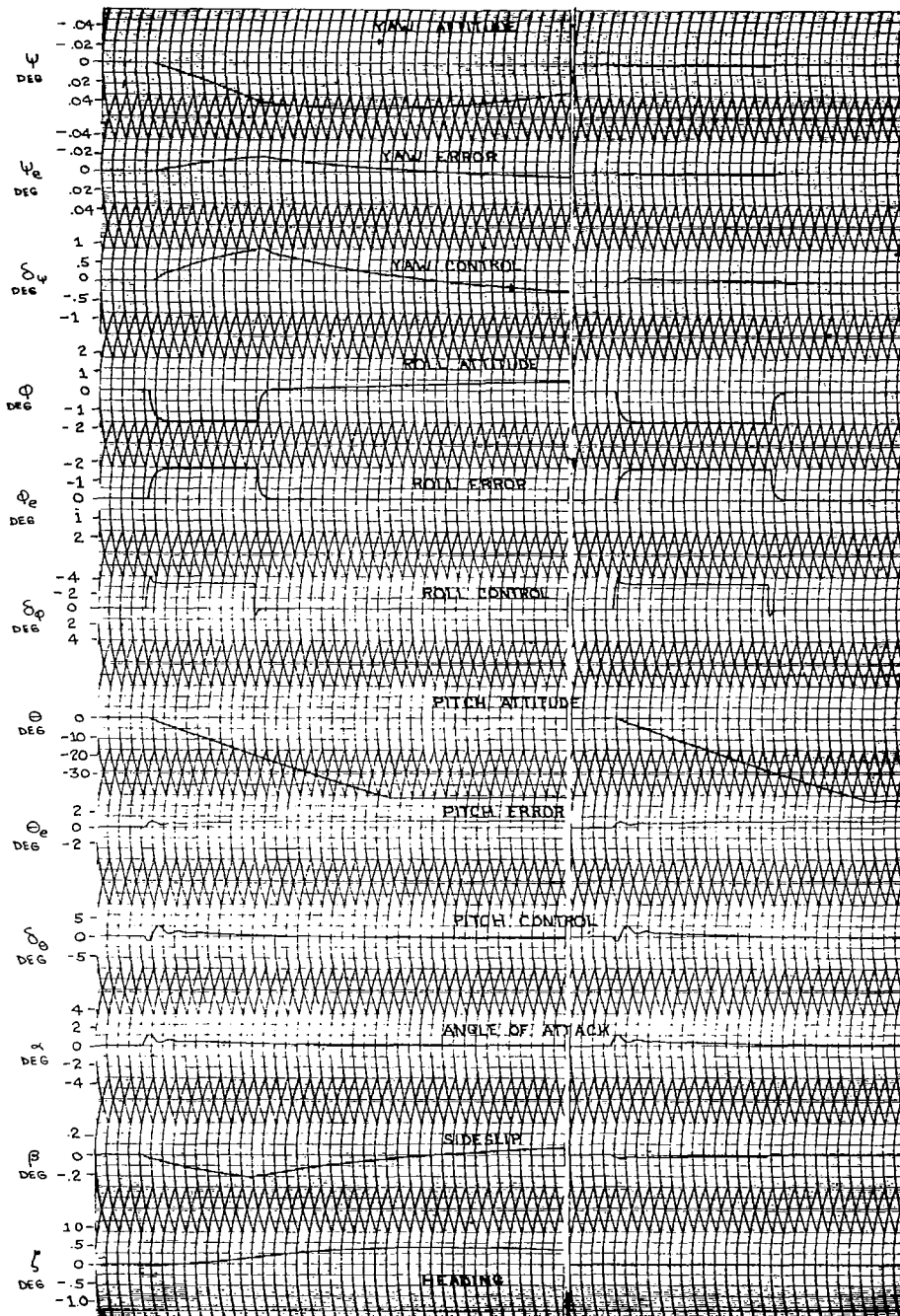


WITHOUT ROLL & YAW COMPENSATION

WITH ROLL & YAW COMPENSATION

Scout First Stage at  $t = 30$  sec  
 Response to sidewind ( $\beta = -4.1^\circ$ )  
 Pitch Rate Command =  $-2.2$  deg/sec ( $4 \times$  nominal)  
 Euler Angle Rotation Sequence: Pitch-Yaw-Roll

FIGURE 7



WITHOUT ROLL & YAW COMPENSATION

WITH ROLL & YAW COMPENSATION

Scout First Stage at  $t = 30$  sec  
 Response to 1,200 ft-lb Roll Moment  
 Pitch Rate Command = -2.2 deg/sec ( 4 x nominal)  
 Euler Angle Rotation Sequence: Pitch-Yaw-Roll

FIGURE 8

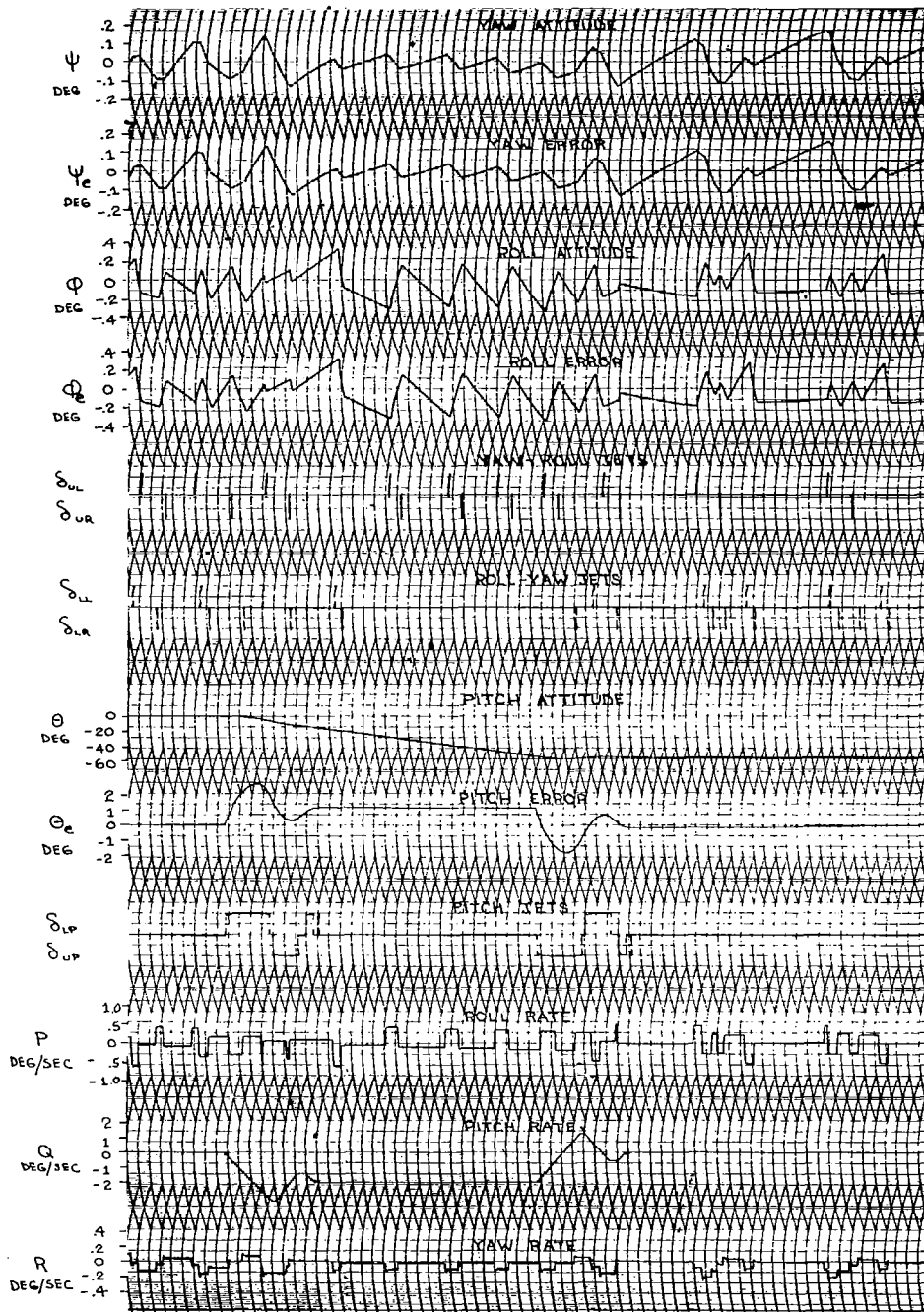
simplified expressions the effect of compensation gain was found to be linear in effect.

Compensation had no noticeable effect on short period stability, although it introduces a long period mode corresponding to a sinusoidal variation at commanded pitch angular frequency as predicted for the geometric variation of yaw Euler angle with pitch attitude.

The third stage pitch maneuver was simulated using six on-off jets with roll-yaw mixing. The response characteristics are shown in Figure 9. Random cycling of the four roll jets occurred with or without the pitch rate command. No difference between gyro errors and Euler angle errors could be seen either with or without compensation indicating that random excursions in roll or yaw during cycling averaged out causing negligible drift in Euler angles. The character of the random lateral motion was not changed by pitch rate commands of either 2 degrees/sec or 4 degrees/second, the approximate limit allowed by the 2 lb. pitch motors without exceeding the  $10^\circ$  pitch limit.

#### 5.2.2 Digital Computer Study

Sensitivities to 99% west wind,  $0.25^\circ$  lateral thrust misalignment and 3  $\sigma$  roll disturbance have been found using 6 degrees of freedom in the first stage, reverting to 3 degrees of freedom at the proper attitude in the upper stages. The conventional yaw-pitch-roll Euler angle system distorts these results relative to simplified analysis. Conversion to the pitch-yaw-roll system in which the yaw and roll angles are always small provides results consistent with the analog study. This conversion is illustrated in figure 2. Pitch disturbances were found to have little effect on roll-yaw compensation. The effect of omitting compensation for the first program step and for the



### SCOUT THIRD-STAGE COAST CONTROL OPERATION

During Pitch Rate Command = -2 deg/dec

With Roll & Yaw Compensation  
Euler Angle Rotation Sequence: Pitch-Yaw-Roll

FIGURE 9

first two program steps was also found. The major contributions occur between 8 and 35 seconds flight time. The wind disturbance is under-compensated by about 12% while the yaw thrust misalignment is over-compensated by 19% in final inclination angle. The roll disturbance was compensated to 1.6%.

### 5.2.3 Trajectory Simulation

A study to determine the effects of incorporating roll and yaw compensation into the Scout vehicle guidance system has been completed and the results are presented in this report. A similar analysis was presented in Reference (1); however, it considered only roll compensation in the first stage. The purpose of roll and yaw compensation, which is an addition to the present Scout guidance system, is to improve Scout orbital inclination accuracy.

This analysis was performed for a 600 n.mi. circular polar orbit developed using the current Scout configuration which consists of the Algol IIB/Castor II/X-259/FW-4S rocket motor and a 34-inch diameter, -25 inch nose station heatshield.

Simulation of the Scout guidance system with roll and yaw compensation was performed using the six degree-of-freedom computer routine described in Reference (2). A nominal trajectory was developed for a 600 n.mi. circular polar orbit using six degrees-of-freedom during operation of the first three stages and three degrees-of-freedom during fourth stage operation. The six degree-of-freedom simulation in the upper stages require simulation of the operation of the reaction control system. In order to activate the reaction controls and establish a limit cycle during second and third stage



operation impulsive disturbances in all three axes were incorporated at ignition of these stages. These disturbances are arbitrary and their only purpose is to activate the reaction control systems to simulate the mode of operation that is assumed in developing a final flight trajectory for a specific vehicle. This mode of operation, for final flight trajectories, is to simulate the first stage as a rigid body in six degrees-of-freedom and the upper stages as a point mass, i.e., three degrees-of-freedom. Simulation of the upper stage in three degrees-of-freedom assumes that: (a) any attitude errors sensed by the guidance system will be completely eliminated instantaneously at stage ignition and (b) the guidance program will be perfectly flown in these stages. This implies then that errors from the first stage and/or the disturbance at ignition will be adequate to activate the reaction control systems and the vehicle attitude will oscillate between the respective deadbands maintaining, on an average, the desired attitude history.

The incorporation of roll and yaw compensation into the Scout guidance system essentially amounts to adding feedback loops to torque the roll and yaw displacement gyros at a rate determined by the product of the commanded pitch rate and the yaw and roll displacement error, respectively. The equations utilized to simulate roll and yaw compensation are:

$$\begin{aligned} P_c &= K Q_c \int R dt \\ R_c &= K Q_c \int P dt \end{aligned}$$

#### 5.2.3.1 Analysis

The significant error sources which produce inclination errors, considered in this analysis, are listed in Table II.

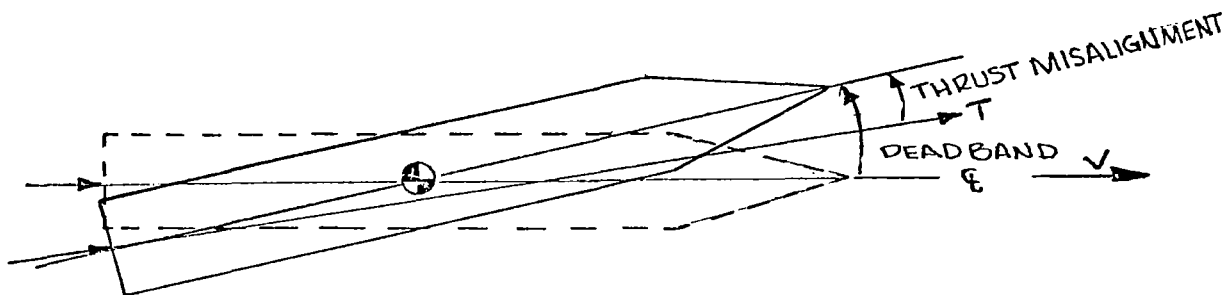
The wind profile, guidance system errors, stage one thrust misalignment, stage two and three roll deadbands and fourth stage tip-off

are presented and discussed in Reference (3). A value of tip-off of 1.5 degrees was considered in this study. First stage roll disturbances are presented in Reference (4). The mean value, from Reference (4) which shows a right roll bias and produces a left inclination bias, is independent of the standard deviation and must be considered separately. An interim fix, on S-150 and sub, for this bias uses cork on the fins to prevent thermal expansion. It is stated in Section 5.3 that the Roll-Yaw Compensation networks considered exhibit no drift and none is shown.

These error sources (Table II) were separately incorporated into the nominal trajectory to determine the inclination deviation that each produces. The resulting deviation in inclination due to the individual error sources is presented in Table II. This procedure was repeated for each error source with roll and yaw compensation incorporated to determine its effectiveness in reducing the inclination deviation due to these error sources. The results are presented in the second column of Table II. It can be seen that a significant decrease in inclination deviation was obtained for all of the error sources with the exceptions of the guidance system errors and second and third stage thrust misalignment. The increase in the inclination deviation from these latter error sources is due to roll compensation eliminating the induced roll error, which was inherently compensating.

This can best be clarified by considering in detail the effect of one of the latter error sources. For example a three sigma yaw thrust misalignment in the upper stages, where the reaction control system maintains the desired yaw attitude within fixed tolerances or deadbands, will force the vehicle to fly, on the average, with a yaw error equal to the deadband value. Thus the thrust vector will not be pointed along the velocity vector,

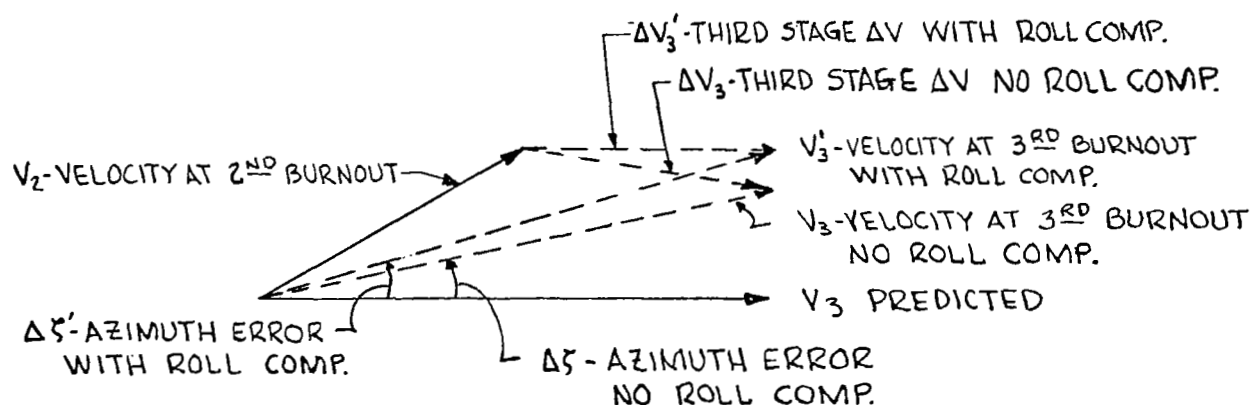
the desired condition, but will be pointed off by an amount equal to the deadband less the thrust misalignment. This is illustrated in the following sketch.



The dashed lines show the conditions with no thrust misalignment. The thrust vector, body centerline and velocity vector are all in the same direction. The solid lines show the conditions that exist with a thrust misalignment forcing the centerline against the yaw deadband. With the vehicle thrusting in the direction shown, a lateral component of velocity will be developed changing the total velocity vector direction, or azimuth, which propagates into an inclination error. Succeeding stages if they thrust in the nominal direction will reduce the azimuth, and corresponding inclination error, but will not completely eliminate it.

A second, more subtle effect of flying the deadband is that a roll error is induced due to a pitch rate acting while the vehicle is against the yaw deadband. This induced roll error is in the same direction as the lateral velocity, i.e., a velocity to the left corresponds to an induced roll to the left. This induced roll error will result in succeeding stages being pitched in a plane skewed to the right. Thus, the roll error that is

induced when the lateral velocity is developed provides an inherent tendency to reduce the effect of this lateral velocity. Roll compensation in the upper stages eliminates this induced roll error and hence the correction for the effect of lateral velocity that it provided resulting in a larger inclination deviation. The following velocity vector diagram illustrates the two effects of a second stage thrust misalignment.



Roll compensation results in the third stage velocity increment being added in the predicted direction. Without roll compensation, the third stage velocity increment is shifted slightly to the right of predicted due to pitching with the induced roll left error. The fourth stage will act in a similar manner, assuming no disturbances, and provide more of a correction.

This example is applicable for both second and third stage thrust misalignments, although more correction is realized for second stage errors since thrusting of subsequent stages contributes a reduction. The effect of roll compensation on guidance system errors is similar to a thrust misalignment.

The velocity vector diagram also applies to any first stage error source which produces yaw attitude errors, such as yaw thrust misalignment and winds. However, if the error source is in the first stage, the vehicle will over-compensate without roll compensation due to the increased angle through which the vehicle pitches. The first stage pitches through about 40 degrees and the second stage pitches through about 10 degrees. Thus, the more the vehicle pitches in a skewed plane, as shown above, the further the velocity vector will move to the right. Therefore, roll compensation in the first stage will decrease the inclination error.

Even though inclination error is not reduced by roll compensation in the second and third stages, it is reduced by yaw compensation. If the vehicle remains on the roll deadband during stage operation, a yaw attitude error will be induced. Yaw compensation will remove this error and the vehicle will pitch in the intended guidance plane but with a roll error. This roll error will not produce an inclination error as long as the induced yaw attitude error is corrected. However, without yaw compensation the vehicle will pitch in a skewed plane, since the yaw error is not corrected, and a velocity vector heading error will result. This error will propagate to injection and produce an inclination error. The only disadvantage to yaw compensation in the upper stages is a slight increase in the inclination deviation produced by the first stage roll bias due to overcompensation. However, this increase is quite small compared to the decrease in inclination deviation due to roll deadband that is realized with yaw compensation.

The inclination deviations without roll compensation and without roll and yaw compensation in the upper stages are presented in Table II.

### 5.2.3.2 Results

The results of this analysis are summarized in Table II which shows the predicted three sigma inclination deviations for the first three stages and for all four stages assuming a tip off of 1.5 degrees. The effect of the first stage roll bias is added directly to the three sigma inclination deviation due to all other error sources, which is obtained by root-sum-squaring the individual deviations. Roll and yaw compensation reduces the three sigma deviation due to the first three stages from 0.799 to 0.317 degrees or approximately 60 percent and the bias from -0.139 to +0.034 degrees. If roll compensation is eliminated from the upper stages, the three sigma value is reduced from 0.799 to 0.275 degrees or approximately 65 percent with the same reduction in the bias as before. Eliminating both roll and yaw compensation from the upper stages provides a reduction in the three sigma inclination of slightly less than 60 percent but the roll bias is further reduced to +0.005 degrees.

The preceding shows the relative gain from roll and yaw compensation since it compensates for errors during the first three stages only. However, the effect considering all four stages cannot be neglected. The three sigma and total (including bias) inclination deviations, assuming a tip off of 1.5 degrees, is presented on the lower portion of Table II. The inclination deviation due to tip off is about the same, 0.705 degrees, as the total deviation of the first three stages, 0.799 degrees. These combine to produce a three sigma value of 1.065 degrees to which the roll bias, -0.139 degrees, is added to obtain the total deviation. It is well to note at this point that the predicted four-stage, three sigma deviation and bias do not agree with the values obtained from flight experience as evidenced by the following comparison.

	<u>Predicted</u>	<u>Flight Data</u>
3 sigma $\Delta i \sim$ deg.	1.07	1.34
Bias or mean $\sim$ deg	-0.14	-0.08

Values for flight data were obtained from the results of 25 flights from the mean and three sigma value of the azimuth deviations and applying a sensitivity coefficient,  $\frac{\Delta i}{\delta \epsilon}$ , of 0.975 to obtain an estimate of the equivalent polar orbit inclination deviation. The flight data shows some indication that the  $3\sigma$  inclination deviation due to fourth stage tip off results from a tip off angle greater than the  $1.5^\circ$  considered in this analysis. The remaining difference between the predicted and observed values resulting from the first three stages has not been accounted for to date; however, if it originates from the operation of the first three stages and is not within the guidance system, it will be reduced with the incorporation of roll and yaw compensation.

Considering the predicted three sigma value, roll and yaw compensation provides a reduction in the inclination deviation of approximately 27 percent. Without roll compensation in the upper stages, the reduction is approximately 29 percent and with no compensation in the upper stages, it is again approximately 27 percent. With compensation, tip off is the predominant error and only large differences in the contribution of the first three stages will be reflected in the final value. The bias again adds directly to the three sigma values to obtain the total inclination deviation.

#### 5.2.3.4 Conclusions

Incorporating roll and yaw compensation into the Scout guidance system will reduce the predicted three sigma inclination deviation of the first three stages by 65 percent and the final deviation by 29 percent.

TABLE II  
INCLINATION DEVIATION DUE TO FIRST THREE STAGES

3 Sigma Error Source	With no Roll or Yaw Compensation	With Roll-Yaw compensation in first three stages	With Roll Comp. in first stage only; yaw comp. in first three stages	With Roll-Yaw Compensation 1st stage only
	Deg	Deg	Deg	Deg
1. Winds	0.443	0.068	0.068	0.068
2. Stage 1 yaw thrust misalignment	0.261	0.056	0.056	0.056
3. Stage 1 roll disturbance	0.529	0.028	0.028	0.028
4. Guidance system error (yaw)	0.164	0.168	0.168	0.168
5. Stage 2 yaw thrust misalignment	0.103	0.166	0.103	0.103
6. Stage 2 roll deadband	0.168	0.020	0.020	0.168
7. Stage 3 yaw thrust misalignment	0.167	0.189	0.167	0.167
8. Stage 3 roll deadband	0.019	0.011	0.011	0.019
RSS	± 0.799	± 0.317	± 0.275	± 0.322
Inclination deviation due to roll bias	- .139	+ .034	+ .034	+ .005
Total 3 $\sigma$ deviation ~ deg	+ 0.660 - 0.938	+ 0.351 - 0.283	+ 0.309 - 0.241	+ 0.327 - 0.317
3 $\sigma$ deviation due to first three stages deg	0.799	0.317	0.275	0.322
Fourth stage tip off (Assumed 1.5 deg) ~ deg	0.705	0.705	0.705	0.705
3 $\sigma$ deviation due to all four stages ~ deg.	± 1.065	± 0.773	± 0.757	± 0.775
Inclination bias ~ deg.	- 0.139	+ 0.034	+ 0.034	+ 0.005
Total 3 $\sigma$ deviation ~ deg.	+ 0.926 - 1.204	+ 0.807 - 0.739	+ 0.791 - 0.723	+ 0.780 - 0.770



Roll and yaw compensation provide a significant decrease in the inclination deviations caused by errors during first stage operation. Yaw compensation reduces the inclination deviations due to roll error in the upper stages. Roll compensation increases the effects of yaw errors and is therefore not desirable. Thus, maximum gains from roll and yaw compensation can be achieved with roll compensation in the first stage only and yaw compensation in all three stages. Further reduction in the predicted total three sigma inclination deviation can only be achieved by reducing the fourth stage tip off.

#### 5.2.4 Propellant Consumption

There is very little effect of roll or yaw compensation on propellant consumption. Theoretically pulses may be added at each time a gyro torquing rate changes. Using standoff errors equal to the deadband and pitch rate command of  $1^\circ/\text{sec}$ , the second stage requires about .06 lb-seconds in roll or about 1 lb-second in yaw per pulse. Assuming two such pulses in yaw due to roll error and four in roll due to yaw error, the added impulse requirement is only 2.25 lb-seconds or less than 0.1% of the propellant supply. The third stage errors require about 10 percent of the second stage impulse values, or 0.1% of the third stage supply.

#### 5.2.5 Accuracy Requirements

The compensator hardware imperfections are essentially errors in slope and intercept of the output  $Q_{cR} \psi_e$  used to drive the roll torquer or  $Q_{cR} \phi_e$  used to drive the yaw torquer. The null error is equivalent to an increased gyro drift rate, while the slope error is equivalent to over or under compensating by the stated tolerance. Since the effect

of compensation on trajectory errors is linear for compensation from zero to its nominal value, the effect of gain tolerance is found by linear interpolation between compensated and uncompensated runs.

Disturbances applied in the presence of 5 percent compensation gain errors would result in an additional r.s.s. inclination error of about 0.044 degrees. This value is considerably smaller than several other error sources and as such will not appreciably increase the r.s.s.'d inclination error of the first three stages. Therefore 5 percent would appear to be a reasonable gain tolerance requirement.

### 5.3 Circuit Analysis

a. Programmed Gain Multiplier System - Schematics of two types of programmed gain multiplier systems considered for the Scout Roll and Yaw Compensation are given in figures 10 and 11 respectively. The system shown in figure 10 provides increased capability if required. The increased capability achieved in this design is provision for obtaining roll-yaw compensation for either pitch up or pitch down programmer signals. Automatic sensing, with contactless switching to condition the Roll-Yaw Compensator correctly for either mode of Programmer signals, is achieved in this design. The contactless IGFET\* switches in the gyro signal input stage are actuated by the 13V (+) or (-) Programmer voltage to select the proper phase of gyro error signal from the secondary winding of the gyro signal input transformer. The gyro signal is required to be stepped down by the transformer to achieve the proper operating level for the IGFET's. Only one IGFET is actuated by the Programmer voltage at a time. One IGFET is on for a (+) voltage and off for a (-) voltage and vice versa. Since transformer losses limit the maximum impedance obtainable by its turns ratio, the output of the transformer is fed

---

\* Insulated gate field effect transistor

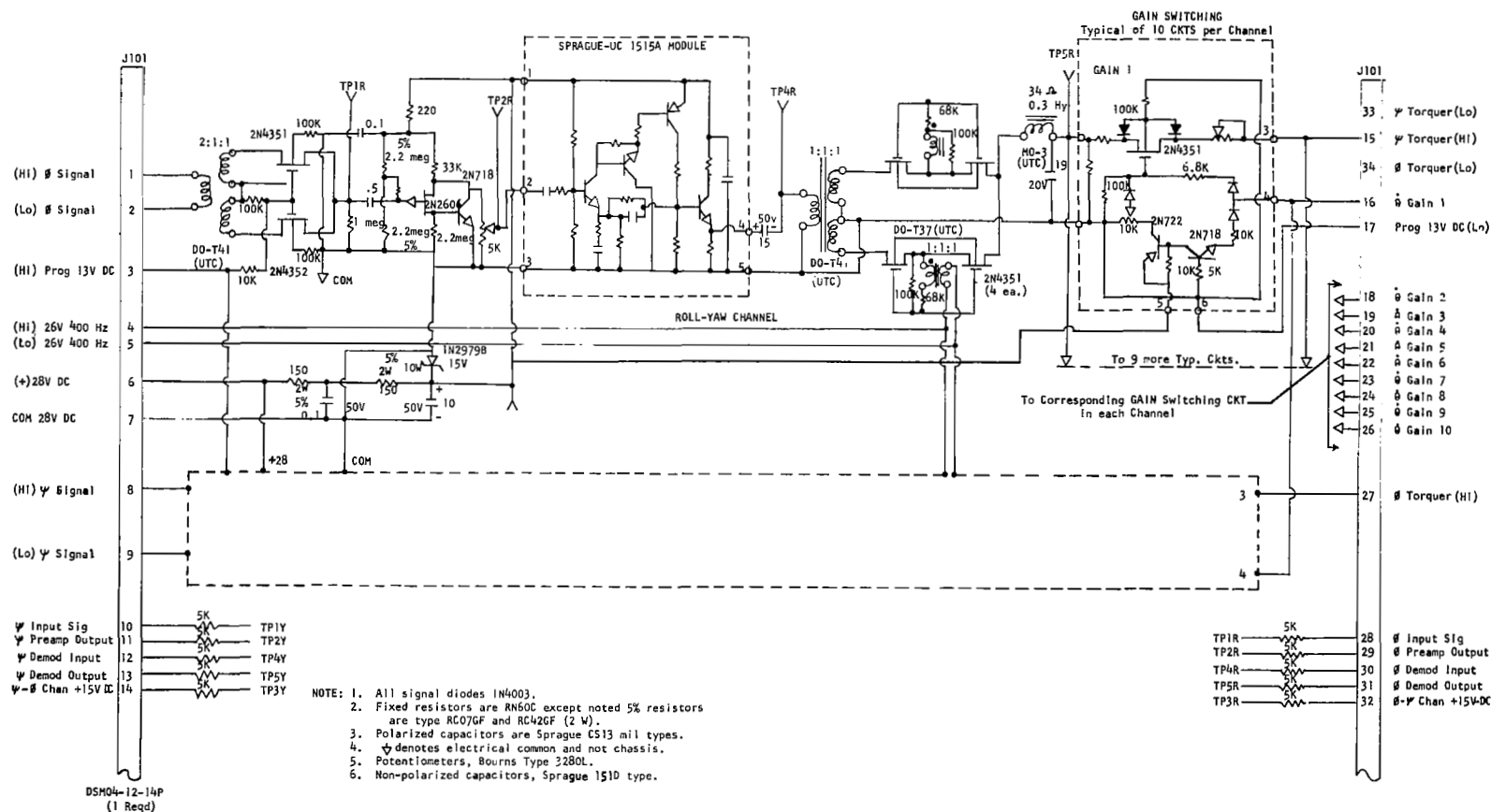
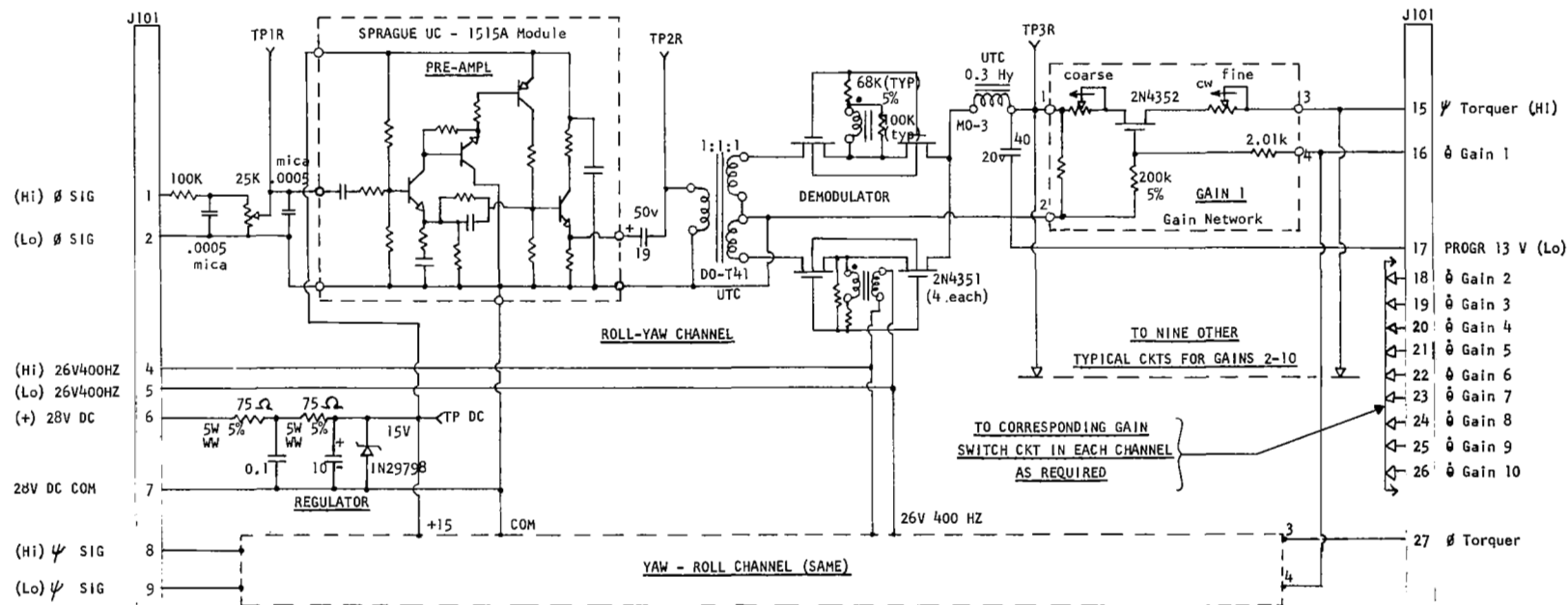


FIGURE 10.- ROLL &amp; YAW COMPENSATION SCHEMATIC



## NOTES

1. Fixed resistors type RN60C (1%) unless noted.
2. Polarized capacitors are Sprague Type CS13.
3. Potentiometers Bourns Type 3280L or equivalent.
4. Nonpolarized capacitors Sprague Type 151D except mica capacitors are Elemento Type CM-15.

$\psi$  Input SIG 10 TP1Y

$\psi$  Preamp OUT 11 TP2Y

$\psi$  Demod OUT 13 TP3Y

(+) 15V DC 14 TPDC

DSH04

TP1R  $\psi$  Input SIG

TP2R  $\psi$  Preamp OUT

TP3R  $\psi$  Demod OUT

FIGURE 11.- SIMPLIFIED SYSTEM ROLL &amp; YAW COMPENSATION.

into a high impedance isolation amplifier to design against any further decrease in this impedance due to loading. The output of the isolation amplifier is fed into a high level amplifier chosen to drive the relatively low input impedance demodulator. This pre-amplifier and amplifier require 15 VDC zener regulated power which is derived from the guidance 28V battery. A voltage gain of approximately 20 db from the gyro input to the demodulator input is required by the design. To achieve a zero off-set required by the performance characteristics, an IGFET demodulator was developed and tested for the system. Test results proved excellent linearity and no off-set; although final design components could not be used in the test, basic performance characteristics were determined. The demodulator uses four N-channel IGFET's as isolated contactless switches. Switching is achieved by the 400 Hz reference voltage. An L-C smoothing filter is used in the demodulator output to reduce ripple voltage to less than 3 percent. The demodulator is designed for 400 Hz input signals of 0 - 10V (p-p). The output of the demodulator is fed to contactless gain switching networks which control the system gain in discrete steps according to the Scout Programmed pitch rate signals. IGFET's are used in the gain switching channels to achieve contactless switching. This increased capability system provides automatic sensing of the Scout Pitch Programmer voltage to enable the gain switching channels to function on either a (+) or (-) Programmer voltage signal. The gain channels use a bipolar transistor inverter stage and diode logic to steer the proper gating signal to each IGFET in the gain switching channels. Only one gain switch in each channel (Roll-Yaw and Yaw-Roll) is on for any given pitch Programmer signal.

The system shown in figure 11 has performance characteristics which limit its operation to pitch down Programmer signals only. Further, the dynamic range of operation for this system is 0.06 to 4.0 degrees per second pitch programmed signals, which is consistent with actual flight requirements, whereas the increased capability system was designed for 0.03 to 10 degrees per second pitch programmed signals. Decrease in the dynamic range of operation as well as elimination of response to pitch up programmer signals permitted deletion of the following circuits:

Phase switching circuit at gyro input

Isolation amplifier circuit

Gain switching channel inverters and logic circuits.

The performance and operation of this system is similar to the system previously described except it operates properly only for pitch down programmer signals and over the lower dynamic range given above. Of course, cost of design and fabrication of the simple system is reduced and reliability is increased with respect to the more complex Roll-Yaw Compensation system.

b. Pre-amplifier - The gyro signal pre-amplifier is a four stage direct coupled semi-conductor amplifier with a medium input impedance and a low (emitter follower) output impedance. The unit is available in a hybrid thin-film construction from Sprague Electric Company. Whereas the basic amplifier module is satisfactory, better performance can be achieved for this application with minor modifications. These modifications consist of reduced bandwidth, higher input impedance, and connections for an external gain change potentiometer. The schematic of the pre-amplifier is shown in figure 10. The electrical characteristics are given in Table III. The input potentiometer, resistor, and capacitor network to the amplifier provide proper impedance match, gain control and high frequency filtering for the gyro signal input.

TABLE III

PRE-AMPLIFIER ELECTRICAL CHARACTERISTICS

<u>Parameter</u>	<u>Min</u>	<u>Typ</u>	<u>Max</u>	<u>Units/Remarks</u>
Voltage gain	39	40	41	db
Voltage gain stability	--	$\pm 0.006$	$\pm 0.008$	db/ $^{\circ}\text{C}$
Bandwidth		40 40	50 50	Hz (low) MHz (high) *
Output at 1 KHz	11	12	--	Volts (p-p) undistorted
Input Z	25	27	--	Kohms * midband
Output Z	--	10	15	ohms
Input noise volts		85	90	VRMS open ckt
Pwr dissipation	--	--	80	mW quiescent
Power supply	12	15	18	volts
Temperature	-55	--	+100	$^{\circ}\text{C}$ operating
Temperature	-55	--	+125	$^{\circ}\text{C}$ storage

\* Desired change

(1) bandwidth 40 Hz to 40 KHz

(2) input Z 150 Kohms

c. DC Power Supply - The Scout 28VDC guidance battery is used as the primary power source for the Roll-Yaw Compensator shown in figure 10. Filtering of the source transients and noise voltages is achieved by the R-C networks which preceded the zener regulator. The zener regulator provides regulation of the DC bias required by the pre-amplifier. The power supply design is based on  $\pm 5$  percent regulation at 15VDC and 30 ma total load current. The minimum battery voltage of 24 VDC sets the minimum zener current requirements for a fixed total series resistance and 30 ma load current. Similarly the maximum battery voltage of 32 VDC determines the maximum zener current requirements. The series resistors are selected as follows:

$$(3) \quad E_B - E_Z = I_T (R_T)$$

$$R_T = \frac{9}{60 \times 10^{-3}} = 150 \Omega$$

$$\text{where: } E_B = 24 \text{ VDC}$$

$$E_Z = 15 \text{ VDC}$$

$$I_T = 60 \times 10^{-3} \text{ amps}$$

With the total series resistance determined for the minimum battery voltage, the maximum zener current, zener power and resistor power ratings may be determined from (3) using the maximum battery voltage of 32VDC. Performing these operations the maximum zener current is approximately 84 ma, maximum resistor wattage rating is 2.9 watts, maximum zener dissipation is 1.26 watts. Based on these results and the temperature range of operation five watt resistors and ten watt zeners are chosen.

d. IGFET Demodulator - The demodulator schematic is given in figure 12. The demodulator is designed for zero off set voltage with no input signal. This is achieved by using the insulated gate field effect transistor which isolates the reference switching voltage from the signal voltage, and by the absence of junction voltages in the IGFET as opposed to bipolar transistors.



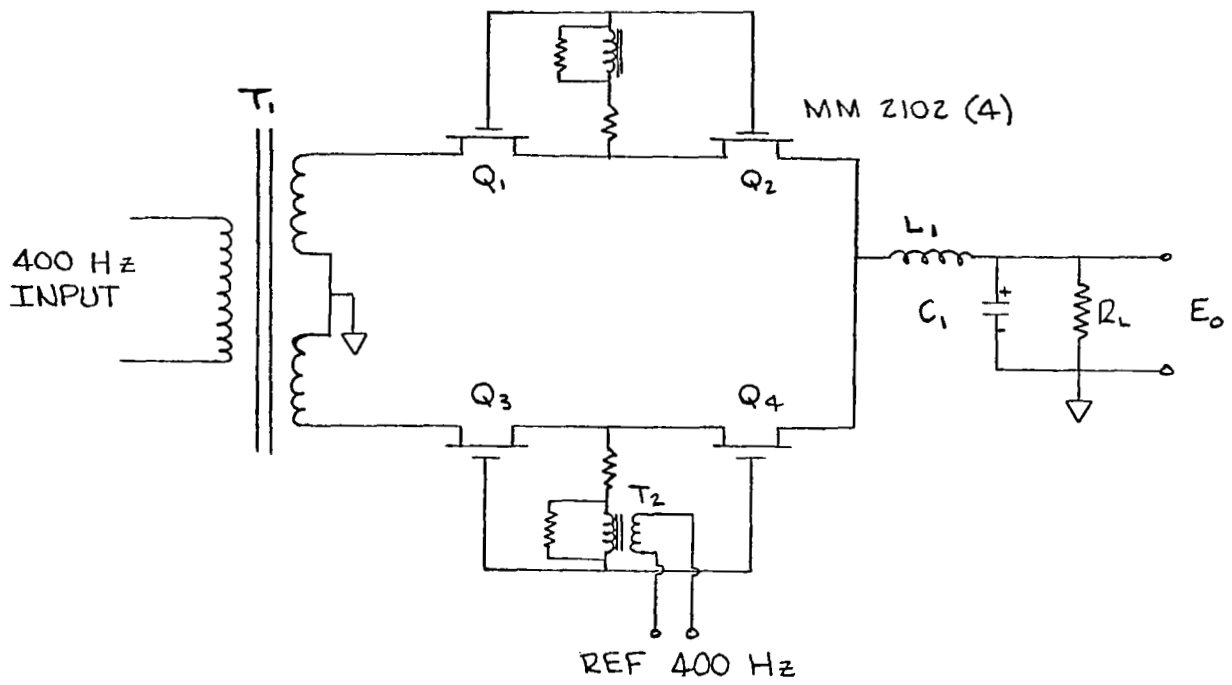


FIGURE 12  
IGFET DEMODULATOR

The demodulator is designed to supply 3.5 ma DC to the gyro torquer. The requirements of the demodulator are given approximately as follows.

$$(1) \quad E_m = \frac{\pi E_o}{2} \left( 1 + \frac{R_c}{R_L} \right) + I_o R_F$$

where:  $R_c$  = DC resistance of  $L_1$   
 $R_F$  = DC resistance of IGFET's  
 $E_o$  = DC Voltage across  $R_L$   
 $R_L$  = Load resistance  
 $E_m$  =  $T_1$  secondary maximum AC voltage  
 $I_o$  = DC current through  $R_L$

From equation (1) the maximum input signal is determined which satisfies the load requirements. Substituting the worst case conditions for the parameters:

$R_c$  = 28 ohms  
 $R_F$  = 300 ohms  
 $R_L$  = 400 ohms  
 $I_o$  =  $3.5 \times 10^{-3}$  amps  
 $E_o$  = 1.4

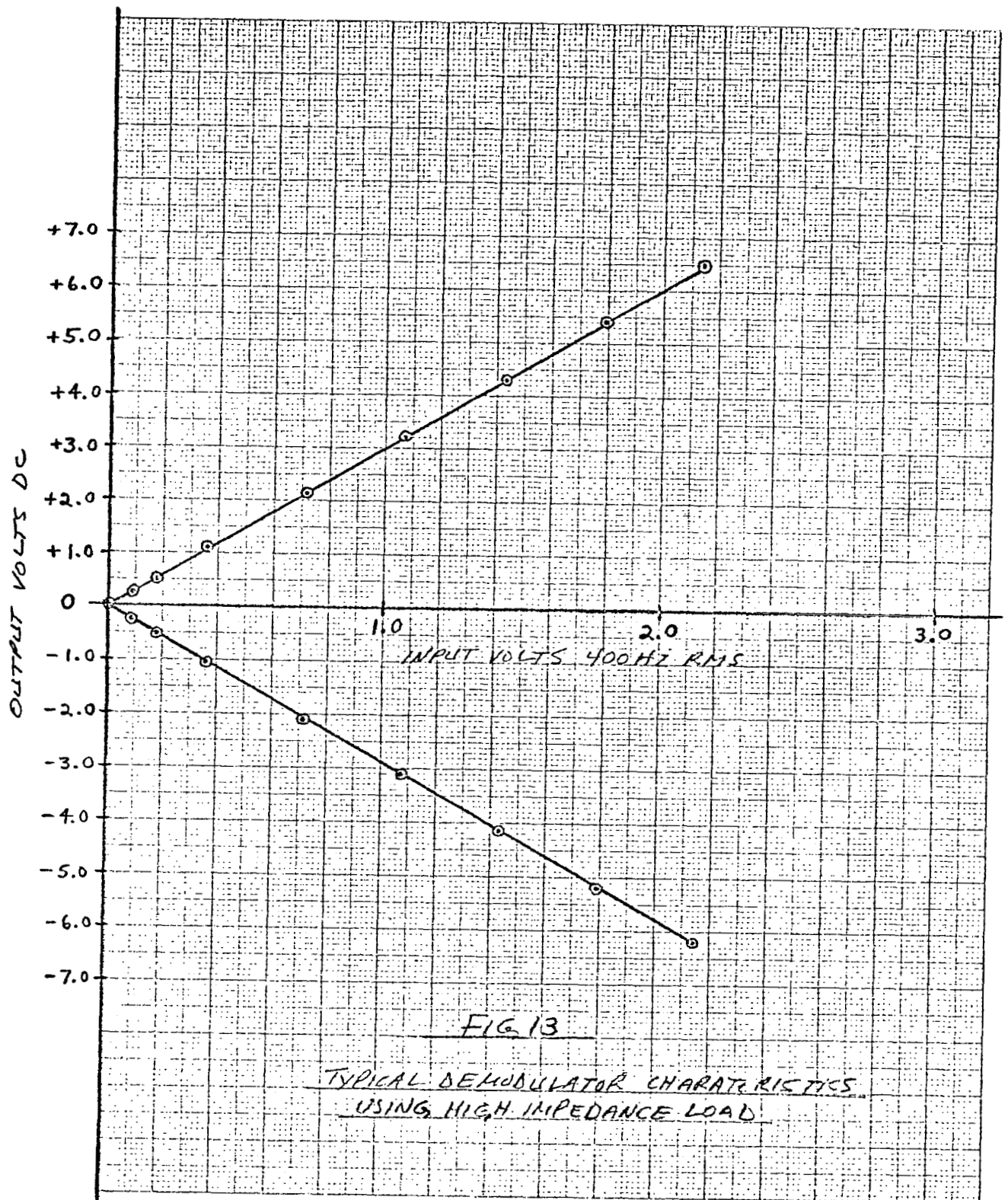
Using these values  $E_m = 3.4V$ . With the turns ratio of  $T_1$  set to 1:1:1 the minimum input signal requirement is 3.2VAC maximum. The demodulator L-C filter is designed to reduce the ripple voltage from the demodulator to less than 3 percent RMS which is determined from the relation:

$$(2) \quad \frac{e_r}{E_o} = \frac{1}{6\sqrt{2}\omega^2 LC}$$

where:  $e_r$  = ripple voltage  
 $E_o$  = 0.7 VDC

Figure 13 gives the IGFET demodulator static response characteristics using a step-up input transformer (1:2:2), a R-C filter and a  $R_L$  of 47K ohms. This test was required to be performed with available components to verify linearity and zero off-set design requirements imposed on the demodulator.

e. Gain Change Switch - The schematic of the gain change switch is given in figure 10. Contactless switching using an insulated gate field effect transistor (IGFET), is used for each gain switch. Each gain change IGFET is actuated by the Scout Intervalometer pitch program switch contacts according to a preset gain program. Each IGFET in the Roll-Yaw Compensation in turn switches in the proper gain resistors which are preset. The preset gain resistors determine the gain of the Roll-Yaw Compensation channels. The sequenced IGFET switch gains provide roll and yaw gyro torquer rates of 0.0105 to 0.698 degrees per second for pitch program rates of 0.06 to 4.0 degrees per second. This requires the IGFET gain switch channels to cover a resistance range of 1.54K to 102.4K ohms for a gyro torquer current range of 0.0459 to 3.05 DC milliamperes. Each IGFET gain channel is designed to use a fixed precision resistor for coarse gain and a multiturn trimming potentiometer for fine gain presetting. The IGFET exhibits approximately 200 ohms on-resistance and  $(10)^7$  ohms off-resistance. Resistance variation of the IGFET through the design temperature range is within  $\pm 10\%$  of its design center value at  $35^\circ\text{C}$ . Since this resistance variation contributes maximum gain error when the gain preset resistors are at a minimum value this total resistance variation is required to determine the maximum gain error which occurs. For this condition the fixed resistors and potentiometer contribute less than a 0.1% error and are neglected. The total resistance of the fixed resistors and potentiometer



for the worst case condition is very near 800 ohms. Therefore the percent change in total gain resistance is approximately one fifth the change in the IGFET or  $\pm 2$  percent.

Contactless switching using an insulated gate field effect transistor (IGFET) is used for each gain switch instead of an electro-mechanical relay. The IGFET can be switched on and off by the existing programmer switching voltage level and requires only a resistor isolation network for each IGFET switch. Relays for this application require separate semi-conductor amplifiers for each switching relay used. To meet the reliability requirements using relays would most likely require using the latching relay types which require additional circuitry to achieve cutoff. Because of the above complexity using relays, IGFET's are specified for this application.

#### 5.4 Reliability

The Reliability evaluation and comparison of the two design approaches is presented in the following paragraphs. Unit I consists of the following functional units: (1) Inverting Amplifier, (2) Operational Amplifier, (3) Demodulator, and (4) Gain Switching. Unit No. II is of the same basic design; however, it is modified for the pitch up condition only. Unit No. II consists of the following functional units: (1) Operational Amplifier (2) Demodulator, and (3) Gain Switching. Failure rates used in the evaluation are derived from the LTV Astronautics Failure Rate Journal and the RADC Reliability Notebook. Expected operating times are based on previous analyses of Scout subsystem components.

Reliability block diagrams are presented in figures 14 and 15. Part and functional component failure rate tabulations are included in Tables V through VIII. Equations for reliability calculations are included in figures 14 and 15. Table IV summarizes the results of the evaluation and presents a comparison of the estimated reliability of each unit.

TABLE IV  
RELIABILITY SUMMARY

Component	Failure Rate (Failures/ $10^6$ hrs.)	MTBF (Hours)	Estimated Reliability
Unit No. I	16.543	$6.0 \times 10^4$	.99900
Unit No. II	12.740	$7.8 \times 10^4$	.99920

As indicated in the summary, the estimated reliability of Unit No. I is .99900 and for Unit No. II is .99920. These estimates are based on the conceptual electronic design only. Parts and materials were not evaluated; however, a cursory evaluation of parts selected for use in the unit indicates that they are adequate for the application.

In comparing the estimated failure rates for each unit (No. I and No. II) it is noted that the difference in failure rates is significant. This difference comes about due to the increased complexity of Unit No. I over Unit No. II. In other words, the higher estimated failure rate of Unit No. I is due to the fact that it requires more parts than Unit No. II. In either case the basic design represents a sound and reliable approach.

#### 5.5 Trade Study

As previously discussed, the trade study is based on two versions of the pre-programmed gain changing multiplier. The assumptions made for the simplified system are that the compensation is not required for pitch up program commands and that the range of pitch program steps is limited to 0.06 to 4 degrees per second. Both assumptions are made based on the history of Scout flight programs. For example, the typical maximum program rate is

TABLE V  
UNIT I  
PART FAILURE RATE TABULATION

Part Type	Part Number	Circuit Designation & Part Value	Quantity	Derating Parameter	Maximum Rating	Stress Level Actual/Rated	Failure Rate (Failures/10 <sup>6</sup> hrs.)	Total Failure Rate (Failures/10 <sup>6</sup> hrs.)
Resistors:								
Metal Film	RN60C	R1	2	Power	125 mw	< .01	.040	.080
"	"	R2	2	"	"	< .01	.040	.080
"	"	R5	2	"	"	.012	.040	.080
"	"	R6	2	"	"	.011	.040	.080
"	"	R7	2	"	"	.09	.040	.080
"	"	R8	2	"	"	.13	.040	.080
"	"	R9	20	"	"	< .01	.040	.800
"	"	R10	20	"	"	< .01	.040	.800
61	"	R12	2	"	"	.09	.040	.080
	"	R15	2	"	"	< .01	.040	.080
	"	R16	2	"	"	.01	.040	.080
	"	R17	2	"	"	< .01	.040	.080
	"	R19	2	"	"	< .01	.040	.080
	"	R21	2	"	"	.13	.040	.080
	"	R24	2	"	"	.056	.040	.080
	"	R25	20	"	"	.032	.040	.800
	"	R26	20	"	"	.064	.040	.800
	"	R27	20	"	"	< .01	.040	.800
"	"	R23	20	"	"	.06	.040	.800
Variable	3280L,Brns	R20, 5K	2	"	250 mw	.02	.014	.028
"	"	R11, 5K	20	"	"	.02	.014	.280
"	"	R22, 10K	20	"	"	.02	.014	.280

TABLE V (Cont'd)  
UNIT I  
PART FAILURE RATE TABULATION

Part Type	Part Number	Circuit Designation & Part Value	Quantity	Derating Parameter	Maximum Rating	Stress Level Actual/Rated	Failure Rate (Failures/10 <sup>6</sup> hrs.)	Total Failure Rate (Failures/10 <sup>6</sup> hrs.)
Resistors Continued:								
Carbon Comp.	RC07GF	R3	2	Power	250 mw	< .01	.004	.008
"	"	R4	2	"	"	< .01	.004	.008
"	"	R18	2	"	"	< .01	.004	.008
Carbon Comp.	RC42GF	R28	1	"	2.0 w	.53	.004	.004
"	"	R29	1	"	"	.53	.004	.004
Capacitors:								
62	Difilm-Metal							
	Clad	118P Sprg	C1, .5 $\mu$ f	2	Voltage	200 VDC	< .01	.045
	"	"	C4, .1 $\mu$ f	1	"	"	.24	.045
	"	"	C6, .1 $\mu$ f	2	"	"	.075	.045
	Solid Tantalum	CS13, Sprg	C2, 15 $\mu$ f	2	"	"	.20	.600
	"	"	C3, 19 $\mu$ f	2	"	"	.40	.600
	"	"	C5, 10 $\mu$ f	1	"	"	.56	.600
Connectors:								
	DSMO4-12-14P	J101	1	Active Pins	---	.24	.190	.190
Diodes:								
Silicon G.P.	1N4003	CR3	20	Power	730 mw	< .1	.020	.400
"	"	CR4	20	"	"	< .1	.020	.400
"	"	CR5	20	"	"	< .1	.020	.400
Zener Reg.	1N2979B	CR6	1	"	10 w	.50	.700	.700



TABLE V (Cont'd)  
UNIT I  
PART FAILURE RATE TABULATION

Part Type	Part Number	Circuit Designation & Part Value	Quantity	Derating Parameter	Maximum Rating	Stress Level Actual/Rated	Failure Rate (Failures/10 <sup>6</sup> hrs.)	Total Failure Rate (Failures/10 <sup>6</sup> hrs)
Transistors:								
IGFET, Field Effect	2N4351	Q1	2	Power	300 mw	.07	.050	.100
" " "	2N4352	Q2	2	"	300 mw	.07	.050	.100
JFET, Field Effect	2N2606	Q9	2	"	"	< .01	.020	.040
	2N718	Q3	2	"	400 mw	< .01	.020	.040
	2N4351	Q4	2	"	300 mw	< .1	.050	.100
	2N4351	Q5	2	"	300 mw	< .1	.050	.100
	2N4351	Q6	20	"	300 mw	< .1	.050	1.000
	2N718	Q7	20	"	400 mw	< .1	.020	.400
	2N722	Q8	20	"	400 mw	< .1	.020	.400
	2N4351	Q10	2	"	300 mw	< .1	.050	.100
	2N4351	Q11	2	"	300 mw	< .1	.050	.100
Inductors:								
Iron Cove	MO-3, UTC	34 $\Omega$ L2, 0.5 Hy	2	No. of Terminals	--	2 terms	.012	.024
Transformers:								
Toroid	DO-T41, UTC	T1, 2:1:1	2	No. of Terminals	--	6	.054	.108
"	DO-T41, UTC	T2, 1:1:1	2	"	--	6	.054	.108
"	DO-T37, UTC	T3, 1:1:1	2	"	--	6	.054	.108
Operational Amplifiers:								
Op. Ampl. Mod.	UC-1515A, Sprg	OAM-1	2	--	--	--	1.065	2.130

$\lambda_t$  (Total Failure Rate) = 16.543/10<sup>6</sup> hrs.  
R<sub>t</sub> (Roll-Yaw Compensator Unit) = .99900

MTBF (Mean-Time-Between Failures) = 6 x 10<sup>4</sup> hrs.

TABLE VI  
UNIT II  
PART FAILURE RATE TABULATION  
(Modified for Pitch up Only)

Part Type	Part Number	Circuit Designation & Part Value	Quantity	Derating Parameter	Maximum Rating	Stress	Failure Rate (Failures/10 <sup>6</sup> hrs)	Total
						Level Actual/Rated		Failure Rate (Failures/10 <sup>6</sup> hrs)
Resistors:								
Metal Film	RN60C	R2, 68K	2	Power	125 mw	.09	.040	.080
"	"	"	R3, 100K	2	"	125 mw	.13	.080
"	"	"	R4, .5-200K	20	"	"	< .01	.800
"	"	"	R7, 100K	2	"	"	.13	.080
"	"	"	R8, 68K	2	"	"	.09	.080
"	"	"	R9, 200K	20	"	"	< .01	.800
"	"	"	R10, 2.01K	20	"	"	< .01	.800
Carbon Comp.	RC42GF	R11, 40 $\Omega$	1	"	2.0 w	.53	.004	.004
"	"	"	R12, 40 $\Omega$	1	"	2.0 w	.53	.004
Variable	3280L	R1, 5K	2	"	250 mw	< .01	.014	.028
"	"	R5	20	"	"	.02	.014	.280
"	"	R6	20	"	"	.02	.014	.280
Capacitors:								
Solid Tantalum	CS13,Sprg	C1, 15 $\mu$ f	2	Voltage	50 V	.20	.600	1.200
"	"	"	C2, 19 $\mu$ f	2	"	20 V	.40	1.200
"	"	"	C4, 10 $\mu$ f	1	"	50 V	.56	.600
Difilm Metal Clad	118P,Sprg	C3, 0.1 $\mu$ f	1	Voltage	200 V	.24	.045	.045

9.5

$$\lambda_T(\text{Total Failure Rate}) = 12.740/10^{-6} \text{ hrs.}$$

$$R_t(\text{Koll Yaw Unit}) = .99920$$

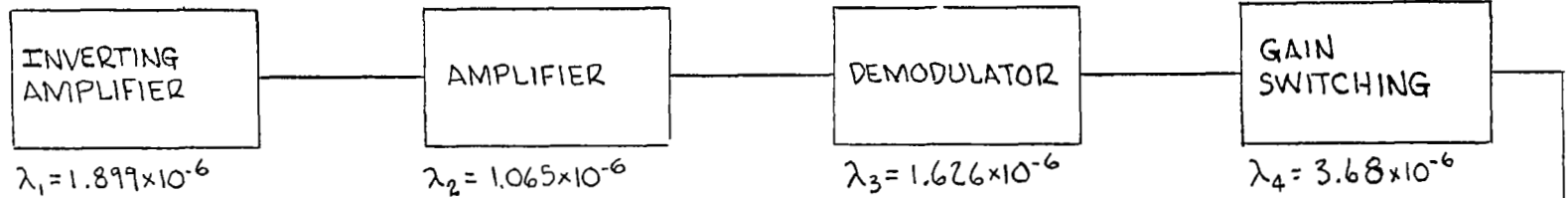
TABLE VII  
UNIT I  
FAILURE RATE TABULATION BY FUNCTIONAL COMPONENT

Functional Component	Quantity	Failure Rate (Failures/ $10^6$ hrs)	Total Failure Rate (Failures/ $10^6$ hrs)	MTBF (Hours)	Reliability t = Mission Time
Inverting Amplifier	2	1.899	3.798	$26.4 \times 10^4$	.99976
Amplifier	2	1.065	2.130	$46.8 \times 10^4$	.99986
Demodulator	2	1.626	3.252	$30.6 \times 10^4$	.99979
Gain Switching	20	.368	7.360	$13.5 \times 10^4$	.99954

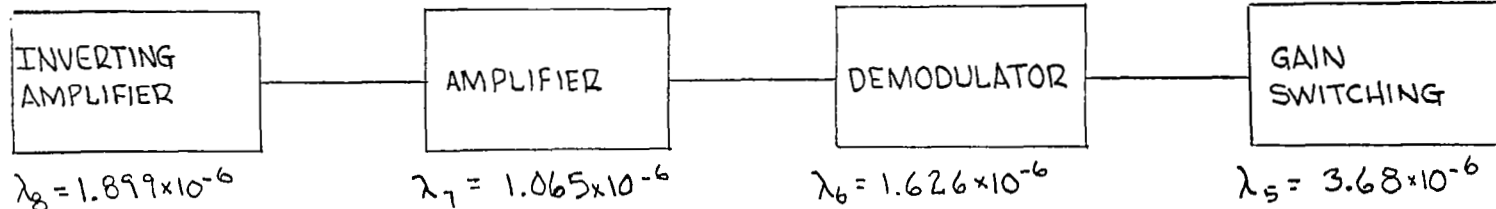
TABLE VIII  
UNIT II  
FAILURE RATE TABULATION BY FUNCTIONAL COMPONENT

Functional Component	Quantity	Failure Rate (Failures/ $10^6$ hrs)	Total Failure Rate (Failures/ $10^6$ hrs)	MTBF (Hours)	Reliability t = Mission Time
Amplifier	2	1.065	2.130	$46.8 \times 10^4$	.99986
Demodulator	2	1.626	3.252	$30.6 \times 10^4$	.99979
Gain Switching	20	.368	7.360	$13.5 \times 10^4$	.99954

## YAW COMPENSATION



## ROLL COMPENSATION



67

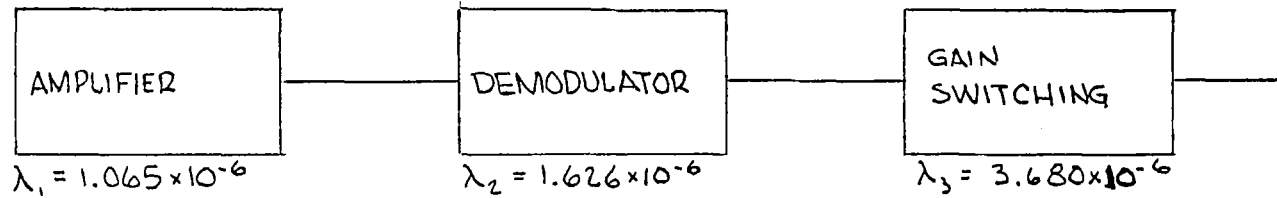
$$\lambda_T = \lambda_1 + \lambda_2 + \lambda_3 + \lambda_4 + \lambda_5 + \lambda_6 + \lambda_7 + \lambda_8 = 16.543 \times 10^{-6}$$

$$R_{(\omega t)*} = e^{-(\lambda_T)(\omega t)} = e^{-(16.543 \times 10^{-6})(62.65)} = .99900$$

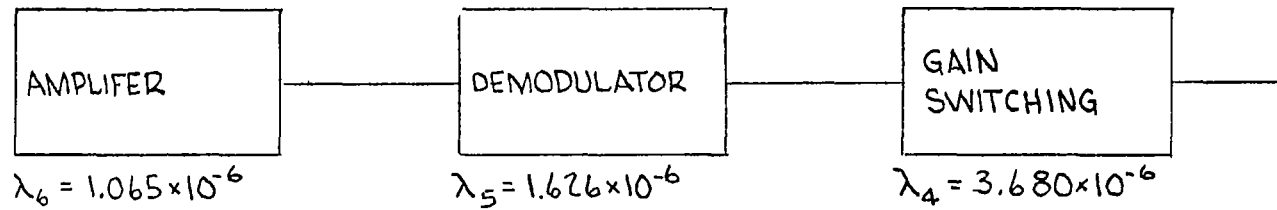
\*  $\omega t = 62.65$  BASED ON PREVIOUS ANALYSES  
ON SCOUT THIRD STAGE COMPONENTS

FIGURE 14 RELIABILITY BLOCK DIAGRAM  
UNIT NO. I

## YAW COMPENSATION



## ROLL COMPENSATION



$$\lambda_T = \lambda_1 + \lambda_2 + \lambda_3 + \lambda_4 + \lambda_5 + \lambda_6 = 12.740 \times 10^{-6}$$

$$R(\omega t) = e^{-(\lambda_T)(\omega t)} = e^{-(12.740 \times 10^{-6})(62.65)} = .99920$$

FIGURE 15 RELIABILITY BLOCK DIAGRAM  
UNIT NO. II

3.5 degrees per second and the typical minimum rate is 0.09 degrees per second. Also, since Roll and Yaw Compensation is required to reduce orbital inclination errors and pitch up program commands have occurred only for probe and re-entry missions, pitch up commands are not needed for Roll and Yaw Compensation.

The values for the parameters listed in the trade study (Table IX) are based on the analyses performed in the preceding paragraphs. The size and weight numbers used are based on the summation of the volume and weight of the individual components in the circuit. A factor of three is used for the volume of the package and an addition of one pound is used for the weight of the package. The cost is based on component parts cost only and does not include package, design, testing, etc. The final schematics for Roll and Yaw Compensation are shown in figures 10 and 11. The studies have concluded that Yaw Compensation is identical to Roll Compensation.

## 5.6 Conclusion

Based on the results of the analyses and computer simulations, it is concluded that the simplified version of the pre-programmed gain changing multiplier is best suited for the requirements of Roll and Yaw Compensation. Therefore the following sections describe the breadboard tests and final design of the selected system.

TABLE IX  
COMPARISON OF ORIGINAL AND REVISED REQUIREMENTS

	Original Requirements	Revised Requirements
70		
1. Complexity	Parts Count a. Transistors 50 b. Field Effect Transistors 34 c. Resistors 228 d. Capacitors 20 e. Diodes 102 f. Transformers 6 g. Potentiometers 42 h. Inductors 2	Parts Count a. Transistors 8 b. Field Effect Transistors 28 c. Resistors 96 d. Capacitors 18 e. Diodes 1 f. Transformers 4 g. Potentiometers 42 h. Inductors 2
2. Accuracy	± 5% of output over the expected temperature range.	Same
3. Reliability	.99900 Reliability 16.543/10 <sup>6</sup> hrs Failure Rate	.99920 Reliability 12.740/10 <sup>6</sup> hrs Failure Rate
4. Pre-Flight Preparation	Requires adjustment of gain to match pitch program rate for each channel.	Same
5. Power Requirements	28 VDC at 120 ma 26 V 400 Hz at 1 ma	Same except 110 ma @ 28 VDC
6. Size and Weight	2 pounds-30 cubic inches	1.7 pounds - 20 cubic inches
7. Cost	Parts Cost \$859	Parts Cost \$596



## 6.0 BREADBOARD RESULTS

### 6.1 Circuit Changes

The control electronics circuits specified for the original breadboard are shown schematically in figure 11. During the fabrication and testing of the breadboard, the following necessary changes were incorporated. Since certain vendor delivery schedules for breadboard components were incompatible with the required test schedule, component substitutions were made which would not invalidate the test results. These substitutions are given in Table XI. A LTV designed pre-amplifier was used in the test instead of the Sprague model UC1515A pre-amplifier which could not be delivered in time for the test. The specifications for the LTV pre-amplifier are given in Table X. After preliminary testing the FET demodulator was redesigned to achieve the required gain margin at the higher temperatures for the maximum load condition (highest torquer current). Additional bias voltage had to be added to the gain switching FET's to meet the null requirements with the increased signal levels from the demodulator at high temperatures. Testing revealed that decoupling networks were required and these were added to the DC power leads feeding the LTV pre-amps to prevent cross coupling between channels. A 20V bias was incorporated for the LTV pre-amp to achieve adequate gain margin at elevated temperatures with minimum distortion. Damping resistors were added in series with the input transformers to the demodulators to eliminate instability caused by the non-linear (switching) demodulator load on the pre-amplifier. Trim circuits were added in series with the gyro signal inputs to compensate for gyro null offsets inherent in the guidance gyros which provide the inputs to the roll and yaw compensation control electronics.

TABLE X  
LTV PRE-AMPLIFIER CHARACTERISTICS\*

<u>Parameter</u>	<u>Min</u>	<u>Max</u>	<u>Units/Remarks</u>
Voltage gain	26	30	db
Voltage gain stability	$\pm 0.01$	$\pm 0.014$	db/ $^{\circ}$ C
Bandwidth	10 12	30 14	H <sub>Z</sub> (low) KHz (high)
Output 400 H <sub>Z</sub>	9	12	Volts (p-p)
Input Z 400 H <sub>Z</sub>	40	70	Kilohms
Output Z	15	50	ohms
Output noise voltage	50	100	microvolt (p-p) with input shunted by 25 kilohms and 0.005 microfarad
Power dissipation	120	200	milliwatts
Power supply	18	22	Volts DC
Operating temperature	25	71	degrees C (range tested)
Storage temperature	-55	125	degrees C

\* With 600 ohm load

**TABLE XI**  
**CONTROL ELECTRONICS COMPONENTS**

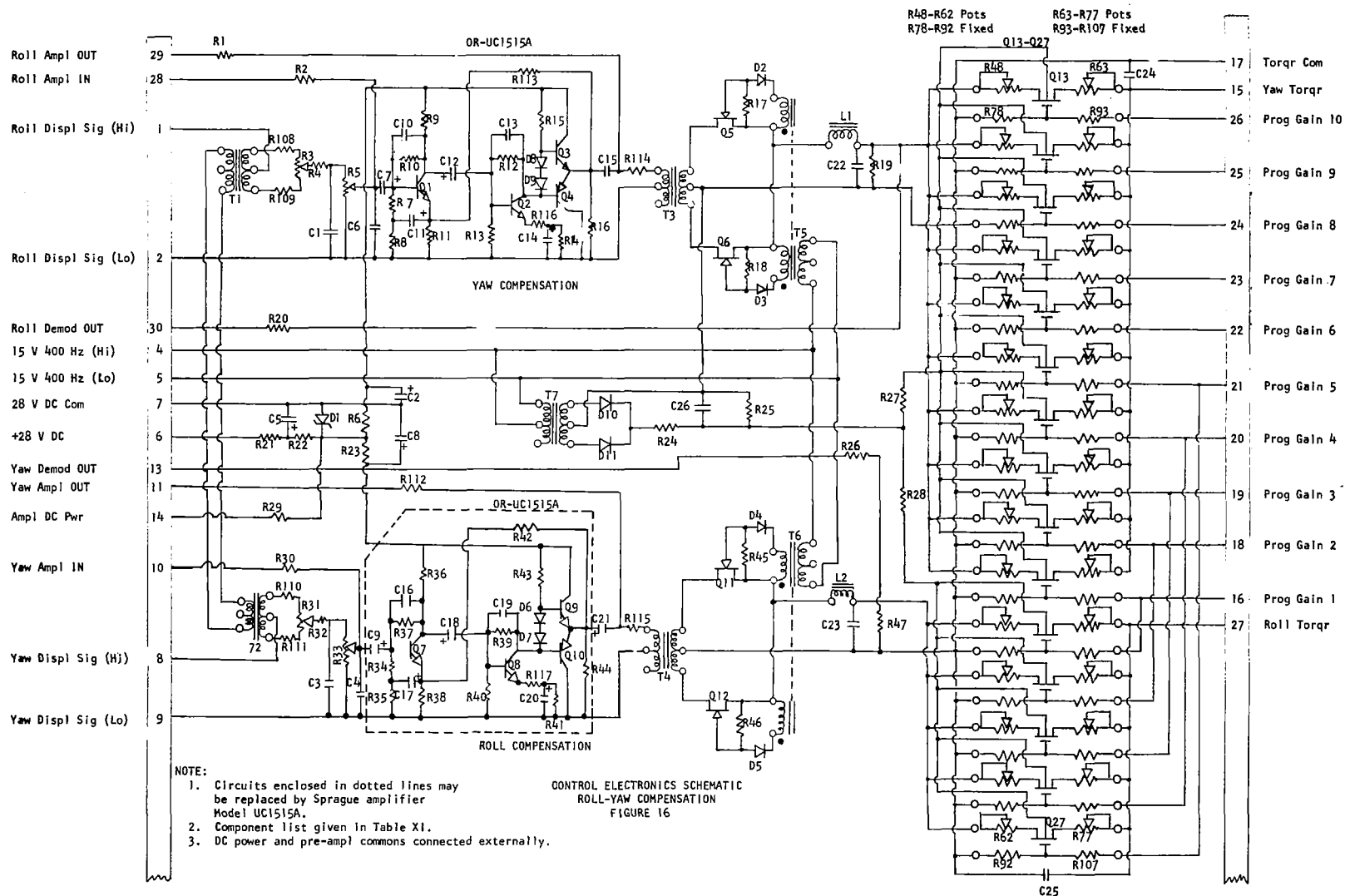
<u>Schematic Symbol (s)</u>	<u>Part Number</u>	<u>Vendor</u>	<u>Specifications</u>
T1, T2	DO-T40	UTC	TF4RX13YY Pin Terminals
T3, T4	DO-T41	UTC	TF4RX17YY Pin Terminals
T5, T6, T7	DO-T37	UTC	TF4RX13YY Pin Terminals
L1, L2	MO-.3	UTC	TF5RX20ZZ Pin Terminals
Q1-Q3, Q7-Q9	2N926	TI	T072 Case
Q4, Q10	2N2906	TI	T072 Case
Q5, Q6, Q11, Q12	2N4860	TI	Spec per Table XII
Q13-Q37	2N4352	Motorola	Spec per Table XII
D1	1N3796A	Motorola	
D2-D11	1N914	TI	
R3, R31	3280W-1-101	Bourns	MIL-R-27208A
R5, R33	3282W-1-503	Bourns	MIL-R-22097B
R63, R77	3282W-1-103	Bourns	MIL-R-22097B
R48-R62	3282W-1-104	Bourns	MIL-R-22097B
R1, R2, R26, R29	RN55D5901F	IRC	MIL-R-10509
R30, R112			
R4, R32	RN55D1003F	IRC	MIL-R-10509
R78-R92			
R9, R36	RN55D9091F	IRC	MIL-R-10509
R7, R8, R16, R34, R35, R44	RN55D5621F	IRC	MIL-R-10509
R10, R37	RN55D1103F	IRC	MIL-R-10509
R6, R23, R14, R41	RN55D1000F	IRC	MIL-R-10509
R116, R117, R108-R114			
R17, R18, R45, R46	RN55D3921F	IRC	MIL-R-10509
R19, R27, R28, R47	RN55D5111F	IRC	MIL-R-10509
R21, R22	RS-1A-100 ohm	DALE	MIL-R-26C
R11, R24, R38	RN55D1001F	IRC	MIL-R-10509
R25	RN55D2211F	IRC	MIL-R-10509
R13, R40	RN55D5111F	IRC	MIL-R-10509
R12, R39	RN55D3922F	IRC	MIL-R-10509
R42, R113	RN55D1822F	IRC	MIL-R-10509
R114, R115	RN55D1500F	IRC	MIL-R-10509
C1, C3, C4, C6	CKR05AX471K	Spague	MIL-C-39014
C10, C13, C16			
C19, C25, C24			
C7, C9, C11, C12	CS13BF226K	Spague	MIL-C-26655B
C15, C17, C18, C21			
C2, C5, C8	CS13BJ225M	Spague	MIL-C-26655B
C14, C20	CS13BC107K	Spague	MIL-C-26655B

NOTE: Components shown for pre-amplifier, within dashed lines on Figure 16 schematic may be replaced with Sprague Type UC1515A amplifier module when module has been tested in the circuit.

## 6.2

### Final Circuit

The recommended circuit configuration for roll and yaw compensation is presented in figure 16. This circuit is intended to provide for any pitch rate from 0.6 to 4.0 degrees per second for any of the ten yaw compensation and five roll compensation outputs. It is also intended to provide the capability of disabling the compensation circuit for program commands other than pitch down (pitch up, yaw torquing, zero rate). The disabling of the compensation for these commands can only be accomplished by providing for an open circuit at the required output. A shorting strap on each output would provide this capability and therefore the pitch up, yaw torquing, or zero rate commands could be used for any of the channels. However, increased complexity as well as a significant increase in package weight and volume make this scheme undesirable. Studies have concluded that the shorting straps are unnecessary if proper assignments are given to the programmer outputs. For example if step number ten is always zero rate, only nine channels are required for yaw compensation. The zero rate command must be used in each flight as the last pitch command and before yaw torquing. It is further concluded that yaw torquing, when required, will be assigned to programmer channel eleven. Pitch up commands, when used, take the place of one of the nine pitch down commands. If pitch programmer channel number nine is assigned for the pitch up command, only eight channels are required for yaw compensation. When the pitch up command is not used, the pitch down command for channel nine will always occur during third stage coast when the compensation is not required. Therefore the circuit given in figure 16 requires only eight channels for yaw compensation instead of the ten shown. The component parts required for this circuit are given in Table XI.



### 6.3 Test Results

#### 6.3.1 Gain, Room Temperature: Yaw Compensation

##### Channel #1

##### AC Input

##### DC Output (torquer)

1.0 v in-phase	+ .595
.8 "	+ .471
.6 "	+ .353
.4 "	+ .236
.2 "	+ .118
0	- .0008
.2 out-of-phase	- .118
.4 "	- .233
.6 "	- .346
.8 "	- .456
1.0 "	- .577

##### Channel #2

##### AC Input

##### Pre-Amp Out

##### Demod Out

##### Torquer Out

1.0 in-phase	2.739 vac	+ 1.533 vdc	+ .455 vdc
.8 "	2.209	+ 1.2269	+ .363
.6 "	1.659	+ .9259	+ .273
.4 "	1.120	+ .6199	+ .184
.2 "	.5649	+ .3129	+ .091
0	.0039	- .0019	- .0006
.2 out-of-phase	.5689	- .3190	- .091
.4 "	1.120	- .6329	- .179
.6 "	1.659	- .9499	- .269
.8 "	2.210	-1.2670	- .355
1.0 "	2.789	-1.6000	- .441

##### Channel #3

##### AC Input

##### DC Output

1.0 v in-phase	+ .393
.8 "	+ .315
.6 "	+ .236
.4 "	+ .158
.2 "	+ .0786
0	- .0005
.2 out-of-phase	- .0793
.4 "	- .157
.6 "	- .233
.8 "	- .310
1.0 "	- .387

#### Channel #4

##### AC Input

1.0 v in-phase  
.8 "  
.6 "  
.4 "  
.2 "  
0  
.2 out-of-phase  
.4 "  
.6 "  
.8 "  
1.0 "

##### DC Output

+ .3343  
+ .269  
+ .202  
+ .134  
+ .0672  
- .0005  
- .0679  
- .134  
- .200  
- .266  
- .332

#### Channel #5

##### AC Input

1.0 v in-phase  
.8 "  
.6 "  
.4 "  
.2 "  
0  
.2 out-of-phase  
.4 "  
.6 "  
.8 "  
1.0 "

##### DC Output

+ .289  
+ .230  
+ .174  
+ .115  
+ .057  
- .0004  
- .055  
- .110  
- .163  
- .215  
- .265

#### Channel #6

##### AC Input

1.0 v in-phase  
.8 "  
.6 "  
.4 "  
.2 "  
0  
.2 out-of-phase  
.4 "  
.6 "  
.8 "  
1.0 "

##### DC Output

+ .228  
+ .184  
+ .137  
+ .091  
+ .045  
- .0004  
- .044  
- .087  
- .129  
- .170  
- .210

Channel #7

AC Input

DC Output

1.0 v in-phase  
.8 "  
.6 "  
.4 "  
.2 "  
0  
.2 out-of-phase  
.4 "  
.6 "  
.8 "  
1.0 "

+ .169  
+ .136  
+ .102  
+ .069  
+ .035  
- .0002  
- .033  
- .068  
- .101  
- .134  
- .169

Channel #8

AC Input

DC Output

1.0 v in-phase  
.8 "  
.6 "  
.4 "  
.2 "  
0  
.2 out-of-phase  
.4 "  
.6 "  
.8 "  
1.0 "

+ .1117  
+ .0895  
+ .0676  
+ .0450  
+ .0225  
- .0002  
- .0228  
- .0454  
- .0680  
- .0906  
- .1130

Channel #9

AC Input

DC Output

1.0 v in-phase  
.8 "  
.6 "  
.4 "  
.2 "  
0  
.2 out-of-phase  
.4 "  
.6 "  
.8 "  
1.0 "

+ .0561  
+ .0451  
+ .0342  
+ .0228  
+ .0114  
- .0001  
- .0116  
- .0229  
- .0344  
- .0458  
- .0571



Channel #10AC Input

1.0 v in-phase  
 .8 "  
 .6 "  
 .4 "  
 .2 "  
 0  
 .2 out-of-phase  
 .4 "  
 .6 "  
 .8 "  
 1.0 "

DC Output

+ .0079  
 + .0064  
 + .0048  
 + .0032  
 + .0016  
 0000  
 - .0016  
 - .0033  
 - .0049  
 - .0065  
 - .0081

Roll CompensationChannel #1AC Input

1.0 v in-phase  
 .8 "  
 .6 "  
 .4 "  
 .2 "  
 0  
 .2 out-of-phase  
 .4 "  
 .6 "  
 .8 "  
 1.0 "

DC Output

+ .5943  
 + .4826  
 + .3672  
 + .2441  
 + .1220  
 - .0011  
 - .1224  
 - .2407  
 - .3564  
 - .4636  
 - .5642

Channel #2AC Input

1.0 v in-phase  
 .8 "  
 .6 "  
 .4 "  
 .2 "  
 0  
 .2 out-of-phase  
 .4 "  
 .6 "  
 .8 "  
 1.0 "

Pre-Amp Out

3.659 vac  
 2.929  
 2.219  
 1.500  
 .7769  
 .0089  
 .7909  
 1.520  
 2.229  
 2.939  
 3.659

Demod Out

+ 1.2859 vdc  
 +1.0469  
 + .7969  
 + .5399  
 + .2699  
 - .0019  
 - .2749  
 - .5479  
 - .8099  
 -1.0679  
 -1.3169

Torquer Out

+ .4059 vdc  
 +.3267  
 + .2466  
 + .1651  
 + .0820  
 - .0007  
 - .0810  
 - .1594  
 - .2326  
 - .3028  
 - .3688

### Channel #3

#### AC Input

#### DC Output

1.0 v in-phase  
.8 "  
.6 "  
.4 "  
.2 "  
0  
.2 out-of-phase  
.4 "  
.6 "  
.8 "  
1.0 "

+ .2927  
+ .2365  
+ .1803  
+ .1202  
+ .0595  
- .0005  
- .0596  
- .1179  
- .1740  
- .2256  
- .2753

### Channel #4

#### AC Input

#### DC Output

1.0 v in-phase  
.8 "  
.6 "  
.4 "  
.2 "  
0  
.2 out-of-phase  
.4 "  
.6 "  
.8 "  
1.0 "

+ .1701  
+ .1389  
+ .1056  
+ .0714  
+ .0353  
- .0003  
- .0357  
- .0713  
- .1050  
- .1372  
- .1677

### Channel #5

#### AC Input

#### DC Output

1.0 v in-phase  
.8 "  
.6 "  
.4 "  
.2 "  
0  
.2 out-of-phase  
.4 "  
.6 "  
.8 "  
1.0 "

+ .0568  
+ .0465  
+ .0354  
+ .0239  
+ .0119  
- .0001  
- .0119  
- .0238  
- .0351  
- .0459  
- .0559

## 6.3.2

## Gain, 71°C: Yaw Compensation

Channel #2

<u>AC Input</u>	<u>Pre-Amp Out</u>	<u>Demod Out</u>	<u>Torquer Out</u>
1.0 v in-phase	2.999 vac	+1.5880 vdc	+ .4523 vdc
.8 "	2.339	+1.2689	+ .3590
.6 "	1.749	+ .9560	+ .2682
.4 "	1.170	+ .6389	+ .1784
.2 "	.5829	+ .3159	+ .0876
0	.0139	- .0079	- .0021
.2 out-of-phase	.6099	- .3339	- .0911
.4 "	1.200	- .6659	- .1798
.6 "	1.779	- .9998	- .2674
.8 "	2.359	-1.335	- .3531
1.0	2.999	-1.690	- .4433

Channel #10

<u>AC Input</u>	<u>DC Output</u>
1.0 v in-phase	+ .0082
.8 "	+ .0066
.6 "	+ .0050
.4 "	+ .0034
.2 "	+ .0017
0	0000
.2 out-of-phase	- .0017
.4 "	- .0034
.6 "	- .0051
.8 "	- .0068
1.0 "	- .0086

Roll Compensation

<u>AC Input</u>	<u>Pre-Amp Out</u>	<u>Demod Out</u>	<u>Torquer Out</u>
1.0 v in-phase	3.749 vac	+1.366 vdc	+ .3990 vdc
.8 "	3.019	+1.1239	+ .3252
.6 "	2.259	+ .8529	+ .2446
.4 "	1.530	+ .5769	+ .1637
.2 "	.7769	+ .2859	+ .0798
0	.0229	- .0069	- .0019
.2 out-of-phase	.8159	- .3009	- .082
.4 "	1.560	- .5959	- .160
.6 "	2.299	- .8789	- .2319
.8 "	3.049	-1.156	- .3013
1.0 "	3.769	-1.4129	- .3604

Channel #5

<u>AC Input</u>	<u>DC Output</u>
1.0 v in-phase	+ .0607
.8 "	+ .0496
.6 "	+ .0379
.4 "	+ .0254
.2 "	+ .0125
0	- .0003
.2 out-of-phase	- .0130
.4 "	- .0257
.6 "	- .0378
.8 "	- .0492
1.0 "	- .0598

6.3.3 Potentiometer Authority

- (a) Null Adjust - with input shorted measure output of pre-amp  
as trim pots R3 and R31 are adjusted stop to stop:

Roll Compensation: R31,     1.489 v in-phase  
                                  1.639 v out-of-phase  
Yaw Compensation: R3,       1.179 v in-phase  
                                  1.289 v out-of-phase

- (b) Pre-Amplifier Gain Adjust - With the input set at 1.0 volt  
in-phase measure the input and output of the pre-amp as  
gain pots R5 and R33 are adjusted stop to stop:

Roll Compensation: R33,	<u>Input</u>	<u>Output</u>
	max <u>.154v</u>	<u>4.219v</u>
	min <u>.0929v</u>	<u>2.559v</u>
Yaw Compensation: R5,	<u>Input</u>	<u>Output</u>
	max <u>.1549v</u>	<u>4.359v</u>
	min <u>.0929v</u>	<u>2.619v</u>

#### 6.3.4 Load Resistors:

The loads used for the breadboard as measured by a resistance bridge are: Roll Compensation, 197.97 ohms

Yaw Compensation, 202.33 ohms

#### 6.3.5 Regulated Power Supply

Measure the regulated voltage as the input supply is varied,

Room Temperature:	<u>Input Supply</u>	<u>Regulated Voltage</u>
	32 vdc	20.879 vdc
	28	20.859
	26	20.829
	24	20.779
	22	19.360
71°C:	32 vdc	21.349 vdc
	28	21.319
	26	21.279
	24	21.110
	22	19.009

#### 6.3.6 Power Requirements

Measure to current for each power source,

Room Temperature:	<u>Supply</u>	<u>Current</u>
	28 vdc	62.5 ma
	15 v, 400 Hz	8.0 ma
	13 vdc	0.26 ma
71°C:	28 vdc	54 ma
	15 v, 400 Hz	7.5 ma
	13 vdc	0.26 ma

#### 6.3.7 Measuring Equipment

The following equipment is used for the breadboard test:

- |                       |   |
|-----------------------|---|
| (1) Digital Voltmeter | Electro Instruments<br>Model 3000A<br>S/N 00070 |
| (2) Oscilloscope      | Tektronic<br>Model 545A<br>S/N 033986           |

- |  |                                       |
|--|---------------------------------------|
| (3) Differential Voltmeter   | John Fluke<br>Model 803B<br>S/N 03664 |
| (4) 28 VDC Supply  | KEPCO<br>Model ABC 30-.3<br>S/N 22680 |
| (5) 13 VDC Supply  | KEPCO<br>Model ABC 30-.3<br>S/N 01964 |
| (6) 400 Hz from laboratory generator with variac S/N #1<br>in line for 15V source. |                                       |

#### 6.3.8 Gain

Selection, by specification, of the demodulator and gain switching FET's is required to assure optimum gain margin, gain linearity and minimum null offset. Table XII gives the FET switching characteristics together with required selection parameters. The breadboard test results indicate the necessity for restricting certain parameters of the components.

The FET's are required to be selected for minimum and equal on resistances as well as minimum and equal leakage currents for the demodulator application. Selection of the FET's in the gain switching circuits are made on the basis of minimum on resistance and leakage currents.

#### 6.3.9 Null

The null offset voltages achieved by the demodulator and gain switching circuits are actually less than  $\pm 0.0002$  volts from  $25^{\circ} - 71^{\circ}\text{C}$ ; however, the test data (channel 2 for example) measures the demodulator output null as high as  $-0.0079$  volts and the torquer output null as high as  $-0.0021$  volts for a null gyro input signal. This discrepancy was caused by the AC pre-amplifier, which feeds the demodulator, picking up 400 Hz spurious signals on the breadboard and hence the AC-pre-amplifier did not actually have

TABLE XII

SWITCHING TRANSISTOR CHARACTERISTICS \*2N4352 P-CHANNEL MOS IGFET

<u>Parameter</u>	<u>Min</u>	<u>Max</u>	<u>Remarks</u>
Gate Threshold Volts	-1.5 vdc	-6.0 vdc	Spec at -2.0 vdc max.
Drain-Source <u>on</u> Resistance	250 ohms	300 ohms	At -13.5 vdc gate volts and 3 ma drain current. Spec at 250 ohms max.
Drain current at zero gate voltage and -5V drain-to source	--	$5 \times 10^{-9}$ amps	Spec at $2 \times 10^{-9}$ amps with +5V substrate to source bias
Gate leakage current	--	$10^{-11}$ amps	Drain to source = 0V Gate to source = $\pm 25$ V
Drain to gate and gate to source breakdown	$\pm 35$ V	--	

2N4860 (TIXS41) N-CHANNEL JFET

Drain source <u>on</u> resistance	--	40 ohms	Matched 2N4860's required (5%)
Drain cutoff current	--	$10^{-8}$ amps	Drain to source 15V Gate to source 5V
Gate cutoff current	--	$5 \times 10^{-9}$	Gate to source -20V

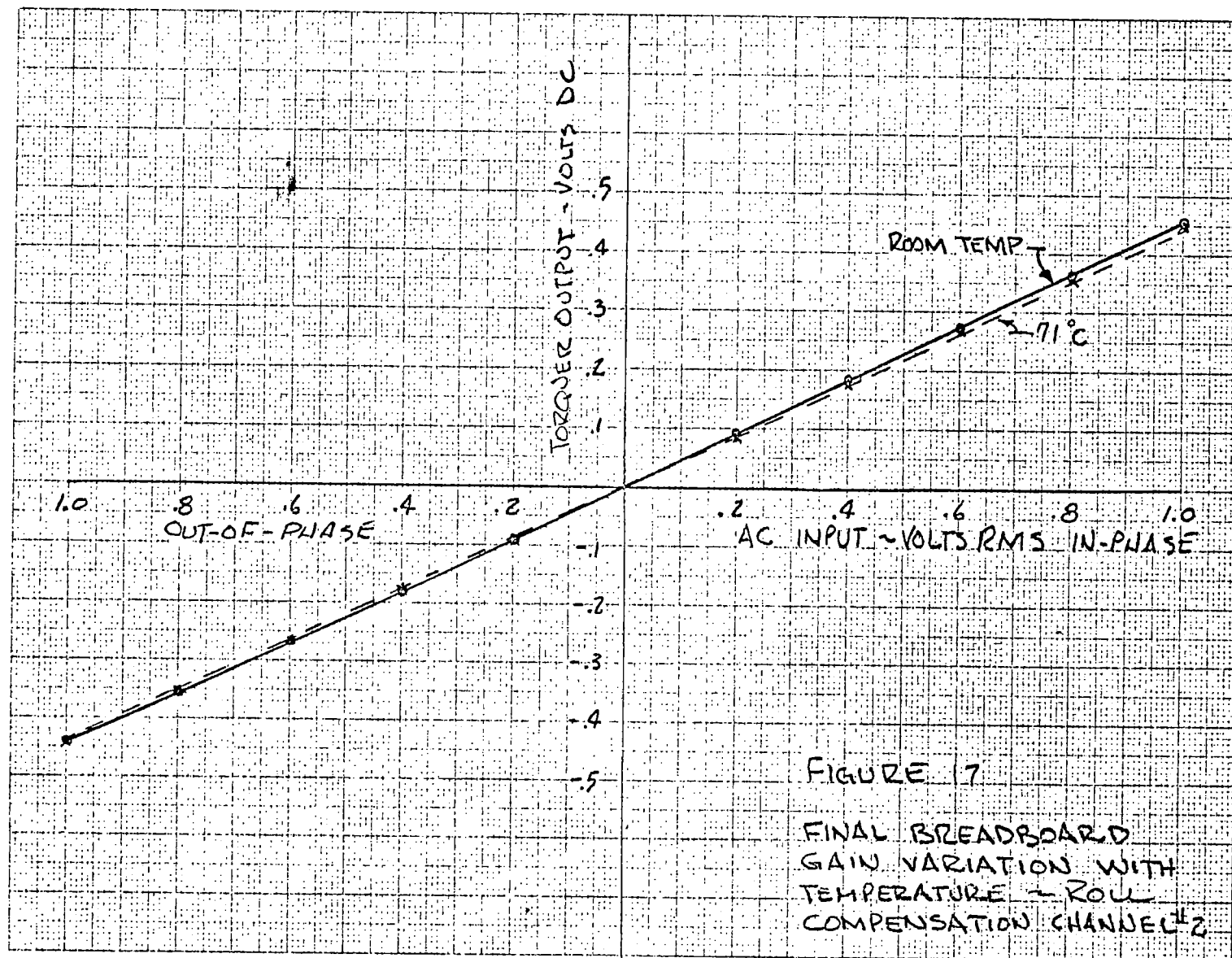
\* Temperature range  $25^{\circ}\text{C}$  -  $71^{\circ}\text{C}$

a zero null output. This is shown in the test results for channel 2 tests where the AC pre-amp actually had a 0.0139 volt 400 H<sub>z</sub> output signal at null. To verify the null qualities of the demodulators and gain switches on the breadboard the AC-pre-amp was disabled (DC power removed) and the nulls re-measured at the output of the demodulator and gain switch circuits. The nulls could not be measured with the instruments available, (less than  $\pm 0.0001$ ). Schedules did not permit re-work of the breadboard to eliminate or minimize the AC-pre-amp 400 H<sub>z</sub> feed-through. This pick-up and/or feed-through of the 400 H<sub>z</sub> varied in a random manner and with arrangement of the test leads terminated at the breadboard. This is considered a discrepancy which can be corrected by proper package and cabling design.

#### 6.3.10 Unbalance

Response of the switching FET's to input signals of opposite polarities varies with the ratio of load resistance to FET on resistance, and the ratio of on gate voltage of the FET to the signal level and polarity which is switched. For the P-channel FET, which requires a negative on gate voltage, a positive input signal acts to decrease the FET on resistance and a negative input signal acts to increase the FET on resistance. For input signals which are much less than the gate voltage this effect is negligible, but for input signals which approach a large fraction of the gate voltage the effect becomes appreciable in most applications where the load resistance is of the same magnitude or less than the FET on resistance. The result of this effect is to cause non-linear signal response which increases at relatively high signal levels. The effect can be minimized for a given load resistance and FET gate on voltage by specifying a low on resistance for the FET's used. For the worst case load and signal condition occurring in this design, the specifications in Table XII for the FET's should give a response that is linear within  $\pm 5\%$  over the temperature range. A typical gain curve of the final breadboard is shown in figure 17.





## 6.4 Reliability

Component changes between the final circuit configuration and the proposed breadboard circuit (figure 11) affect the reliability analysis of paragraph 5.4. However, since the final circuit represents a simplification of the proposed system in terms of total parts, it is concluded that the reliability of the final circuit is superior to the proposed circuit analyzed in paragraph 5.4. Therefore the reliability analysis is not updated but the following table is included to show the reduction in the number of component parts:

	Number of Parts	
	<u>Proposed Circuit</u>	<u>Final Circuit</u>
1. Resistors	70	48
2. Potentiometers	44	30
3. Capacitors	6	13
4. Diode	1	5
5. Field Effect Transistors	28	17
6. Inductors	2	2
7. Transformers	6	6
8. Operational Amplifiers	2	2

## 7.0

### CHECKOUT METHOD

The checkout requirements for Roll and Yaw Compensation are the measurement and adjustment of the torquing rates for each of the eight yaw channels and five roll channels. The checkout philosophy will be similar to that presently used for checkout of the pitch programmer torquing rates:

1. Component acceptance testing using a standard program.
2. Component acceptance testing with flight program.
3. System bench testing with flight program torquing rates.

Since the design of the Roll and Yaw Compensation is such that only the adjustment of potentiometers, rather than the soldering of jumper wires and fixed resistors, is required for the setting of torquing rates, step 2 above can be eliminated.

It is recommended that the Roll and Yaw Compensation Unit be acceptance tested using a standard flight program and then torquing rates adjusted at the system bench level. The torquing rates will then be verified at the vehicle level.

The compensation torquing rates will be set to  $\pm 3\%$  to assure the required  $\pm 5\%$  operational accuracy. The ratio of the checkout requirement to the operational requirement is consistent with the philosophy used in the checkout of other Guidance System components.

## 7.1

### Acceptance Tests

During fabrication of the Compensation unit, the gain potentiometers will be set to a standard flight program that will include the maximum range of pitch program rates. The gain settings will be verified during acceptance testing of the unit. Standard laboratory test equipment will be

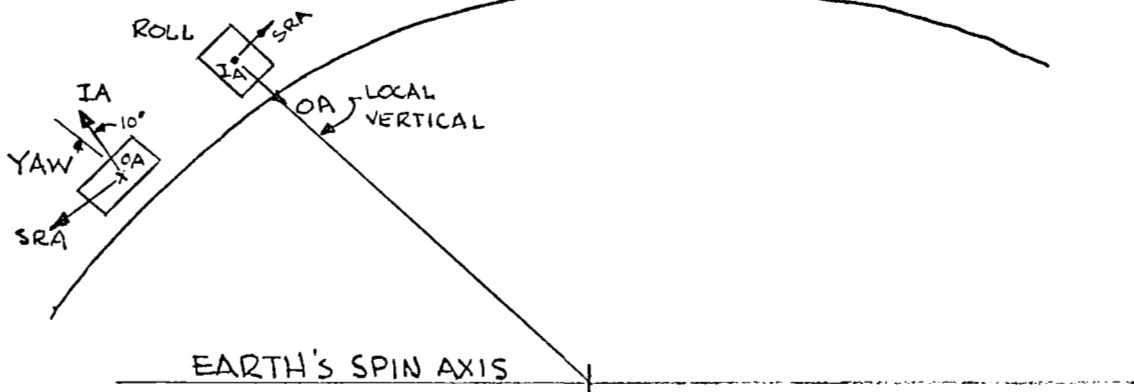
utilized for the acceptance testing. A test cable with a test box will be the only GSE necessary for the acceptance testing. Signal inputs for the displacement and timer commands to the pitch programmer will be applied to the unit and the gain of each channel will be measured.

## 7.2 Bench System Test

The SEI normally released for the installation of the flight profile pitch program torquing rates will be expanded to include the Roll and Yaw Compensation torquing rates. The procedure for roll and yaw torquing rates will be similar to the procedure for determining the pitch program torquing rates.

7.2.1 The roll and yaw gyro torquer voltage scale factors will be determined by applying a known voltage to each torquer and measuring the gyro displacement for a fixed period of time. The measured torquer scale factor will be used to calculate the voltage gain of the Compensator unit.

7.2.2 The following orientation will be used to minimize drift during the gain adjustment.

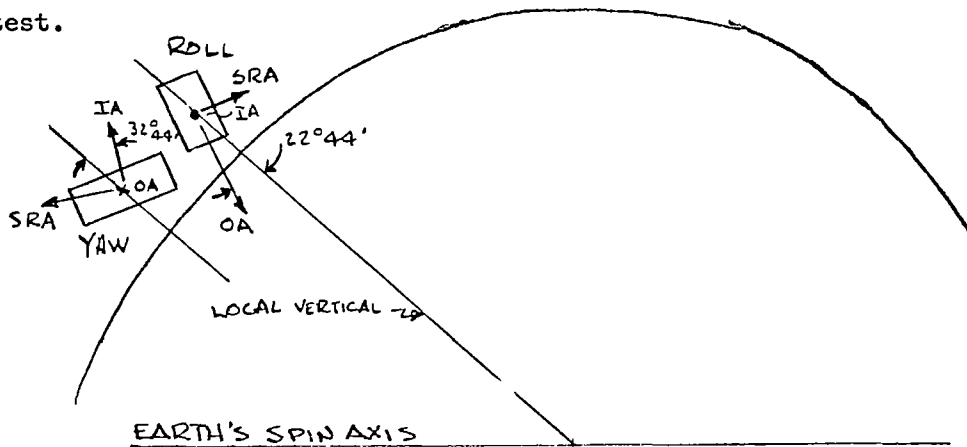


This orientation is used for adjustment of the Yaw Compensation voltage gains. The roll and yaw gyro orientations are interchanged for the adjustment of the Roll Compensation voltage gains. The gyros are uncaged while oriented  $10^\circ$  off of the local vertical and are then rotated about the roll input axis

to the orientation shown. This orientation provides a  $10^0$  roll displacement signal with zero roll gyro drift due to earth's rate and mass unbalance. The yaw gyro will drift in this orientation due to earth's rate and mass unbalance. However, since only the yaw gyro torquer voltage and not the torquing rate is being measured, the yaw gyro drift does not cause a measurement error.

The gain of each channel of Yaw Compensation is set by actuating the appropriate pitch program step and adjusting the potentiometers to the required voltage across the yaw gyro torquer as determined by the measured torquer scale factor. This test is performed using existing Scout GSE.

7.2.3 Torquing rates will then be verified by applying a displacement signal and the timer command for each pitch program step to the compensator and measuring the compensation torquing rate. The rate will be measured by rotating the axis under test for a fixed period of time and measuring the magnitude of rotation. The following IRP orientation is used for this test.



The gyros are uncaged at  $22^0 44'$  south of the local vertical and the yaw gyro is torqued until the input axis is  $32^0 44'$  south of the local vertical to provide a  $10^0$  yaw displacement signal with zero gyro drift due to

earth's rate. This orientation is used for measuring Roll Compensation torquing rate. This orientation results in drift due to mass unbalance about the gyro spin axis and input axis. Since the IRP cannot be orientated to give zero drift due to earth's rate and mass unbalance for two gyros, the gyros are oriented for zero earth's rate drift since its effects are greater than mass unbalance. The resulting maximum drift due to mass unbalance is:

$$\begin{aligned} \text{Roll; } \text{MU}_{\text{IA}} &= \frac{2.9^\circ/\text{hr/g} \sin 22^\circ 44'}{3600} = 0.00031^\circ/\text{sec} \\ \text{MU}_{\text{SRA}} &= 0 \\ \text{Yaw; } \text{MU}_{\text{IA}} &= \frac{2.9^\circ/\text{hr/g} \sin 32^\circ 44'}{3600} = 0.00043^\circ/\text{sec} \\ \text{MU}_{\text{SRA}} &= \frac{2.9^\circ/\text{hr/g} \sin 57^\circ 16'}{3600} = 0.00067^\circ/\text{sec} \end{aligned}$$

In the case of Roll Compensation, the roll gyro drift adds directly as an output error. The yaw gyro drift is a function of the period of the test since the yaw gyro is used as a displacement input to the system. Therefore the testing time must be minimized to minimize the error. Also, since the roll gyro is being rotated about its input axis to measure the torquing rate, the yaw gyro input axis will be displaced off of perpendicular to the earth's spin axis. This displacement causes the yaw gyro to sense a component of earth's rate resulting in a yaw gyro drift. Although this drift is small,  $(12.6512 \sin \alpha^\circ/\text{hour})$ , where  $\alpha$  is the angle displaced from the perpendicular) the angle of rotation must be minimized to minimize the error.

7.2.4 For a  $10^\circ$  displacement input and a pitch program rate range of 0.06 to  $4^\circ/\text{second}$ , the compensation torquing rate will be from 0.0105 to  $0.6981^\circ/\text{second}$ . The measurement of these torquing rates should be accurate to  $\pm 0.00003^\circ/\text{second}$  for the low rate and  $\pm 0.00209^\circ/\text{second}$  for the high rate to achieve a measurement accuracy an order of magnitude greater than

the checkout tolerance. Therefore, it can be seen that mass unbalance alone results in a 3% error for the low rate. It is concluded that the mass unbalance for the roll gyro must be measured and used as a correction factor applied to all program steps which will result in zero measurement error due to this drift. Other measurement error sources are:

- a. Yaw gyro mass unbalance drift
- b. Yaw gyro earth's rate drift
- c. Griswold head reading accuracy
- d. EPUT timer accuracy
- e. Yaw Displacement input uncertainty.

The Griswold head accuracy is  $\pm 10''$  of the scale reading. Therefore, the greater reading accuracy occurs for larger angles. As previously mentioned, the angle of rotation must be small to minimize gyro drift due to earth's rate. To achieve the required  $\pm 0.3\%$  measurement accuracy, a compromise must be made between testing time and angle of rotation. A discussion of the measurement accuracy follows:

Assume the angle of rotation to be  $2^\circ$ .

The measurement errors are:

- (1) Griswold reading error (output) =  $10'' = .138\%$
- (2) Time for  $0.0105^\circ/\text{second} = 190.48$  seconds nominal; and  
EPUT error =  $190.48 \pm .01$  ( $\pm 1$  count) =  $.005\%$
- (3) Yaw gyro error due to  $2^\circ$  component of earth's rate drift =  

$$\frac{12.6512 \sin 2^\circ}{3600} \times 190.48 = 0.0228^\circ \quad \text{or for a } 10^\circ \text{ yaw}$$
displacement, yaw error is  $1/2 (0.0228/10) = 0.114\%$

The factor of  $1/2$  is included since the displacement error due to earth's rate drift will increase from zero to  $.0228^\circ$  as the Griswold head is rotated from zero to  $2^\circ$ .

(4) Yaw error due to mass unbalance for 190.48 seconds is:

$$(.00043^{\circ}/\text{sec} + .00067^{\circ}/\text{sec})190.48 = 0.21^{\circ}$$

The resulting yaw displacement error of 2.1% approaches the required checkout tolerance of 3%. Therefore, it is concluded that the yaw gyro mass unbalance must be measured and used as a displacement correction factor. The mass unbalance error will then be the component added due to the rotation of the gyro axes from the given orientation -

$$\text{or } MU_{IA} = 0.00043 \sin 2^{\circ} = 0.000015^{\circ}/\text{sec}$$

$$MU_{SRA} = 0.00067 \sin 2^{\circ} = 0.00023^{\circ}/\text{sec}.$$

Since the change in mass unbalance drift increases from zero to 0.000038<sup>0</sup>/sec as the IRP is rotated, the yaw displacement error due to this rotation is:

$$\frac{1/2(0.000038 \times 190.48)}{10} = 0.036\%$$

(5) The uncertainty in setting the 10<sup>0</sup> yaw displacement input is:

$$\frac{10''}{10^{\circ}} \times \frac{1}{3600} = .03\%$$

The total maximum error for this test method is the summation of the error sources, or (1) + (2) + (3) + (4) + (5)

$$\text{err} = .138 + .005 + .114 + .036 + .03 = .323\%$$

This measurement accuracy is considered sufficient to meet the required checkout tolerance of  $\pm 3\%$ .



## 8.0 FINAL DESIGN

### 8.1 GSE Requirements

As previously determined, the only GSE necessary for acceptance testing is a test box and cable. Bench system tests will be performed with the Guidance test point unit modified as required for the addition of roll and yaw compensation. Vehicle tests will use existing GSE.

#### 8.1.1 Acceptance Test Set

The Acceptance Test Set for the roll and yaw compensation package will be fabricated from off-the-shelf commercial hardware. The test set will be housed in a portable container and provide the controls, displays and test points as shown in figure 18. The test set is shown in figure 19. The cables will be an integral part of the test set with storage provisions, when not in use, provided on the rear of the test set. New drawings will be provided to cover documentation of the test set. The test set will have the capability of being used as a break-out box in the vehicle. This capability will be used for trouble shooting only.

#### 8.1.2 Guidance Test Point Unit Modification

The modification of the Guidance Test Point Unit will be by modification kit and drawing revision of existing drawings. The test point unit presently has spare binding posts which are not connected or identified. The addition of the roll and yaw compensation package connector test points will require 37 binding posts on the front panel, the addition of a connector at the rear and a cable. The test points will be in three separate groups of twenty (20), ten (10) and seven (7) due to the location of available spares. A cable will be provided to connect the compensation package to the rear of the test point unit. The additional wiring required in the test point unit is shown in figure 20.

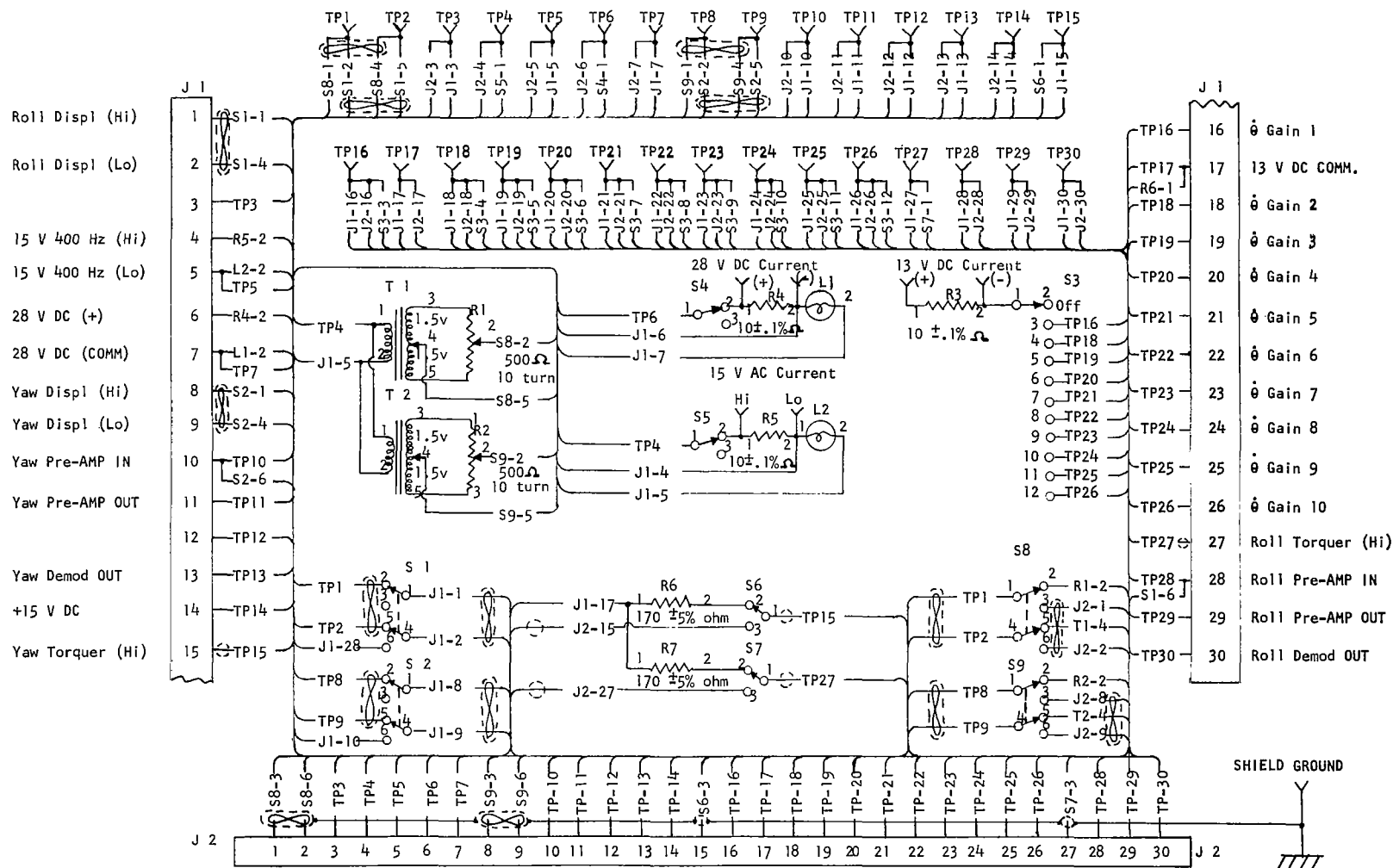


FIGURE 18.- ACCEPTANCE TEST BOX: ROLL &amp; YAW COMPENSATION

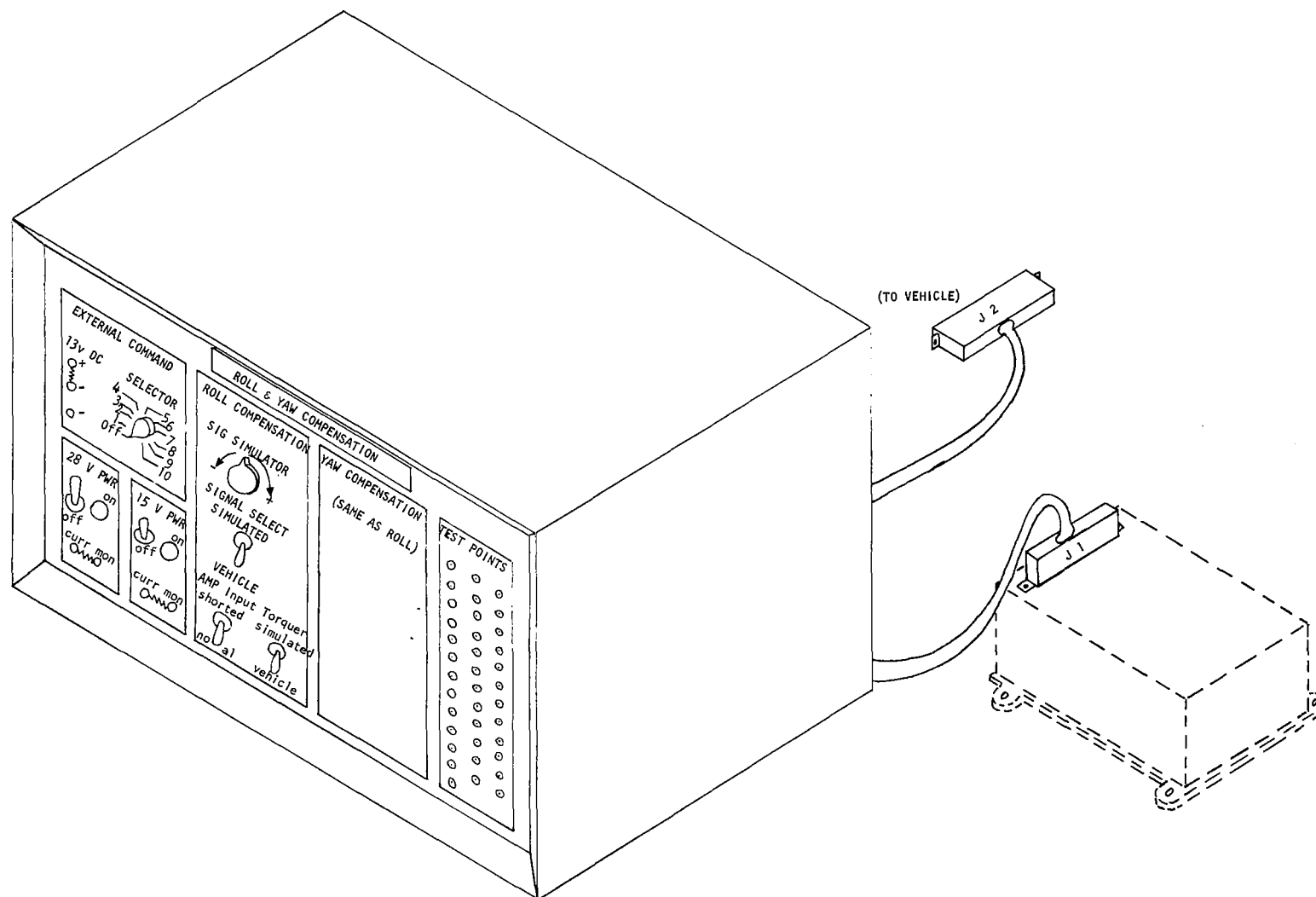
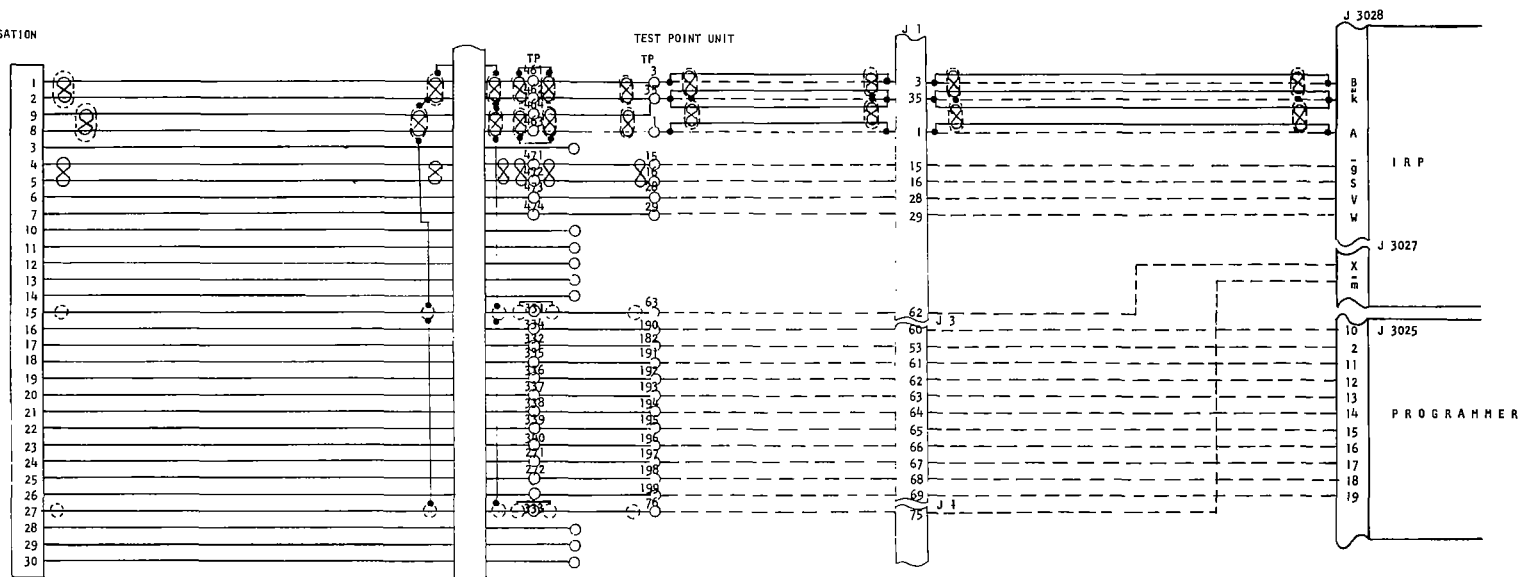


FIGURE 19.- ACCEPTANCE TEST SET

## ROLL AND YAW COMPENSATION

Roll Displ Hi  
 Roll Displ Lo  
 Yaw Displ Lo  
 Yaw Displ Hi  
 Spare  
 15 V 400 HZ HI  
 15 V 400 HZ Lo  
 28 V DC (+)  
 28 V DC COMM  
 Yaw Pre-AMP IN  
 Yaw Pre-AMP OUT  
 Spare  
 Yaw Demod OUT  
 +15 V DC  
 Yaw Torquer HI  
 Gain 1  
 13 V DC COMM  
 Gain 2  
 Gain 3  
 Gain 4  
 Gain 5  
 Gain 6  
 Gain 7  
 Gain 8  
 Gain 9  
 Gain 10  
 Roll Torquer HI  
 Roll Pre-AMP IN  
 Roll Pre-AMP OUT  
 Roll Demod OUT



## NOTES:

1. All wiring #20 AWG.
2. Solid lines indicate new wires;  
dotted lines indicate existing wires.
3. New shields shown at connectors J1 and J3028  
should be tied to existing shields in those  
connectors.

FIGURE 20.- TEST POINT UNIT WIRING CHANGES.

## 8.2 Package Design

The packaging design will utilize proven concepts and materials and will provide a unit of minimum size and weight consistent with this packaging concept.

The various circuit components will be mounted on two (2) double sided printed circuit boards. The design study indicates that the lower board will contain the roll and yaw amplifiers and demodulators. The upper board will contain the output field effect transistors and associated adjustment potentiometers. The compensation unit will be packaged in a drawn aluminum box or other suitable housing with a flat base plate. The proposed package configuration is shown in figure 21. A thirty-seven (37) pin Cannon "D" series miniature connector is proposed for electrical connection to the unit. The overall size of the compensation unit will be approximately 5.25 long, 3.50 wide and 2.00 high. The calculated weight of the proposed unit is 1.96 pounds.

## 8.3 Vehicle Changes

### 8.3.1 Package Installation

The package will be mounted inside the existing delta structure in Scout lower "D" section, as shown in figure 22.

### 8.3.2 Vehicle Wiring Changes

The proposed changes, to the existing vehicle wiring, required to accept the roll and yaw compensation unit are illustrated in figure 23. Circuit splices using standard proven Scout crimp splices will be used to minimize harness rework and reliability impact. Existing components will not be reworked to provide internal junctions.

### 8.3.3 Weight

It is estimated that the installation provisions and additional wiring will weigh one-half (.5) pounds, or a total of 2.46 pounds for the installed unit.

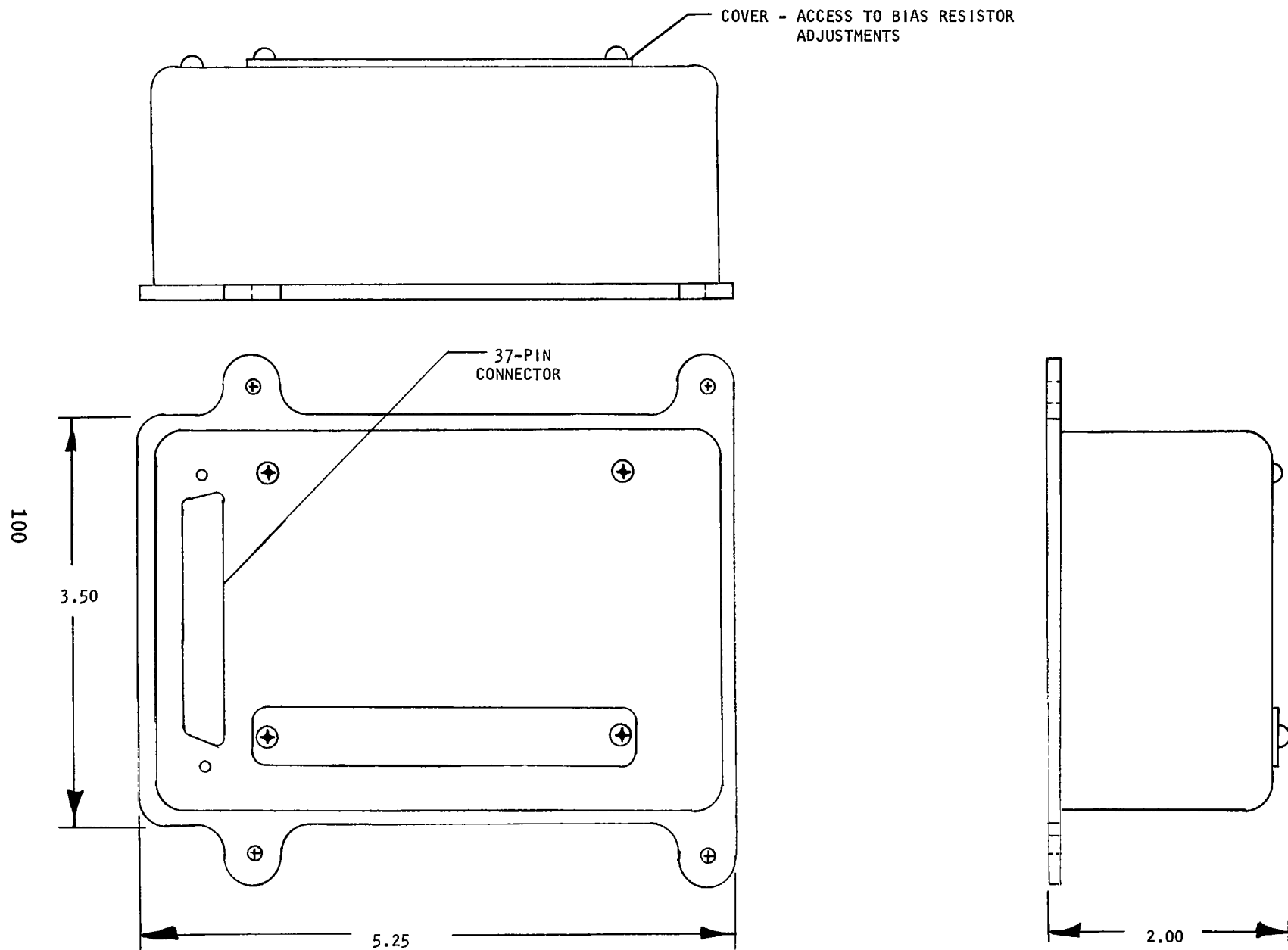


FIGURE 21.- ROLL & YAW COMPENSATION UNIT

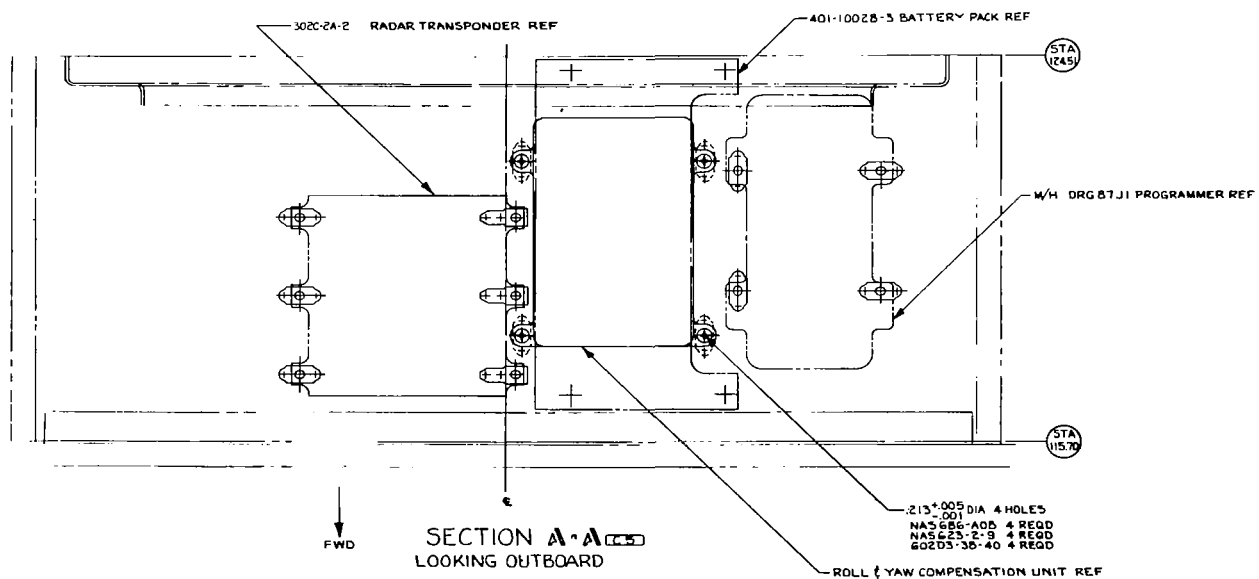
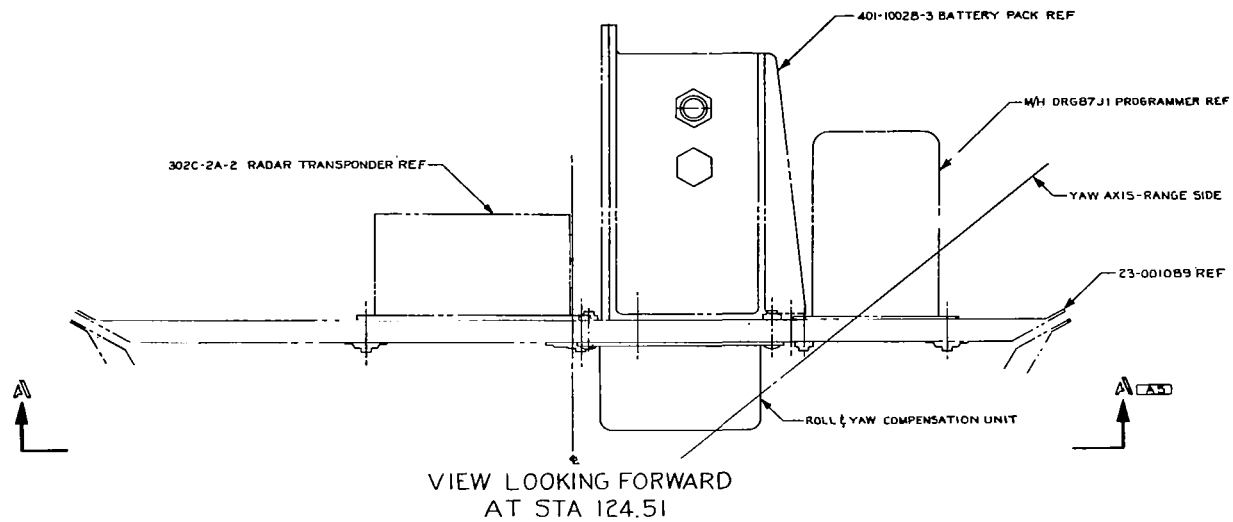


FIGURE 22.- UNIT INSTALLATION ROLL & YAW COMPENSATION GUIDANCE SYSTEM.





CONCLUSIONS AND RECOMMENDATIONS

The important conclusions resulting from the Roll and Yaw Compensation Study are:

1. Hardware can be produced capable of meeting the design objectives and accuracy requirements of Roll and Yaw Compensation analyses and simulation.
2. The addition of Roll and Yaw Compensation to the Scout launch vehicle results in a significant improvement in the orbital inclination accuracy as affected by the lower stage errors.
3. The greatest improvement in inclination accuracy occurs with incorporation of Roll Compensation in the first stage only and Yaw Compensation in the first, second, and third stages.
4. The Roll and Yaw Compensation circuit is best mechanized by a pre-programmed multiplier with the gain changed on command from the Guidance System Intervalometer for each pitch program step.
5. Pre-flight adjustment of the compensation can be accomplished by the setting of potentiometers and therefore no special pre-flight wiring is required.
6. Roll and Yaw Compensation is not used for pitch up commands or yaw torquing commands. The compensation is required for orbital missions only.

Based on the results of this study, LTV recommends that the necessary action be taken to immediately implement the final design, qualification testing, and incorporation of Roll and Yaw Compensation in the Scout Vehicle.

10.0

REFERENCES

- (1) Scout Orbital Inclination Study, LTV Report No. 23.222, dated 17 June 1965.
- (2) The Near Earth Mission Analysis Trajectory Routine, LV-VC-27, LTV Report No. 00.251, dated 4 October 1963.
- (3) Mission Accuracy Analysis for the Scout Launch Vehicle, LTV Report No. 23.41, dated 30 November 1962.
- (4) Scout First Stage Roll Moment Disturbance, LTV 23-DIR-405, dated 7 November 1966.